International specialized medium for agricultural mechanization in developing countries

ISSN 0084-5841

AMA

AGRICULTURAL MECHANIZATION IN ASIA, AFRICA AND LATIN AMERICA

VOL.51, NO.1, WINTER 2020

FARM MACHINERY INDUSTRIAL RESEARCH CORP.


ECHO
ECHO
ECHO
ECHO

International specialized medium for agricultural mechanization in developing countries

ISSN 0084-5841

AMA

AGRICULTURAL MECHANIZATION IN ASIA, AFRICA AND LATIN AMERICA

VOL.51, No.1, WINTER 2020

Edited by

YOSHISUKE KISHIDA

Published quarterly by

Farm Machinery Industrial Research Corp.

in cooperation with

The Shin-Norinsha Co., Ltd.

and

The International Farm Mechanization Research Service

TOKYO

ADVERTISING

(Tel.+81-(0)3-3291-3674)
Yuki Komori, Director (Head Office)
Advertising Rate: 300 thousand yen per page

CIRCULATION

(Tel.+81-(0)3-3291-3674)
(Fax.+81-(0)3-3291-5717)
Editorial, Advertising and Circulation Headquarters
1-12-3, Kanda Nishikicho, Chiyoda-ku, Tokyo 101-0054, Japan
URL: https://www.agriculturalmechanization.com/
E-Mail: ama@shin-norin.co.jp

This is the 182th issue since its maiden issue in the Spring of 1971

EDITORIAL

The year 2020 has begun. Twenty-one years have passed since the beginning of the 21st century, but human beings are still engulfed in political struggles and various conflicts on this small planet earth. Currently Japan's population is 120 million, but among them, about 36 million people are over the age of 65 and this number is going to stay as it is. The population of Japan will be reduced by 40 million in 30 years and thus it is expected to be 80 million by 2050.

Furthermore, after twenty more years later, that is by 2070, the population of Japan is expected to decrease to half (60 million) of the current level of 120 million. Japan demographic structure is aging and the number of young people is decreasing and the number of elderly people is increasing.

The reason has not been determined. It was announced that one in four adult males in Japan had azoospermia, but why the number of sperm has decreased is also a terrible thing, the cause of this has not been determined. Some scholars say it's due to chemicals taken up by food or may the result of atomic radiation from one generation to the next. If so, further research on food safety and health issues are needed.

In Europe and the United States, it is said that the Round-up herbicides that are used everywhere are dangerous, so it will be banned. Weeding is an important and important part of agricultural work, but most is accomplished by using herbicides. There are many farmers who want to practice however, there is still no information about the relationship between food safety and chemical substances, organic farming may have to be expanded in every country.

Research and development of a new mechanized system is needed to develop organic farming. Agricultural machines are evolving into robotic agricultural machines. Last year's AGRITECHNICA, Naïo Technologies of France announced inter-tillage robot that was awarded a silver medal. In Japan, a company called INAHO is starting to sell asparagus harvesting robots. These movements also have a major impact on mechanization in developing countries. Small revolving robots must be mass-produced and made available very cheaply in any of the country.

AMA has been in operation for over 50 years since it began in 1971, 'Appropriate Technology' was reconsidered, including the latest available technology during those days. Humans have to become in more harmony with the life systems, An appropriate and better agricultural mechanization is required worldwide.

The next spring issue will be published on May 25 and will include a special field with the title 'SDGs (Sustainable Development Goals) and the world's agricultural mechanization' as a special issue commemorating the 50th anniversary.

Yoshisuke Kishida
Chief Editor
January, 2020

CONTENTS

AGRICULTURAL MECHANIZATION IN ASIA, AFRICA AND LATIN AMERICA

Vol.51, No.1, Winter 2020

Evaluation Parameters Afeccting the Performance of Vibrating Vertical Tillage Equipment – First Stage

by
Guillen Sánchez Juan
Posgraduate student at Instituto Tecnológico de Aguascalientes
MEXICO

Santos G. Campos Magaña
Universidad Autónoma Agraria Antonio Narro
MEXICO
Corresponding author: camposmsg@hotmail.com

Carlos Sánchez López
Instituto Tecnológico de Aguascalientes
MEXICO

Oscar M. González-Brambila
Centro de Ingeniería y Desarrollo Industrial
MEXICO

Gabriela Ramírez-Fuentes
Universidad Autónoma Agraria Antonio Narro
MEXICO

Abstract

The aim of this work was to evaluate an alternative to reduce energy consumption applied to primary soil tillage. To do this an experimental apparatus was developed to evaluate the operation of vibration induced tillage parameters. The components that integrated the system for field valuation were: frame tool carrier that includes a system of three-point hitch and depth control mechanism; three sensors were included to measure tillage force, torque and the frequency of the subsoiler oscillation. Oscillatory impact force was applied through a rod and crank mechanism through a subsoiler tine whose movement is provided by a hydraulic motor. The apparatus evaluation was complemented by a system of data acquisition and signal conditioner that allows the registration of the variables of interests such as draft power, penetration force, applied torque and speed of oscillation of the system. The results of the calibration of the sensors showed a system correlation higher than 95%. The results obtained during field system verification at different speed, amplitude and depth of tillage showed a reduction of the draft force up to 50% using the oscillated induced tillage compared to the non-vibrating tine condition. The study shows a significant increase in the magnitude of the draft force and torque applied by 33% when the working depth increased from 0.30 to 0.40 m and an increase of 21% of draft force was produced when the amplitude of oscillation was reduced from 0.070 to 0.060 m. No significant difference was found when the tractor speed was increased from 1.5 to 2.5 km h^{-1}. For future work the developed apparatus will allow to determine how the amplitude and the working depth and oscillation frequency of the tine could affect the draft force in tillage work.

Keywords: oscillatory subsoiler, draft force, energy consumption, amplitude of oscillations.

Introduction

Vertical conventional tillage implements have soil-working tools, which do not move relative to the implement frame. Their draft requirements are comparatively high as they are always in contact with the soil and the power for operating these implements is transmitted through traction with tractive eficiency varying between 40 to 75% (Witney, 1995). To improve the tractive efficiency, the tractor drive wheels are ballasted with additional weights. However, this practice causes soil compaction, which is detrimental crop efficiency. Several researchers have reported that oscillating soil-working tools have lower draft requirements and break up the soil better than do their non-oscillating tine implements when working under identical conditions. Therefore, an oscillating soil-working tool may reduce the number of operations to prepare an acceptable seedbed and minimize soil compaction, thus providing a better physical environment for plant growth. In addition, oscillatory tillage uses more eficient tractor power-take-off by 90 to 95% to mechanically oscillate tines (Hendrick, 1980). Lower draft requirement of oscillatory tillage reduces the reliance on less ef?cient drawbar power; leading to a lower overall demand on engine power may occur (Slattery and Desbiolles, 2003), also is generally recognized that the draft force of a vibratory tillage implement can be reduced by 30% to 80%.

Bandalan et al. (1999) performed an experimental study on the tillage performance of an oscillatory subsoiler, determining the optimum combination of operating parameters of the subsoiler such as frequency of oscillation, amplitude and working speed the pull-force and the total power consumed were measured.

Sahay et al. (2009) developed the equipment induced vibration tillage that change the transmission frequency of vibration from 9 to 13 Hz and from 15 to 35 Hz. Experiments showed that the real depth of the oscillatory system work was 0.153 m while the same equipment without vibration was 0.074 m.

Shahgoli et al. (2009) in their study reported the evaluation of the effect of the angle of swing of the tine in the performance of the subsoiler. The objective of this study was to quantify the optimal angle of oscillation for the reduction of the strength of pull, low requirement of power, low specific draft-force, maximum disturbed area and minimum vibration transmitted to the operator's seat. In terms of performance, –22.5° was the optimum angle of oscillation for the reduction of the draft force and power.

Shahgoli et al. (2010[a], 2010[b]) claimed in his study on the optimization of the oscillatory frequency of vibratory tillage, the tines were oscillated with amplitude of ±69 mm at an angle of 27° using a working speed of 3 km h^{-1}. The frequency of oscillation was changed from 1.9 to 8.8 Hz. There was an optimal frequency near 3.3 Hz (1.5 speed ratio), which minimized the total engine power required to operate a subsoiler. It was estimated a decrement of engine power demand above 26% compared to a rigid tillage equipment.

Studies of oscillatory tillage cited by (Shahgoli et al., 2009 and 2010[a]) reported that the induced oscillation of a longitudinal or vertical tillage in directions tool can significantly reduce by 50% the draft-force requirements. They also mentioned that the oscillatory frequency, amplitude of swing, swing angle, speed of the tractor, tool design and soil properties those are important factors affecting the functioning of a vibrating tool.

Campos et al. (2015[a]) modified a vertical tillage implement call multicultivador and conducting a series of investigations by applying the theory of critical depth in tillage equipment. The modifications that were made by the researchers team, basically consist of place shallow tines on the front; and greater length at the rear tines. In the tines of the rear, wings of different sizes were evaluated to increase the disturbed cross sectional area. Field tests were conducted with this arrangement and experimentally was demonstrated that there is a decrease in the specific soil resistance by more than 20% in comparison with primary tillage using tines at the same working depth.

The purpose of the present research work was to develop an apparatus that allows determining the effect that has the variation of the most important parameters in vibration induced tillage such as amplitude and frequency of oscillation, as well as the effect of this vibration on the reduction of the draft force on the vertical tillage.

Materials and Methods

The experimental apparatus was design to be mounted to a tractor category II with three points hitch system, and the oscillatory system was powered by the hydraulic system of the tractor. This device al-

Fig. 1 Side view of the vibrating tillage equipment. Oscillating tine (1); oscillatory mechanism (2); extended octagonal ring transducer (3)

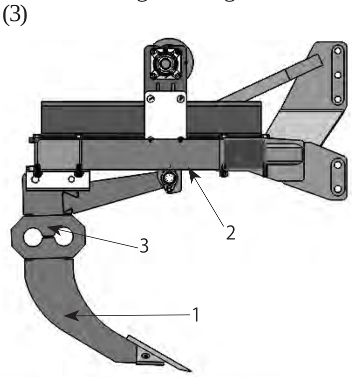

Fig. 2 Isometric view of the vibrating tillage equipment. Chassis (4); hydraulic motor (5); torque transducer (6); frequency sensor (7)

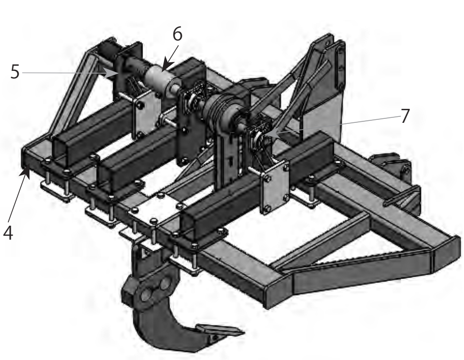

low adjustment of the frequency of oscillation from 3.3 to 4.9 Hz and amplitudes from 0.060 and 0.070 m. **Figs. 1** and **2** show the main components of the device designed and built by the Tecnomec Agricola S. A. de C.V. Company. The apparatus is integrated by an oscillation tine (1), an oscillatory mechanism connecting rod crank (2), an extended octagonal transducer (3), structure or chassis (4), a hydraulic motor (5), a torque transducer (6) and an oscillation frequency sensor (7).

The chassis corresponds to the structure of the apparatus in which all the components including the three-point hitch system are mounted. A crank connecting rod mechanism provides the swing of the tine as shown in **Figs. 1** and **2**. This mechanism is operated by means of a hydraulic motor for high torque and low speed of rotation. The frequency of rotation is controlled by a flow regulator valve. A torque transducer with a capacity of 25 kW at a frequency of 9 Hz was coupled between the hydraulic motor and oscillating mechanism to measure the torque that is generated at the time of soil tillage.

To measure horizontal and vertical forces applied to the soil an extended octagonal ring transducer (OAE) with capacity of 40 kN was built which dimensions are shown in **Fig. 3**.

An electronic card was developed to determine the frequency of oscillation in real time of the vibrating apparatus, using an infrared optoelectronic sensor H21A1 (Fairchild Semiconductors, USA) and a microcontroller PIC 16f84 (Microchip company, USA) to eliminate rebounds produced by the effect of magnetic noise.

The construction of the apparatus and mounting of sensors were built at Tecnomec Agricola S. A. de C. V., Aguascalientes State, Mexico, during the period from February to December 2014. Laboratory research and field test was carried out from January to October 2015 in the Agricultural Engineering Department and the experimental Station "El Bajío" at the Universidad Autónoma Agraria Antonio Narro. Located at the State of Coahuila, Mexico, at 25° 21.52" N, 101° 50" W and at altitude of 1,740.5 m over the sea level in a clay soil with resistance to penetration of 2.45 kPa, and average soil moisture of 18%.

A John Deere tractor JD6403, single traction with 105 HP at the engine, was used for the field test. Instrumented tractor include the following equipment: analog to digital converter Logbook360 (Iotech Company, USA), calibrated at a frequency of 20 Hz sampling rate and signal conditioner model DBK43A from the same made, calibrated to a gain of 2,500 micro strain (μδ).

In order to measure forces in the horizontal and vertical direction (**Figs. 4** and **5**), it was necessary to make a static calibration of the transducer (OAE) using known loads of (470.8, 470.8, 716.13, 343.35, 343.35, 294.30, and 294.30 N). To run the calibration, the loading and unloading of the weights

Fig. 4 Calibration of transducer OAE for horizontal force

Fig. 5 Calibration of the transducer OAE to determine vertical force constant

Fig. 3 Dimensions and characteristics in the extended octagonal ring transducer in mm

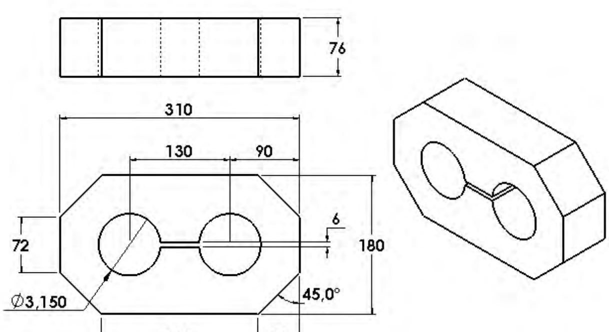

Fig. 6 Calibration of torque transducer

were carried out with 5 replicates each.

In order to measure the torque applied to the tine from the hydraulic system of the tractor was necessary a torque transducer calibration, the same Logbook360 data acquisition system was used. Calibration was performed with two-arm lever (0.65 and 0.85 m) and four loading and unloading weights: 294, 294, 343 and 343.5 N, each position was replicated 5 times (**Fig. 6**).

Data analysis was performed with the method of spectral analysis described by Campos and Wills, (1995) using Matlab V2010a and Fast Fourier Transform algorithm to obtain the mean values, curves and calibration constants, using a linear regression of the data analysis. Analysis of variance was performed using Minitab V15 statistical analysis software. The field Treatments performed for two depths of 0.30 and 0.40 m, two working speed at 1.5 and 2.5 km h^{-1} and two amplitudes of 0.060 and 0.070 m for a single oscillatory speed of 3 Hz. A control test with not vibrating tine at two working depths of 0.30 and 0.40 m at a speed of 1.5 km h^{-1} was also performed. A total of 10 treatments were conducted and four replications were carried out by each arrangement; each trial was carried out on plots of 50 m long by 2.5 m wide.

Results and Discussion

Construction of the Apparatus

Fig. 7 shows instrumented apparatus (a) for vibrating tillage, a transducer OAE (b) that (c) was employed to measure the torque required for impact the soil, an infrared optoelectronic sensor (d) to measure the frequency of the oscillating mechanism and a data acquisition system (e) for collecting all data information from the transducers in real-time to be subsequently analysed.

To obtain the same reliability of measurement in the two transducers, it was necessary to standardize the coefficient of constant by means of the calibration adjustment on 3 channels of the amplifier that correspond to each sensor and adjust the input gain, the compensator and the excitation voltage. **Fig. 8** shows an example of a step graph of OAE corresponding to the vertical force transducer calibration. **Fig. 9** shows the equation of regression with a constant of 75.00 mV N^{-1}, with a correlation coefficient of 99.8%.

Fig. 10 shows an example Graph corresponding to the horizontal force of OAE transducer calibration and **Fig. 11** shows the linear calibration of horizontal force. In addition, shows the equation of regression with a constant of 47.74 mV N^{-1} with a correlation coefficient of 99.7%.

Fig. 12 shows an example of the graph of the deformation in mV generated from the ascent and descent of four loads with a lever arm of 0.85 m and **Fig. 13** shows the equation of regression with constant 0.4538 mV N m^{-1} with a correlation coefficient of the 98.8%. Similar results were obtained by (Campos et al., 2015[b]) for the calibration of sensors of the type of OAE.

Tests Under Field Conditions

Fig. 14 shows the forces obtained in field for the vertical force by comparing the amplitudes of 0.060 and 0.070 m for both working at a depth of 0.40 m and a speed of 1.5 km h^{-1}. It can be seen that the applied

Fig. 7 Instrumented Apparatus for field evaluation

(a) apparatus for vibratory tillage

(b) transducer OAE

(c) torque transducer

(d) sensor optoelectronic

(e) data acquisition system

Fig. 8 Cycles of loading and unloading of the OAE transducer during calibration with different weights for the vertical force

Fig. 9 Graph showing the linearity of calibration of OAE transducer for vertical force. The obtained equation was: Force (N) = 8.073 + 75.00* Voltage (mV)

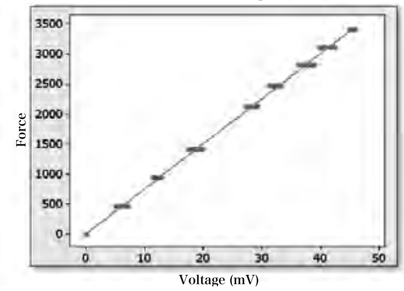

Fig. 10 Cycles of loading and unloading of the OAE transducer during calibration with different weights for the horizontal force

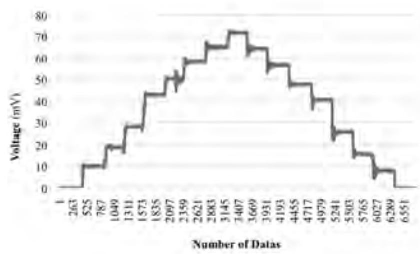

Fig. 11 Shows the Linearity of calibration of horizontal force. The obtained equation was: Force (N) = 21.97 + 47.74 Voltage (mV)

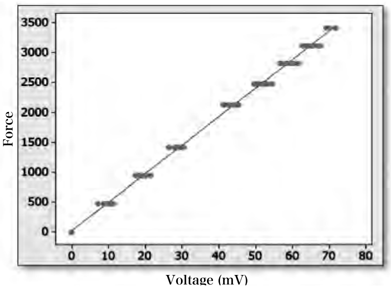

forces for higher oscillation amplitude (7040A1) are charged towards the positive part of the graph, while in the lower oscillation amplitude forces (6040A1) are distributed both in the positive as negative zone.

Fig. 15 shows an example of the behaviour of horizontal force generated by the rigid tine subsoiler, where it can see the difference between two depths of tillage (0.30 and 0.40 m) at a speed of work of 1.5 km h^{-1}.

Fig. 16 compares the draft-force obtained in field with the rigid and vibration tine for a forward speed (1.5 km h^{-1}), at the same depth of 0.40 m, which shows a lower draft-force demand when applying an induced vibrations to 0.070 m amplitude.

From **Fig. 17** can be appreciated the magnitude of the torque obtained in field. Where shows that exist two directions of registered torque magnitude applied to the soil one for the forward working condition into compacted soil and the another magnitudes for the reverse when the tine is acting in loose soil. The results of this analysis are shown in **Table 1**.

In **Table 1**, the variance analysis of the effect of depth of tillage of 0.30 to 0.40 m shows a highly significant difference on the magnitude

Fig. 12 An example graph of cycles of loading and unloading during calibration the torque transducer with different loads and arm lever

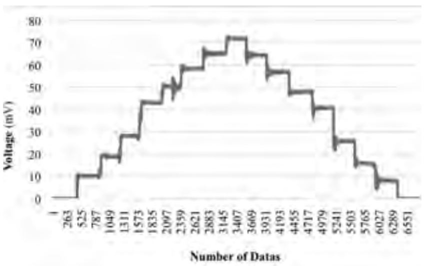

Fig. 13 Graph showing the linearity and constant of calibration for torque transducer. Torque (Nm) = 29.34 + 0.4538 Voltage (mV)

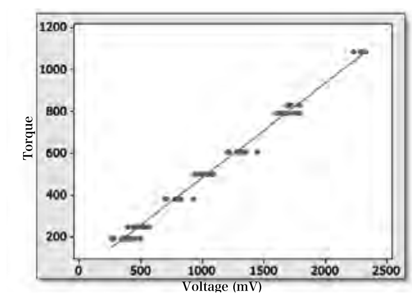

Fig. 14 Comparison of vertical forces to different amplitudes for a depth of 0.40 m. The graph (7040A1) is for amplitude of 70 mm and first replicate. The graph (6040A1) is for amplitude of 70 mm and first replicate

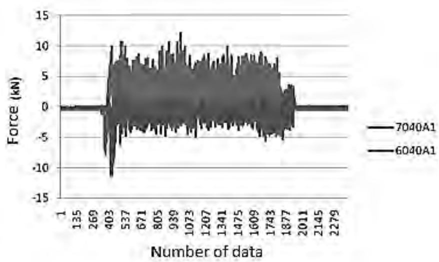

Fig. 15 Comparison of the horizontal force at rigid tine at two depths. Graph (40A1) shows the tine working at 0.40 m depth for the first replicate. Graph (30A1) shows the tine working at 0.30 m depth for the first replicate

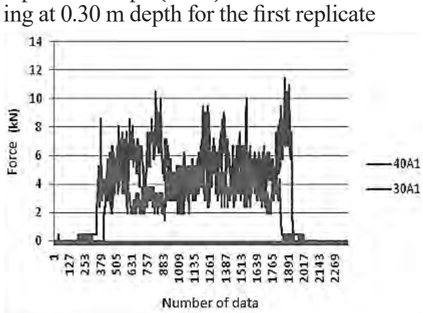

Fig. 16 Comparative force demand at rigid tine and vibration (amplitude of 0.070 m) to the same depth of 0.40 m and speed of 1.5 km h^{-1}. Graph (7040A1) shows the draft force for vibrating tine working at 0.40 m depth. Graph (40A1) shows the draft force for rigid tine working at 0.40 m depth

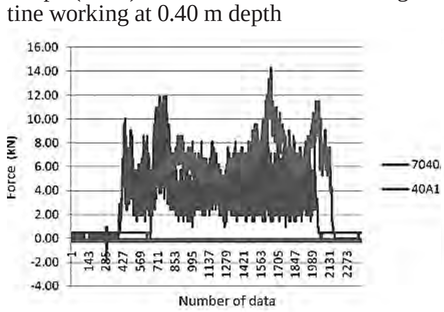

Fig. 17 Graph showing the applied torque for the oscillating amplitude of 0.070 m and a working depth of 0.40 m

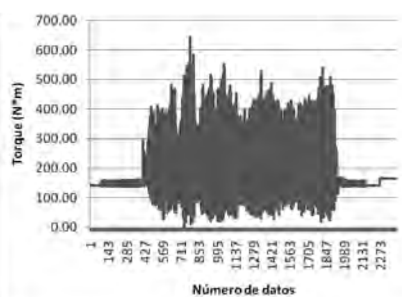

of the draft force, as well as the force applied for tillage with oscillation chisel to three different magnitudes of swing (0.01, 0.06 to 0.07 m)

For the oscillatory tine, the mean values showed a decrease of 50.1% in the force of pulling, compared with the rigid tine. Similar results were reported by Shahgoli et al. (2010[b]). The significant reduction in the magnitude of the draft force by change of depth of tillage, from 0.40 to 0.30 m, was also reported by (Spoor and Godwin, 1978; Campos et al., 2015[a]).

An analysis of variance was performed as shown in **Table 2**, whereas only the magnitudes of the draft force to the two assessed oscillation amplitudes of 0.060 and 0.070 m finding significant difference. Variance analysis shows the effect is also at two-tillage speed, 1.5 and 2.5 km h^{-1} on the draft force, finding not significant difference in force for the effect of change of speed. In this analysis was corroborated the significant effect that produces the depth of tillage on draft-force (Campos et al., 2015[c]).

In comparison to the change of amplitude of oscillation, **Table 3** shows a significant difference in the measurement of the draft force in the order of 21.0% when increases the oscillation amplitude from 0.060 to 0.070 m. Similar results were obtained by (Shahgoli et al., 2010[a]).

From **Table 4**, the oscillation of the tine increases the magnitude of the vertical force to a 47.0% between the vibrating and the rigid tine when tillage speed increases from 1.5 to 2.5 km h^{-1}. Likewise, the magnitude of the torque is increased up to 33.0% when tillage depth is increased from 0.30 m to 0.40 m unless this increase has to do with the increased speed of 1.5to 2.5 km h^{-1}. Similar magnitudes were reported by (Xin et al., 2013).

Conclusions

The device designed and built by Tecnomec Agricola S. A. de C. V. allowed mounting of sensors for the on-field measurement of horizontal and vertical forces acting on the tine tool as well as frequency of oscillation and torque of impact of the tine in a satisfactory manner.

In the field-testing for verification of the system functions, data recorded at different amplitudes of swing revealed that the apparatus could reduce the draft force up to 50% using the oscillated induced tillage compared to the non-vibrating condition. There was a significant increase in the magnitude of the draft force and torque applied by 33% when the working depth increased from 0.30 to 0.40 m. Besides, an increase of 21% draft force was produced when the amplitude of oscillation was reduced from 0.070 to 0.060 m.

No significant difference was found when the tractor speed was increased from 1.5 to 2.5 km h^{-1}. Then, based on the above results, it was confirmed that there is a significant reduction in the draft-force between a rigid tines versus one vibrating at lower oscillation amplitude.

REFERENCE

Bandalan, E. P., V. M. Salokhe, C. P. Gupta and T. Niyamapa. 1999. Performance of an oscillating subsoiler in breaking a hardpan. Journal of Terramechanics, 36(2): 117-125.

Campos-Magaña, S. G. and B. M. D. Wills. 1995. Force Measure-

Table 1 Analysis of variance of the effect depth (0.30 and 0.40 m) and swing (0.00, 0.06 to 0.07 m) on the magnitude of the pulling force

FV	GL	SC	CM	FC	F_{05}	F_{01}
Blocks	3	4.313	1.438	0.725		
Oscillation factor (O)	2	167.267	84.633	42.670**	5.14	10.92
Oscillation inaccuracy	6	11.901	1.983			
Depth factor (P)	1	2.8380	2.8380	221.21**	5.12	10.56
O × P	2	25.065	12.532	9.768**	4.26	8.02
Depth inaccuracy	9	11.546	1.283			
Total	23	505.892				

FV = Factors, GL = degree of freedom, CM = Mean square, FC = F factor, F_{05} = F for (P < 0.05), F_{01} = F for (P < 0.01), ** = exist a significant difference between variable levels

Table 2 The variance analysis of the effect of working speed and depth, oscillating frequency and amplitude over the magnitude of the draft force

FV	GL	SC	CM	FC	F_{05}	F_{01}
Blocks	3	1.598	0.533	1.251		
Speed factor (V)	1	0.001	0.001	0.002	10.13	
Speed error	3	1.51	0.350			
Oscillation factor (O)	1	14.005	14.005	44.691**	5.99	13.75
V × O	1	1.129	1.129	3.602	5.99	
Oscillation error	6	1.88	0.313			
Depth factor (P)	1	118.157	118.157	186.240**	4.26	7.82
V × P	1	24.939	1.129	39.310**		
O × P	1	2.571	24.939	4.052		
V × O × P	1	3.194	2.571	5.035*		
Total error	24	7.613	3.194			
Total	31	176.138	0.634			

FV = Factors, GL = degree of freedom, CM = Mean square, FC = F factor, F_{05} = F for (P < 0.05), F_{01} = F for (P < 0.01), ** = exist a significant difference between variable levels

ment and Recording and data analysis for tillage tools. Agricultural Mechanization in Asia, Africa and Latin America, 26(1): 13-16.

Campos-Magaña, S. G., M. Cadena-Zapata, G. Ramírez-Fuentes, J. L. Pacheco-Lopez, M. A. Reynolds-Chávez and J. R. Valenzuela-García. 2015[a]. An experimental determination of specific soil resistance of a sandy loam soil using vertical soil tillage in the northeast of Mexico. Agricultural Mechanization in Asia, Africa, and Latin America, 46(1): 53-57.

Campos-Magaña, S. G., J. A. López-López, M. Cadena-Zapata, M. A. Reynolds-Chávez, N. Cuervo-Piña, and G. Ramírez-Fuentes. 2015[b]. Desarrollo de un penetrómetro integrado con tecnología GPS-RTK para la generación de mapas de resistencia a la penetración del suelo. Terra Latinoamericana, 33(2): 119-128.

Campos-Magaña, S. G., M. A. Reynolds-Chávez, M. Cadena-Zapata, J. A. López-López, N. Cuervo-Piña and G. Ramírez-Fuentes. 2015[c]. Desarrollo de un sistema integral de medición de fuerzas para la evaluación de implementos de labranza. Terra Latinoamericana, 33(2): 139-149.

Hendrick, J. G. 1980. A powered rotary chisel. Trans of ASAE 23(4), 1349-1352.

Sahay, C. S., E. V. Thomas and K. K. Satpathy. 2009. Performance evaluation of a novel power tiller operated oscillatory tillage implement for dry land tillage. Biosystems Engineering, 102(4): 385-391.

Shahgoli, G., C. Saunders, J. Desbiolles and J. M. Fielke. 2009. The effect of oscillation angle on the performance of oscillatory tillage. Soil and Tillage Research, 104(1): 97-105.

Shahgoli, G., J. Fielke, J. Desbiolles and C. Saunders. 2010a. Optimising oscillation frequency in oscillatory tillage. Soil and Tillage Research, 106(2): 202-210.

Shahgoli, G., J. Desbiolles, J. Fielke and C. Saunders. 2010b. Simulation of the dynamic behaviour of a tractor-oscillating subsoiler system. Biosystems Engineering, 106(2): 147-155.

Slattery, M. and J. Desbiolles. 2003. Effect of vibrating tines, multi-depth and multi-pass subsoiling on soil loosening and tractor power use, paper presented at the E-Proc. of 13 International Soil Tillage Research Organization Conference, Brisbane, Australia. 1149-1156.

Spoor, G. and R. J. Godwin. 1978. An experimental investigation into the deep loosening of soil by rigid tines. Journal of Agricultural Engineering Research, 23(3): 243-258.

Witney, B. D. 1995. Choosing and Using Farm Machines. Land Technology Ltd., Edinburgh

Xin, L., J. Liang and L. Qiu. 2013. Dynamic analysis and experimental research of vibratory subsoiler system. Journal of Theoretical and Applied Information Technology, 48(4): 1195-1201.

■■

Table 3 Comparison of means values of the magnitude of the draft forces at different frequencies of oscillation and depths of the tine work

Oscillation amplitude (mm)	Average force (kN)	Depth (m)	Average Force (kN)
0.60	7.929a	0.30	5.153b
0.70	6.236b	0.40	8.96a

Means in the same column followed by the same letter do not differ significantly (P < 0. 05) by DUNCAN test.

Table 4 Comparisons of means values of the vertical forces and torque for the evaluated treatments

Treatment	Vertical Force	Applied torque
	kN	Nm
60 mm swing tine + 0.40 m Depth + 2.5 km h^{-1}	8.93a	304.3a
70 mm swing tine + 0.40 m Depth + 2.5 km h^{-1}	7.85a	303.1a
Rigid tine to 0.40 m Depth + 1.5 km h^{-1}	4.13bc	---
70 mm swing tine + 0.40 m Depth + 1.5 km h^{-1}	4.04bc	318.1a
60 mm swing tine + 0.40 m Depth + 1.5 km h^{-1}	3.96bc	310.2a
60 mm swing tine + 0.30 m Depth + 2.5 km h^{-1}	3.28cd	186.5b
60 mm swing tine + 0.30 m Depth + 1.5 km h^{-1}	3.62cd	203.8b
70 mm swing tine + 0.30 m Depth + 2.5 km h^{-1}	2.39de	169.7bc
70 mm swing tine + 0.30 m Depth + 1.5 km h^{-1}	2.14e	108.78c
Rigid tine to 0.30 m Depth + 1.5 km h^{-1}	1.84e	---

Means in the same column followed by the same letter do not differ significantly (P < 0.05) by DUNCAN test

Design, Fabrication and Evaluation of a Power Operated Walnut Grader

by

Syed Zameer Hussain
Division of Post Harvest Technology
Shere-e-Kashmir
University of Agricultural Sciences & Technology of Kashmir
INDIA
zameerskuastj@rediffmail.com

Umbreen Showkat
Division of Post Harvest Technology
Shere-e-Kashmir
University of Agricultural Sciences & Technology of Kashmir
INDIA

Sheikh Idrees
Division of Post Harvest Technology
Shere-e-Kashmir
University of Agricultural Sciences & Technology of Kashmir
INDIA

Monica Reshi
Division of Post Harvest Technology
Shere-e-Kashmir
University of Agricultural Sciences & Technology of Kashmir
INDIA

Abstract

The manual size grading of walnuts is labour intensive, and tedious practice; besides being inconsistent and less efficient. The aim of the present study was thus to design, fabricate and evaluate a power operated walnut grader. The walnuts grown in Jammu and Kashmir State of India were classified into four grades, and all the four grades were evaluated for various dimensional, physical, frictional and mechanical properties to create a database which play an important role in designing of mechanical system for walnut grading. A power operated walnut grader was developed and tested. The machine consists of feed hopper, casing, rotating pipes, delivery chutes, sprockets, driving chain and a control box. The result of the performance tests showed that grading error was significantly affected by feed rate, grader slope and opening size from feeding end to trailing end. The highest mean grading efficiency of 96.3% (least grading error 3.7%) was recorded at a feed rate of 400 kg/hand 80 of grader slope. The effective throughput capacity of the machine was estimated to be 337 kg/h. Adoption of this technology will help walnut growers, processors and other stakeholders to make quality graded walnuts available in the competitive markets. This paper describes the design and performance evaluation of the walnut grader as well as the implications of results obtained.

Keywords: Walnut Grader, Feed Rate, Grader slope and Dimensional properties

Notations

P = Power requirement of machine
N_1 = rotation per minute of motor
T = Torque generated in the motor
N_2 = Worm gear output
T_1/T_2 = Gear ratio
M_t = Torsional moment of shaft
F_{pt} = Pure torsional load on shaft
d = Diameter of shaft
M_b = Pure bending load on shaft
F_t = Ultimate tensile strength
θ = Torsional deflection induced in shaft
L = Length of shaft
J = Polar moment of Inertia
C = Modulus of rigidity
M_{be} = Equivalent bending moment on shaft
E = Elastic limit of shaft material
I = Moment of inertia
W = Weight on shaft due to load
δ_{linear} = Deflection in shaft
M = Mass of shaft
A = Area of cross section of shaft
δ_{weight} = Static deflection due to own mass of shaft
F_n = Frequency of transverse vibration
V_R = Velocity ratio
N_3 = Speed of driven sprockets
Z_1 = No. of teeth of driving sprocket
Z_2 = No. of teeth of driven sprocket
C_p = Chain pitch
C_d = Centre distance between two sprockets
V = Chain velocity
F = Total load on driving chain
F_s = Shearing force on chain
$W_{breaking\ load}$ = Breaking load strength of chain

F_0 = Force load on chain element
F_f = Frictional force on chain element
K = Lubrication constant
F_c = Tearing force acting on chain
P_B = Check for wear
K_w = Wear constant for chain
A_c = Area of chain
d_p = Duplex chain distance
l_b = Length of chain duplex hub
b_t = Width of chain duplex hub
t_p = Thickness of chain duplex hub
L_c = Chain length
m_1 = Module length of chain
d_1 = Boss diameter
D = Diameter of flange/disc
W_t = Width of slot/tongue
h = Depth of slot/tongue
P_c = Power transmitted by coupling
P_s = Allowable stress between slot/tongue
T_{pipe} = Torque transmitted by hollow pipes
F_{max} = Maximum shear strength of pipe
d_o = outer diameter of PVC pipes
d_i = Inner diameter of PVC pipes
D_p = Design power
C_o = Overload factor
D_{TL} = Design transmitted load
C_v = Velocity factor/dynamic factor
f_b = Bending stress
f = Form factor
y = Shape factor
K_f = Stress concentration factor
m = Distance between the faces of the teeth of sprocket
Z_p = No. of teeth on pinion
d_{pi} = Diameter of pinion
Y = Exact Lewis form factor
F_d = Dynamic load
F_i = Inertial force acting on spun gear
C_f = Correction factor
K_d = Constant for correction factor
e = Permissible error for linear velocity calculation
E_p = Ultimate elastic limit for pinion
E_g = Ultimate elastic limit for gear
f_{cf} = Form correlation factor
F_B = Beam strength for sprocket gear
f_{ef} = Force strength of pitch circle on gear
F_w = Limiting wear load
K_L = Limiting load factor
Q = Q Factor for limiting wear load
f_{es} = Flexural endurance limit
L_w = Length of weld
T_j = Thickness of joint
f_{tw} = Allowable tensile stress for steel under static loading
T_s = Tearing strength of weld
V = Voltage applied to arc welding machine
I = Amperage measured
ɳ = efficiency
F_{normal} = Normal stress
W_w = Weight of walnuts on pipes
a = area of pipes
ρ_b = Bulk density
ρ_t = True density
ρ_f = Fluid density
ϵ = Porosity
D_F = Drag force
D_c = Drag coefficient
A_p = Projected area
N_R = Reynolds No.
V_w = Velocity of walnuts
d_c = Diameter of column
B_F = Bouncy force
μ = dynamic viscosity of water
g = Acceleration due to gravity

Fig. 1 Size based grades of walnuts

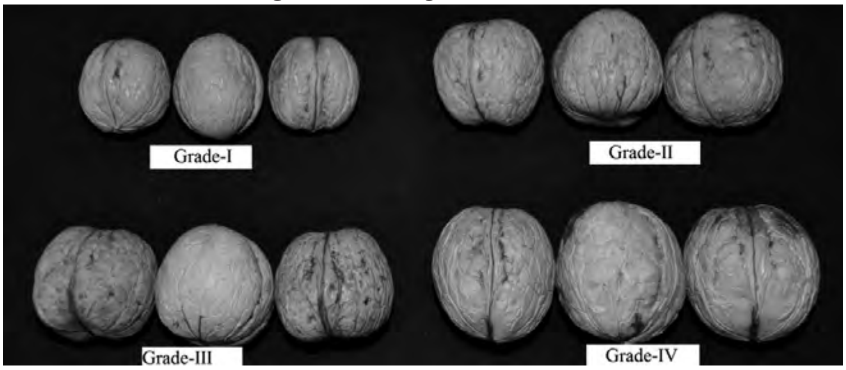

Introduction

Juglans regia L- the English or Persian walnut is one of the most important temperate nuts grown all over the world. In commercial production of Persian walnuts, India ranks seventh in the world. In India, Jammu and Kashmir is major walnut producing State. The State covers an area of 88,900 hectares under walnuts with an annual production of 266,133 MT (Anonymous, 2015).

In Jammu and Kashmir State, there are no regular walnut orchards. Also there are no particularly identified varieties of walnuts grown in the State. The cultivation of walnuts is scattered around home grounds, field bunds, barren lands, road sides and on waste lands. The entire production of walnuts is from seedling trees and each tree behaves as a variety and thus exhibits heterogeneity in size and shape of nuts.

About 90% of the un-shelled walnuts in the State are marketed as mixed lot. These mixed lots are not preferred by the consumers and therefore, fetch less return. Further, the kernels from the mixed lots are also non- uniform in size, which subsequently affects the consumer acceptability. Only 10% of the walnuts are graded manually on the basis of shell colour, thickness and nut size. Manual grading is an expensive and time consuming process and even the operation is affected due to non-availability of labourers during the peak season.

Sensing the aforesaid problems, a need was felt to develop an efficient and economical grader for walnuts. This study extends our previous work in which we have developed and evaluated walnut dehuller (Syed et al., 2016) and walnut bleacher (Syed et al., 2016).

Materials and Methods

During the year 2015, a survey was conducted in the major walnut growing districts of State to identify the dimensional ranges in walnuts. The survey revealed that there is huge variability in walnut size. The length (major diameter) was found in the approximate range of 23-44 mm. Based on the range obtained, walnuts were classified into four grades (**Fig. 1**). Such size characteristics differences are essential criterion to conduct mechanical grading of walnuts. The dimensional, physical, frictional and mechanical properties of walnuts are indispensable properties for designing of size based walnut grading system.

Dimensional Properties

100 walnuts from each grade were selected randomly and major diameter (length), intermediate diameter (width) and minor diameter (thickness) of selected nuts were measured using electronic digital caliper of 0.001mm accuracy. The equivalent diameter, geometric diameter, arithmetic diameter, area of transverse surface, sphericity, surface area, aspect ratio, volume and projected area were calculated from the principal dimensions (L, W, T) using the relationships given by Mohsenin 1980.

Physical Properties

Bulk density and true density of each walnut grade was determined using the standard test weight procedure (Singh and Goswami, 1996) and toluene displacement method (Sacilik et al., 2003) respectively. The porosity was determined using the following equation:

$\epsilon = [1 - (\rho_b / \rho_t)] \times 100$

ρ_b = Bulk density

ρ_t = True density

Frictional Properties

The coefficient of frictions of each walnut grade was measured by a frictional device. Maximum frictional force was recorded when the box started operating. This value was used to calculate the static coefficient of friction. While the box continued to slide on frictional surface, the dynamic coefficient of frictions was determined (Sacilik et al., 2003). Angle of repose was measured by pouring method (Mirzabe et al., 2013).

Mechanical Properties

Bouncy force and drag force are the forces encountered for and against the movement of walnuts. For determining these properties a cylindrical glass column was used. The column was filled with tap water and walnuts were placed in flat position in the bottom of column. In order to determine the velocity, a stop watch was used for recording the time for movement of walnuts from releasing point to top of the water column (Vanoni, 1975). The drag force (D_F) and Bouncy force (B_F) were thus calculated using the following formula:

$D_F = D_C A_p [\rho t (V_W)^2 / 2]$

Where A_P is projected area, ρt is true density of walnut, V_W is velocity of walnuts and D_C is drag coefficient and was calculated as:

$D_C = 24 / N_R$

N_R is Reynolds No. and was calculated as:

$N_R = V_W d_C / \mu$

d_C is diameter of walnuts and μ is dynamic viscosity of water

The Bouncy force (B_F) was calculated as

$B_F = \rho f (g \pi d_C^3 / 6)$

ρf is fluid density and g is acceleration due to gravity

Design, Development and Evaluation of Walnut Grader

A power operated walnut grader was designed and developed by Srinagar Centre of All India Coordinated Research Project on Post Harvest Engineering and Technology (AICRP on PHET), Sher-e-Kashmir University of Agricultural Sciences and Technology of Kashmir, India during the year 2015-16. **Fig. 2** shows different schematic views of the walnut grader.

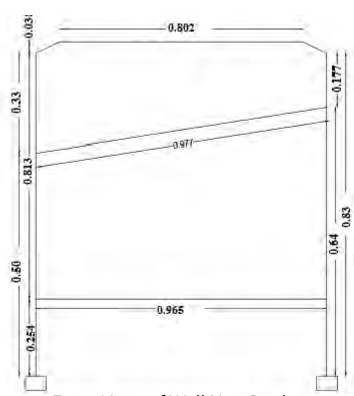

Front View of Wall Nut Grader

Fig. 2 Schematic views of walnut grader (All dimensions in meters)

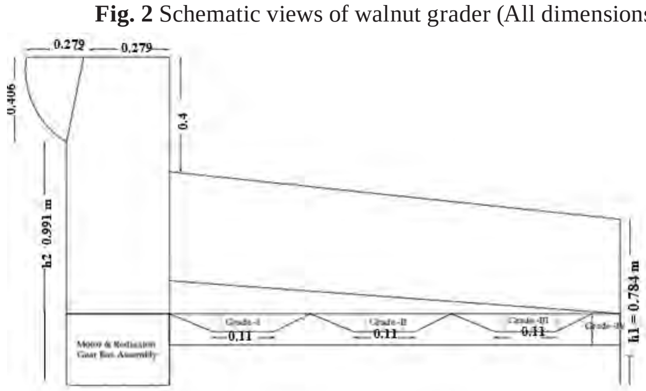

Side View of Wall Nut Grader

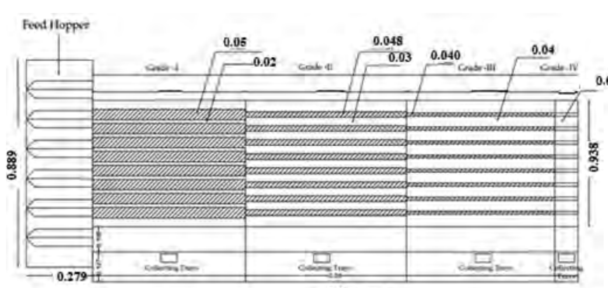

Top View of Wall Nut Grader

Design of Machine Components

In the design, machine parameters that include power requirement, reduction gear, rotating shaft, chain drive, old hams coupling, PVC pipes, chain sprockets, welded joints and stress on inclined pipes due to load were determined as:

Power Requirement

Power requirement of machine (P) was calculated using the equation (Hannah and Stephens, 1984):

$P = 2\pi N_1 T / 60$

N_1 = rotation per minute of motor = 1400 rpm

T = Torque generated by moving parts of 1HP motor used = 5.08 Nm

Therefore, Power requirement (P) = 0.744 kW, which can be easily provided by the 1 hp motor.

Reduction Gears

Reduction gear has a gear ratio of 1/20. The worm gear output (rpm) transmitted to the reduction gear pulley was calculated using the equation (Aaron, 1975):

$N_2 / N_1 = T_1 / T_2$

N_2 = worm gear output (rpm)

Gear ratio (T_1 / T_2).= 1/20

Therefore, rpm of worm gear output (N_2) was calculated as 70

Rotating Shaft

Torsional Moment of Shaft

Torsional moment (M_t) of the shaft was calculated using the equation (Shigley et al., 1983):

$M_t = (9550 / N_1) \times P = 5.08$ kN

Pure Torsional Load on Shaft

Pure torsional load on shaft (F_{PT}) was calculated using the equation (Shigely et al., 1983)

$F_{PT} = (M_t \times 16) / (\pi \times d^3) = 3.23$ MN/m^2

d = diameter of shaft = 0.02 m

Pure Bending Load on Shaft

Pure bending load on shaft (M_b) was calculated using the equation (Shigley et al., 1983)

$M_b = (F_t. \times \pi \times d_3) / 32 = 86.39$ Nm

F_t = ultimate tensile strength of shaft = 110 MN/m^2 (for C- 45 Mild Steel Shaft)

Torsional Deflection Induced in Shaft

Torsional deflection induced in shaft (θ) was calculated using the equation (Norton et al., 1992):

$\theta = (Mt \times L) / (J \times C) = 8.75°$ ($\theta > 0.5°$ indicates that torsional deflection induced in shaft is in safe range)

L = Length of shaft = 2.136 m

C = Modulus of rigidity = 79 × 109 N/m^2 (for M.S Shaft)

J = Polar Moment of inertia (MOI)

J is calculated using the equation $J = (\pi d^4) / 32$

$J = 1.57 \times 10^{-8}$ m^4

Equivalent Bending Moment

Equivalent bending moment (M_{be}) on Shaft was calculated using equation given by (Norton et al., 1992)

$M_{be} = 1/2\ (M_b + \sqrt{M_b^2 + M_t^2})$

M_{be} = 2.55 kNm

Deflection in the Shaft

Deflection in shaft (δlinear) was calculated using the equation Mott (1992)

$\delta linear = WL^3 / 48EI$

W = Weight on shaft due to load (Assume 1 kg walnuts are on the center of shaft during grading)

E = Elastic Limit of Shaft Material = 200 GPa

I = Moment of inertia, is calculated as:

$I = \pi d^4 / 64 = 7.85 \times 10^{-9}$m^4

Thus, $\delta linear = 1.29 \times 10^{-4}$ m

Static Deflection Due to Own Mass of Shaft

Static deflection due to own mass of shaft (δweight) was calculated using the equation (Orthwein,1990)

$\delta weight = 5ML^4 / 384EI$

M = Mass of Shaft per unit Length = area × length × denisty = 5.02×10^{-3} kg

Density of Shaft material = 40 × 103 kg/m^3

Area of cross section of shaft = $\pi d^4 / 4$.

Therefore, δ weight = 8.65×10^{-7} m

Frequency of Transverse Vibration

Frequency of transverse vibration (F_n) is calculated using the equation (Juvinall and Marshek, 1992)

$F_n = 0.4985 / \sqrt{\delta linear + (\delta weight / 1.27)}$

F_n = 43.77 Hz

Assume the whirling speed of shaft (rpm) is equal to the frequency of transverse vibration in Hz.

Therefore, whirling speed of Shaft (N_c) = 43.77 × 60 = 2626.2 rpm

Chain Drive

Velocity Ratio

In order to determine the velocity needed at the output shaft, the velocity ratio (VR) was calculated using equation from (Tonoshenko, 1989).

$VR = N_2 / N_3 = 1.4$

N_3 = Speed of driven Sprocket = N_2 / 1.45 (Tomoshenko, 1989) = 70 / 1.45 = 48.27 ≈ 50 rpm

In order to determine the no. of teeth of driving sprocket, the below mentioned equation (Shigley and Mischkee, 1989) was used

$Z_2 = Z_1 \times VR = 42$ (To be on safer side, value of Z_2 was taken as 48 for design purpose)

Z_2 = No of teeth of driven sprocket

Z_1 = No of teeth of driving sprocket = 30

Shear and torque on shaft

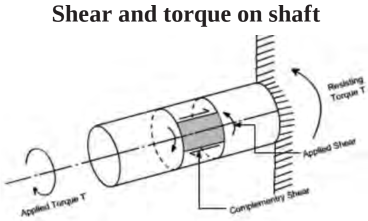

Twist and torque on shaft

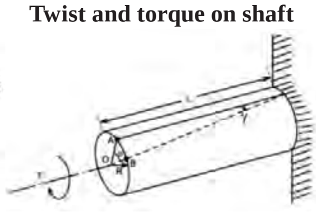

Stress on shaft

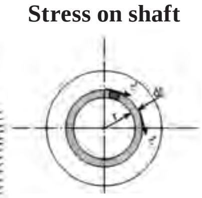

Chain Pitch

Chain pitch (CP) was calculated using the equation (Shigley and Mischkee, 1989)

$C_p = C_d$ / (30 to 60) = 16.9 mm = 0.0169 m (Keeping in view the fabrication constraints value 30 was taken in the denominator)

C_d = Center distance between two sprockets = 0.508 m

Chain Velocity

Chain velocity (V) was determined by equation given by (Shigley and Mischkee, 1989).

$V = (C_p \times N_2 \times Z_1) / (60 \times 1000) = 5.915 \times 10^{-4}$ m/sec

Total Load on Driving Chain

Total load on driving chain (F) was determined by equation given by (Shigely and Mischkee, 1989).

$F = (P \times 1000) / V = 1261.2$ kN

Shearing Force on Chain

Shearing force on chain (F_s) was calculated using equation given by (Shigely and Mischkee 1989).

$F_s = (W_{breaking\ load} \times 1000) / F_0$

$W_{breaking\ load}$ = Breaking load strength of chain = 45.40 kN

F_0 is force load on chain element

$F_0 = 1820 + F_c + F_f = 1857.63$ N

F_f = frictional force on chain element = $K \times W_{duplex\ chain} \times C_d$ = 36.98 N

K = Lubricating constant = 4 k (Design procedure)

$W_{duplex\ chain}$ = 18.2 (constant)

F_c is tearing force acting on chain

$F_c = (W_{duplex\ chain} \times V^2) / g$ (Ertas and jones, 1992) = 6.49×10^{-7} N

Therefore, FS = 24.43 N

$F_s > 11$ indicates that design is safe. Hence chain 10B was used

Check for Wear

Check for wear (PB) in chain was determined by equation given by (Arora, 1989)

$P_B = (F \times K_w) / Ac = 12.25$ kN/mm^2 which is within the safe limits

K_w = wear constant for chain = $K_1 \times K_2$ = 1.3 (For periodic lubrication of chain $K_1 = 1.0$, $K_2 = 1.3$)

A_C = Area of chain = $d_p \times l_b \times 2$ (Arora, 1989) = 133.81 mm^2

d_p = duplex chain distance = 5/16 × C_P = 5.28 m = 5.28×10^{-3} m

l_b = length of chain duplex hub = $b_t + 2t_p$ = 12.672 mm

b_t = width of chain duplex hub = 5/8 × C_P = 10.56 mm

t_p = Thickness of chain duplex hub = 0.1 × b_t = 1.056 mm

Chain Length

Length of chain (L_C) was determined using the equation (Khurmi and Gupta, 2004)

$L_C = m_1 \times C_P = 1679.57$ mm^2

m_1 = Module length of chain = $(2C_d / C_P) + (z_1 + z_2) / 2 + CP(z_2 - z_1)^2 / 4\pi^2 \times C_d$ = 99.38 mm

Oldhams Coupling

Oldhams flexible coupling was used to connect motor drive to the reduction gear box drive. As per the design considerations, following parameters were determined.

Boss Diameter (d_1) = 2d = 40 mm = 0.04 m

Diameter of flange/Disc (D) = 3d to 4d = 80 mm = 0.08 m

(4d was taken in order to have safe stress and high torque transmission)

Width of slot/tongue (wt) = 0.45d = 9 mm = 0.009 m.

Depth of slot/tongue (h) = wt/2 = 0.0045 m

Power transmitted by the coupling (P_c) was calculated using the equation (Raimond and Boyd, 1985)

$P_C = (Ps(D)^2hN) / 57 = 6012.63$ kW

p_s = Allowable stress between slot/tongue = 8.5 N/mm^2

PVC Pipe

Torque transmitted by hollow pipes (T_{pipes}) was calculated using equation (Hall et al., 1999):

For Grade-I

$T_{pipes} = 3.14/16\ F_{max} \times (d_o^4 - d_i^4) / d_o$ = 1.24 kNm

d_o = Outer diameter of PVC pipes (0.05 m)

d_i = Inner diameter of PVC pipes (0.02 m)

f_{max} = Maximum Shear Strength of pipe =52 MPa (PVC material)

For Grade-II

d_o = 0.048m

T_{pipes} = 1.092 kNm

For Grade-III

do = 0.040 m

$T_{pipes} = 61 \times 10^{-2}$ kNm

Chain Sprockets

Design power (D_p) was calculated by equation given by (Shighley and Mischkee, 1989):

Design Power (D_p) = $P \times C_o$ = 0.9325 kW

C_o = Overload factor taken as 1.25 for machines with light shock production and moderate transmission

Design transmitted load (D_{TL}) = (D_p × 1000) / Linear velocity of chain (V) = 157.65 kN

Velocity factor or Dynamic factor $C_v = 4.5 / (4.5 + V) = 0.998$

Using Lewis Equation

$D_{TL} = (f_b \times f \times m \times y \times c_v) / k_f$

m = 0.0268 m = 26.8×10^{-3} m (For safety of design, 4 mm module was taken for sprocket)

f_b = Bending stress = 140 MPa (for cast steel)

f = Form factor =10 m (as per design procedure)

y = Shape factor =0.25 (as per design procedure)

K_f = Stress Concentration factor = 1.6 for 14(1/2)° teeth

m = Distance between the faces of the teeth of sprocket

No. of teeth on pinion (Z_p) was calculated as

$Z_p = d_{pi}/m = 38 \approx 42$ (for safety precaution)

d_{pi} = Diameter of pinion = 0.15 m

Exact value of Lewis form factor (Y) for sprocket was determined:

$Y = \pi(0.124 - 0.684 / Z_p)$

Y = 0.338

Checking for Dynamic Load (F_d) by Buckingham's Equation

$F_d = D_{TL} + F_i$ = 15772.78N = 157.72 kN

F_i = Inertial force acting on spur

gear = $[21V(C_f \times f_{cf} + D_{TL})] / [21V + \sqrt{}C_f \times f_{cf} + D_{TL}] = 78.78$ N

C_f = Correction factor = $K_d \times e / (1/E_p + 1/E_g) = 1056.09$ MN/m

$K_d = 0.107$ for 14(1/2)º teeth, e = permissible error for linear velocity calculation = 0.094

Since the material for pinion and gear is same, hence $E_p = E_g$ = ultimate elastic limit of material = 210 GPa.

f_{cf} = form correlation factor lies between 9.5 module to 12.5 module (Module = 4) = 9.5 × 4= 38 mm = 0.038 m

Beam Strength for Sprocket Gear

Beam Strength for sprocket gear (F_B) was determined as:

$F_B = f_{ef} \times f_{cf} \times m \times Y = 8990.8$ N

f_{ef} = Force strength of pitch circle of gear, (forged steel C-30) = 175 MPa with BHN = 150

Value of F_b which is less than Fd which implies that gear will not fail.

Checking for Wear

Wear of gear sprocket (F_w) was calculated using equation given by Shigely and Mischkee (1989)

The limiting wear load

$F_w = d_{pi} \times f_{cf} \times K_L \times Q = 1258.73$ N

d_{pi} = diameter of pinion=0.15 m

K_L = limiting load factor and calculated as:

$K_L = [(f_{es}^2 \times \sin\theta) / 1.4] (1/E_p + 1/E_g) = 208.33$ kN/m^2

f_{es} = flexural endurance limit = 2.8 × BHN – 70 = 350 MPa

Sin θ = sin 14.5° = 0.25 (Spur gear has helix angle of 14.50)

Q factor was calculated as:

$Q = 2Z_2 / (Z_2 + Z_p) = 1.06$

Therefore, $F_w = 1258.73$ N

Value of F_w is less than Fd value, which indicates that sprocket will wear. Therefore it will be necessary to heat treat the sprocket. Hence C-40 was used as sprocket material due to its high strength.

Welded Joints for Grader

Electric arc welding was used to weld the main frame and other moving component. The necessary length of weld was calculated using the equation given by (Buceli and Beganaru, 1980)

$L_w = M_t / (0.7 \times T_j \times f_t) = 2.07$ mm ≈ 3 mm

T_j = Thickness of Joint = 3.175 cm

As per design procedure factor 12.5 is to added to each weld

Therefore, Length of welded joint = 3 + 12.5 = 15.5 mm

Tearing strength of weld was calculated as:

$T_s = 0.7 \times T_j \times L_w \times 2 \times F_{tw} = 0.7 \times 0.317 \times 222.5 \times 2 \times 110 = 75{,}787.25$ N

Energy/Power Consumption During Welding

Voltage applied to arc welding machine = 26 volts

Amperage measured by ampere meter= 75.5 ampers

Power consumed = V × I = 1963 W

Heat input to work piece = power × η = 1.66 kW (η = 85%)

η = efficiency of machine

Stress on Inclined Pipes Due to Load W

Stress on inclined pipes due to load was determined using equation given by (Appelle, 1941)

Normal stress (F_{normal}) = $W_w \sin 2\theta / a$

Considering an average weight of 50 kg walnuts remain at a time on the surface of pipes (W_w) Area of pipes (unit area). Grader inclination was tested at 8º, 12° and 16º.

(F_{normal}) at 8º slope = 50 × sin2(8) = 13.7 kg/m^2

(F_{normal}) at 12º slope = 50 × sin2(12) = 20.33 kg/m^2

(F_{normal}) at 16º slope = 50 × sin2(16) = 26.49 kg/m^2

The force is acting on 8 pipes

Thus, $F_{(normal)}$ on individual pipes at 8º, 12º and 16º slope = 1.722, 2.54 and 3.31 kg/m^2 respectively which is very well within the yield strength and ultimate strength of PVC/MS shaft

Shear Stresses (FShear) = $W_w \cos 2\theta / a$

Therefore, Fshear on individual pipes at 8°, 12° and 16° slope= 6.00, 5.71 and 5.30 respectively, which is again within safe range

Electric Motor Specifications

For providing driving force to the machine, a single phase 1 hp, AC motor having a rotational speed of 1400 rpm and power rating of 240 V AC, 50 Hz was used. In order to limit the overload current in minimum time, type C MCB with rated amperage of 32 A and short circuit breaking capacity of 1 kA was used in the grader.

Machine Descriptions

The main features of the machine are casing, rotating shaft, chain drive, delivery chutes and control box (**Fig. 3**). Keeping in mind the availability, durability, cost, maintenance and ease of constructions, the material was selected for construc-

Fig. 3 Pictorial view of walnut grader

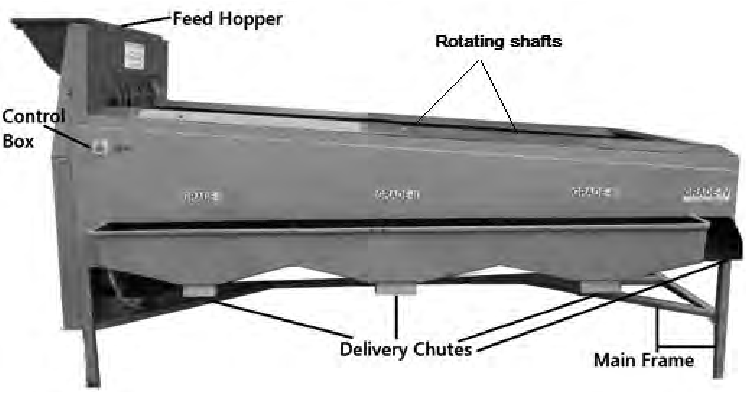

tion of different components of machine. The materials of construction and machine specification details are given in **Table 1**.

Casing forms the outer rigid structure of the machine and prevents the shocks, vibrations and direct contact of moving parts of the machine with the workers. Feed hopper is rectangular in shape with edges narrowing towards downside. For efficient grading system, the hopper has 6 triangular protruding gyrations which allow the walnuts to fall between the pipes. For comfortable feeding the height of the feed hopper has been kept as 4.2 feet above the ground. The motion to the pipes is transmitted by means of chain and sprocket mechanism. Two sprockets (reduction gear sprocket and shaft sprocket) were used to transmit power from reduction gear to rotating shaft. As soon as the walnuts leave the hopper, they fall over the slanting rotating pipes. The pipes rotate at a speed of 70 rpm. Due to the rotation of pipes the walnuts roll downwards and as they reach a distance where the inter-pipe distance is more than the walnut size, they fall down by gravity action and are discharged through delivery chutes. For easy operation of machine, a provision of control box having necessary indicator and a motor switch for controlling the motor has been made in the machine.

Performance Evaluation

The grader was tested to study the effect of grader slopes (80, 120 and 160) and feed rates (400, 700 and 1000 kg/h) on grading efficiency. A known sample weight of 100 kg of walnuts comprising of all grades was fed to the machine for each parameter combinations. The walnuts coming out through four outlet chutes of the machine were collected and under/oversized walnuts from each grade were separated and weighed for determining the grading error on weight basis.

Statistical Analysis

Analysis of variance of the data was performed by SPSS 11.0. All the data are means of triplicate assays, unless otherwise mentioned. The least significance test at 5% level of significance was used to test the difference among the mean values (Steel et al., 1997).

Results and Discussion

Dimensional, Frictional and Mechanical Properties of Walnuts

The dimensional, physical, frictional and mechanical properties of walnut grades are depicted in **Table 2**. All the dimensional properties (equivalent diameter, geometric diameter, arithmetic diameter, area of transverse surface, sphericity, surface area, aspect ratio, volume and projected area) followed an increasing trend from grade-I (very small) to grade-IV (extra-large). Sphericity range 88.92 to 93.0% indicates that all the four walnut grades can be considered as spherical shaped. Physical properties such as (bulk density and true density), frictional properties (coefficient of static friction, dynamic friction and angle of repose) and mechanical properties (drag force and bouncy force) showed an increasing trend from grade-I to grade-IV, whereas, porosity showed a decreasing trend. The

Table 1 Material of construction and brief specification of the machine

A. Material of Construction

Sl. No	Component of machine	Material used	Purpose of material selection
1	Feed hopper	Mild Steel sheet (16, 18 gauge), angle iron 1.25 inch square	Stiffness and rigidity
2	Casing	Galvanized Iron (GI Pipes 1.25 inch square)	Rigidity, strength and vibration absorption.
3	Rotating Pipes	PVC made with silver coating, Inside shaft (dia 20 mm) made of mild steel	Light weight with reduction friction, strength
4	Delivery Chutes	Mild Steel (16, 18, 22 gauge), carpet cloth.	Stiffness, rigidity and noise absorption
5	Sprockets	Stainless steel	Better performance, corrosion resistance
6	Driving chain	Industrial chain	Better power transmission
7	Foundation pads	Rubber	Vibration and noise absorption
8	Electrical components	Conducting and insulating material	Electrical transmission and safety of operator

B. Brief Specification of Machine

1	Over all dimensions of machine, Length = 2.186 m, Breadth = 1.066 m, Height at feeding end (h1) = 1.397 m, Height at trailing end (h2) = 0.784 m
2	**Power source**: 1 Hp single phase, AC induction Motor
3	**Hopper**: Length = 0.279 m, Width at Top = 0.889 m, Width at bottom = 0.1016 m, Height = 0.406 m
4	**Casing**: Length = 2.186 m, Breadth = 0.938 m, Height at feeding end (h1) = 1.397 m, Height at trailing end (h2) = 0.784 m
5	**Pipes**: **Grade I**: Outer diameter (D_0) = 0.05 m, Inner diameter (D_i) = D_i = 0.02 cm **Grade II**: Outer diameter (D_0) = 0.048 cm, Inner diameter (D_i) = 0.02 cm **Grade III**: Outer diameter (D_0) = 0.040 cm, Inner diameter (D_i) = 0.02 cm
6	**Delivery Chutes**: Length = 2.159 m, Breadth = 1.092 m, Height = 0.2286 to 0.381 m, Inclination of delivery chutes, Θ = 300
7	**Drive Mechanism**: Chain drive

porosity is a function of bulk density and true density. The increase in bulk density and true density was about 1.24 and 1.06 folds from grade-I to grade-IV respectively. Therefore the increase in true density might have a lower effect on porosity than that of bulk density. The increasing trend of true density from grade-I to grade-IV was reflected in bouncy force as well. The larger walnuts displace more fluid which leads to the increased value of bouncy force. The drag force values also showed an increasing trend from grade-I to grade-IV. The reason behind could be the increase in surface area from grade-I to grade-IV. The large surface area offers more drag (resistive force) to the motion of walnuts. The increase in coefficient of friction (static and dynamic) from grade-I to grade-IV may be due to the reason that larger size walnuts offer a higher cohesive force on the surface of contact. Overall the recorded values of static/dynamic coefficient of friction were much lower than one, which indicates that no wearing of rotating shafts will take place due to friction. Further keeping in mind that material to be handled during grading is in-shelled walnuts, thus friction will no way affected the quality of kernels. The increase in angle of repose from grade-I to grade-IV could be possibly due to the reason that large size walnuts create a large surface layer, which helps in holding the walnuts together by producing higher surface tension.

These investigations on dimensional, physical, frictional and mechanical properties of walnuts helped in designing of walnut grader. This information will also be useful for design and development of walnut handling/processing machines in the near future also. Values of most of the properties were found slightly different than the ranges reported by various researchers for whole walnuts (Ebubekir and Mehmet, 2010; Ragab et al., 2011 and Hossein et al., 2012). Such dissimilarity in values can be due to the reason that there are no recognized varieties of walnuts in Jammu and Kashmir. The entire production of walnuts is from seedling trees and each tree behaves as a variety and thus exhibits heterogeneity in walnut characteristics.

Table 2 Dimensional, physical, frictional and mechanical properties of walnut grades

Properties	Grade-I	Grade-II	Grade-III	Grade-IV
Eq. diameter (mm)	≤21.57	>21.57 - ≤28.30	>28.30 - ≤35.00	>35.00
Geometric diameter (mm)	≤22.23	>22.23 - ≤29.26	>29.26 - ≤36.27	>36.27
Arithmetic diameter (mm)	≤22.23	>22.23 - ≤29.33	>29.33 - <36.33	>36.33
Sphericity (%)	≤88.92	>88.92 - ≤91.43	>91.43 - <93.00	>93.00
Surface area (mm^2)	≤1,551.70	>1,551.70 - ≤2,688.30	>2,688.30 - <4,130.71	>4,130.71
Aspect ratio	≤0.88	>0.88 - ≤0.90	>0.90 - <0.92	>0.92
Volume (mm^3)	≤5749	>5,749 - ≤13,109.9	>13,109.9 - <24,970.1	>24,970.1
Projected area (mm^2)	≤431.79	>431.79 - ≤728.48	>728.48 - ≤1,102.14	>1,102.14
Bulk density (kg/m^3)	≤245.09	263.36 - 264.70	288.30 - 289.10	≥303.92
True density (kg/m^3)	≤735.29	764.70 - 766.29	773.29 - 775.18	≥784.31
Porosity (%)	≥66.66	65.38 - 65.63	62.70 - 62.71	≤61.25
Coefficient of static friction	≤0.190	0.197 - 0.210	0.224 - 0.245	≥0.257
Coefficient of dynamic friction	≤0.220	0.231 - 0.243	0.250 - 0.260	≥0.274
Angle of repose (º)	≤37.21	43.50 - 45.26	49.36 - 53.54	≥58.12
Drag force (N)	≤20.50	22.71 - 25.19	27.45 - 41.42	≥72.26
Bouncy force (N)	≤0.056	0.056 - 0.128	0.128 - 0.24	≥0.24

Grades	Length (mm)	Width (mm)	Thickness (mm)
Grade-I (very small)	≤25	≤22	≤20
Grade-II (small)	>25 - ≤32	>22 - ≤29	>20 - ≤27
Grade-III (large)	>32 - ≤39	>29 - ≤36	>27 - ≤34
Grade-IV (extra large)	>39	>36	>34

Performance Evaluation of Walnut Grader

The data regarding the grading errors at different treatment combinations depicted in **Table 3** reveals that feed rate, grader slope and opening size had significant effects ($p \leq 0.05$) on grading error. A decreasing trend was observed in grading error with the decrease in feed rate. Highest mean grading error (13.18%) was recorded at highest test feed rate of 1000 kg/h, whereas least grading error of 3.70% was recorded at lowest feed rate of 400 kg/h. With the decrease in slope, the grading error was found to decrease. Highest mean grading error (12.80%) was recorded at 160 slope and the least (6.55%) at 80 slope. The increase in grading error with the increase in feed rate and grader slope could be justified by the reason that higher feed rate blocks the grader openings and higher slope causes walnuts to roll down at higher velocities, due to which some small size walnuts drop through large openings. These results are in concomitance with the findings reported by various researchers in mechanical sorting/grading of food materials (Shyam et al., 1979 in potato sorting; Devries et al., 1997 in Soybean separation; Syed et al., 2002 in raw mango grading and Muhammad et al., 2007 in apple grading). The grading error was found significantly decreased with the increase in opening size from feeding end to trailing end. Highest grading error of 11.14% was observed in O_1 (10-25 mm) near the feeding end and least (7.22%) in O_3 (32-39 mm) near the trailing end. This could be due to the reason that torque transmission decreases from O_1 (1.24 kNm) to O_3 (61×10^{-2} kNm). The perusal of the results clearly shows that 8º grader slope and 400 kg/h feed rate were most appropriate machine parameters to achieve maximum mean grading efficiency (96.3%) and least grading error (3.70%).

Conclusions

Keeping in view the requirements of walnut growers/processors of India, particularly Jammu and Kashmir, locally available raw material and ease of operation a power operated walnut grader was developed and tested. The effective throughput capacity of the machine (337 kg/h) is much better than the existing manual grading capacity of 15 kg/person/h. Besides, mechanical interventions can solve the boredom, drudgery and other constraints associated with the manual size grading of walnuts. Performance of the grader was evaluated for grading error, occurred during the operation. The highest grading efficiency (96.3%) was obtained at 8º grader slope and 400 kg/h feed rate. This study also concludes with some information on engineering properties of walnuts grown in the State which may be useful for further designing of equipment/machinery for walnut processing in future.

Conflict of Interest

The authors report no conflict of interest.

Acknowledgement

Authors acknowledge the funding support of All India Coordinated Research Project on Post Harvest Engineering and Technology (AICRP on PHET), Indian Council of Agricultural Research (ICAR) New Delhi and are grateful to Prof. Nazeer Ahmed, Vice Chancellor, Sher-e-Kashmir University of Agricultural Sciences & Technology of Kashmir (SKUAST-K) and Dr. S. N. Jha, Assistant Director General Agricultural Engineering (ICAR) for supporting the Investigation.

REFERENCES

Aaron. 1984. Shigleys Mechanical Engineering Design, New York; 9th edition; Mc Graw Hill Series in Mechanical Engineering.

Anonymous. 2015. Physical Progress Report. Department of Horticulture, Planning and Marketing, Govt. of J & K.

Apelle. 1941. Shigleys Mechanical Engineering New York, 9th edition, Mc Graw Hill Series in Mechanical Engineering.

Arora. 1989. Design machine elements New York, Tata Mc Graw Hill publication.

Buceli and Beganaru. 1980. Machine Design, New York, Mc Graw Hill Publishing Ltd.

Devries, H. C. P., P. J. Rijpmal and J. E. S. Owaa. 1997. Development of separator for soybean. Agricultural Mechanization in Asia, Africa and Latin America, 28(1): 40-42.

Ebubekir A. and E. Mehmet. 2010. Physical properties of shelled and kernel walnuts as affected by the moisture content. Czech. Journal Food Science 28(6): 547-556

Ertas and Jones. 1992. Design of Chain Elements for Mechanical Links, New York, Mc Graw Hill Publications.

Hall, H. M. 1999. Machine Design, New York, Pearsons Publishing Ltd.

Hannah and Stephens. 1984. Shigley is Mechanical Engineering Design; New York, 9th edition; Mc Graw Hill series in Mechanical Engineering.

Hossein, H. A. A., G. Iman and H. Roya. 2012. Determination of physical properties of two walnut genotypes. International Research Journal of Applied and Basic Sciences. 3(6): 1203-1209.

Table 3 Average grading error (%) values at different machine parameters for walnut grading

Slope	F_1 (400 kg/h)				F_2 (700 kg/h)			
	O_1 (10-25 mm)	O_2 (25-32 mm	O_3 (32-39 mm	Mean	O_1 (10-25 mm)	O_2 (25-32 mm	O_3 (32-39 mm	Mean
S2 (8º)	2.93	2.59	2.16	2.56	9.07	7.51	6.51	7.69
S3 (12º)	4.07	3.36	3.11	3.51	10.61	8.42	6.66	8.56
S4 (16º)	6.40	5.40	3.35	5.05	20.76	15.49	11.45	15.90
Mean	4.46	3.78	2.87	3.70	13.48	10.47	8.20	10.71
Slope	F_3 (1000 kg/h)				Mean			
	O_1 (10-25 mm)	O_2 (25-32 mm	O_3 (32-39 mm	Mean	O_1 (10-25 mm)	O_2 (25-32 mm	O_3 (32-39 mm	Mean
S2 (8º)	2.93	2.59	2.16	2.56	9.07	7.51	6.51	7.69
S3 (12º)	4.07	3.36	3.11	3.51	10.61	8.42	6.66	8.56
S4 (16º)	6.40	5.40	3.35	5.05	20.76	15.49	11.45	15.90
Mean	4.46	3.78	2.87	3.70	13.48	10.47	8.20	10.71

C.D ($P \leq U$ 0.05)
S (Slope) = 0.2911, F (feed rate) = 0.2911, S × F = 0.5042, O (openings) = 0.2911, S × O = 0.5042, F × O = 0.5042, S × F × O = 0.8734

Juvinall and Marshek. 1992. Design of machine components, New York, Mc Graw Hill.
Khurmi and Gupta. 2004. Theory of Machines New Delhi, S. Chand Publications.
Mizrabe, A. H., J. Khazaei, G. R. Chegini and M. H. Amir Pour Rostami Nejad. 2013. Determination of some physical properties of virgin olive fruits. Agricultural Engineering Int: CIGR Journal 15(1): 201-210.
Mohsenin, N. N. 1980. Physical Properties of Plants and Animal Materials. New York: Gordon and Breach Science Publishers.
Muhammad, A., S. S. Muhammad, A. Manzoor and Y. Muhammad. 2007. Design, development and performance evaluation of fruit and vegetable grader. Pakistan Journal of Agriculture Science. 44(4): 704-713.
Orthewein. 1990. Mechanical Design Element, New York, Mc Graw Hill.
Ragab, K., P. Zhongli, G. Atungulu Griffiths, F. Thompson James and S. Dongyan. 2011. Size and moisture distribution characteristics of walnuts and their components. Food Bioprocess Technology. DOI 10.1007/S11947-011-0717.1.
Raimand and Boyd. 1985. Shighleys Mechanical Engineering, New York, 9th edition, Mc Graw Hill series in mechanical engineering.
Robert L. Norton. 1992. Machine Design an Integrated approach: 2nd edition: Dorling Kindersly (India), New York Pvt. Ltd.
Sacilik K, R. Ozturk and R. Keskin. 2003. Some physical properties of hemp seed. Biosytems Engineering 86(2): 191-198.
Shighley and Mischkee. 1989. Shighley's Mechanical Engineering Design, New York, 9th edition, Mc Graw Hill Series in Mechanical Engineering.
Shighley and Nisbett. 1983. Shigleys Mechanical Engineering Design, New York; 9th edition; Mc Graw Hill Series in Mechanical Engineering.
Shyam, M., V. Singh and R. Singh. 1979. Studies on sorting of potatoes into different size grades by mechanical sieving. Journal of Agricultural Engineering 16(3): 115-120.
Singh, K. K. and T. K. Goswami. 1996. Physical properties of cumin seed. Journal of Agricultural Engineering Research 64: 93-98
Steel, R. G. D., J. H. Torrie and D. A. Dricky. 1997. Principles and procedures of statistics: A biometrical Approach, 3rd edition Mc Graw Hill Book Co., New York, USA.
Syed, Z. H., A. Tehmeena, A. H. Rather and H. R. Naik. 2016. Development of walnut dehulling machine and assessment of its performance using ethephon and tween-80 as pretreatment for hull loosening. Journal of Food Science Technology 53(6): 2835-2843.
Syed, Z. H., A. Tehmeena, A. H. Rather, H. R. Naik and I. Sheikh. 2017. Design fabrication and evaluation of walnut bleacher. Journal of Food Process Engineering 40: 3. DOI10.1111/JFpe.12462.
Syed, Z. H., S. C. Mandhar and S. Javare Gowda. 2005. Evaluation and performance of raw mango grader 3(2): 46-48.
Tomoshenko. 1989. Elements of Engineering, Japan.
Vanoni, V. A. 1975. Sedimentation Engineering. ASCE Manual 54. New York, ASCE.

■■

Single Locking Cotton Feeder for Enhancing Ginning Efficiency of Double Roller Gin

by

V. G. Arude
Scientist (FMP)
ICAR- Central Institute for Research on Cotton Technology,
Mumbai-400 019
INDIA
arudevg@gmail.com

S. P. Deshmukh
Professor
Institute of Chemical Technology
Mumbai-400 019
INDIA

P. G. Patil
Director
ICAR- Central Institute for Research on Cotton Technology,
Mumbai-400 019
INDIA

S. K. Shukla
Sr. Scientist (Mech. Engg.)
ICAR- Central Institute for Research on Cotton Technology,
Mumbai-400 019
INDIA

Abstract

Single locking cotton feeder was designed and fabricated with an aim to maintain constant feeding rate of individual locules at the ginning point of Double Roller (DR) gin. It comprises of a pair of feed roller, spiked cylinders, grid, feeder hopper and distributor chute. Spiked cylinder has spikes, its tips were spaced closer to the feed rollers than the thickness of a lock of cotton. The spiked cylinder travel at a greater linear speed than the feed rollers, whereby cotton bolls held between the feed rollers are struck by the spikes of spiked cylinder, thus ensuring single locking of cotton. The effect of single locking of cotton on ginning efficiency of DR gin was studied. Extent of unlocking was determined by measuring the change in bulk density of cotton before and after passing through the feeder which decreased with increase in spike cylinder speed. DR gin output was found to increase by 15-20% with use of single locking feeder as compared to conventional feeding system comprising of auto-feeder and micro-feeder. Cotton quality was also found to improve in terms of colour grade. Single locking feeder observed to be highly useful for Indian cotton ginneries.

Keywords: single locking, feeder, cotton, double roller gin, ginning

Introduction

Cotton is an important commercial crop of India and about 338 lakh (33.8 million) bales of cotton were produced during 2016-17. More than 95% of the cotton produced in India is ginned on Double Roller (DR) gins. The output capacity of DR gins is very low as compared to the Saw gins and Rotary Knife Roller gins which are mostly used in USA, Brazil and China. The output capacity of DR gin ranges from 40-90 kg lint/h depending on the length of the gin machine. The capacities of commercially available Saw gins range from 500-1000 kg lint/h and that of Rotary Knife Roller gin is about from 400-450 kg lint/h. Quality of the cotton ginned on DR gins is better than that of Saw gins (Sharma, 2014). Despite of this, DR are gins are less preferred across the world except in India and some African counties, the main constraint for its wide spread adoption is its low production capacity.

The DR gins are modified on varioua aspects to increase the ginning efficiency which is mainly governed by lint output, lint quality and eneergy conssumption (Patil et al., 2007). The manufacturers of DR gins have developed improved versions of DR gin by increasing roller length from 1,065 to 1,525 mm with an increase in output from 40 to 90 kg lint/h. Improvements are carried out in the material of construction in parts such as beater shaft, knives, gears, connecting rod and eccentric shaft to increase working life of parts and to reduce the downtime due to unexpected breakdown. In an effort to increase the productivity of DR gin, the gear box of the gin is modified to have the roller and beater drives de-linked and were driven independent of each other. This modifiction is referred as ‘Variablle Speed DR gin’. The speed variations of roller and beater are possible for diferent staple cotton to get better quality and productivity (Patil et al., 2003). Self grooving rubber roller was developed to increase the gin productivity and roller life and also to reduce the drudgery of grooving operation associated with the leather roller. These modifications improved working efficiency of the DR gin to some extent.

The efficiency of DR gin in terms of output primarily depends upon the roller speed, beater speed, setting and adjustments, machine condition, moisture content, staple length and trash content in the cotton and cotton feeding mechanism used over the DR gin. Type of feeder plays an important role in deciding the ginning efficiency. The Indian ginneries mostly use auto-feeder in combination with micro-feeder and screw conveyor as feeding system. Commonly encountered problems in auto-feeder are frequent stoppages, feeding of seed cotton in lumps, non-uniform feeding to beater of DR gin, falling of seed cotton outside the DR gin, damage to cloth belts, shifting of belt cloth to one side and seeds coming out of lower portion of hopper. In this systems of feeding, flow rate is often erratic. Feeding becomes difficult due to entanglement and difficult to maintain the optimum feed rate to DR gin. Ginning efficiency of the DR gins gets affected significantly due to these problems. To improve ginning efficiency, careful attention needs to be given to improve the feeding system.

Efficient ginning is achieved on gin machinery with constant and uniform flow rate and uniform of seed cotton. Feeder output must be uniform and steady. The primary function of the feeding device is to feed seed cotton to the gin machine precisely. Seed cotton feeding should be limited to that which is essential to ensure smooth and trouble free ginning in order to obtain optimum bale value (Antony, 1994).

It is necessary to modify and restructure feeders, in order to get efficient ginning with enhanced capacity of DR gin. The efficiency of DR gin can be enhanced by replacing the conventional method of cotton feeding comprised of micro-feeder and auto-feeder with a new concept of feeding individual locules of seed cotton at the ginning point. This principle of single locking of seed cotton is employed in Saw and Rotary Knife Roller gins to achieve the efficient ginning with the desired gin capacity and bale value. Saw and Rotary Knife Roller gins employ extractor feeders to feed seed cotton in single locks uniformly to the gin stand at controllable rates. Feed rollers of the extractor feeder control the feed rate of seed cotton to the gin. It provides even flow of seed cotton to the knife edges of rotary gin and saw tips in saw gins (Lummus, 2003). Single locking of seed cotton ensures controlled feed rate and increases the production capacity with the increased bale value (Baker et al., 1994).

Development of single locking feeder especially for DR gin would help to eliminate the flaws in the existing ginning process and would help in improve the ginning efficiency. It is expected to increase the ginning efficiency in terms of increased output, controlled feed rate, increased ginning percentage, improved grade of lint and yarn, reduced downtime, wastage and contamination. The developed feeder would be useful for ginning machinery manufactures, cotton ginners to understand how the gin feeder affects the overall performance of the ginning machine which would enhance profits of growers and ginners.

Materials and Methods

Spike cylinder type single locking cotton feeder cum cleaner was designed at ICAR-Central institute for Research on Cotton Technology, Mumbai by using standard design methodology and procedure. Each subassembly and its individual component were designed by selecting the appropriate materials so as to achieve the intended function effectively. Two and three dimensional drawings of each machine component and subassembly were prepared using AUTOCAD. The prototype of the designed feeder cum cleaner was fabricated and its performance was evaluated. The effect of single locking of cotton on ginning efficiency of DR gin was studied by evaluating the performance of the prototype in terms of degree of unlocking of cotton bolls, cleaning efficiency, energy consumption and output capacity of DR gin and quality of ginned lint. Extent of unlocking was determined by measuring change in bulk density of cotton before and after passing through the feeder.

The developed prototype was mounted on the commercial double roller gin with roller length of 1,360 mm. The spike cylinder speed was varied from 100-500 rpm with the help of variable frequency drive. Long staple cotton with 2.5% span length of about 30 mm was processed during testing. The moisture content of the cotton varied from 5-9%. The Clamp on Power Meter (CW240) manufactured by Yokogawa, Japan was used for measurement of energy consumption. The fibre quality parameters were measured on High Volume Instrument (HVI) and Advanced Fibre Information System (AFIS). The trash analyser was used to measure the trash content.

Principle of Working

Seed cotton is fed through feed roller assembly. Spiked cylinder has spikes, its tips were spaced closer to the feed rollers than the thickness of a lock of cotton. The spiked cylinder travel at a greater linear speed than the feed rollers, whereby bolls of cotton momentarily held between the feed rollers are struck by the spikes, thus ensuring single locking of cotton. The individual locules so formed are passed over and between the spike cylinders and the grid underneath. Foreign matter gets dislodged from the cotton by the agitating and scrubbing action of the cylinders and falls through grid. The trash gets accumulated in the trash chamber. The individual locules are carried forward by the centrifugal action of the spike cylinder and dropped into the distribution chute mounted below the feeder. The distribution chute equally distributes the cotton in the form of a continuous matt on either side of the beater of the DR gin. Fibres adhere to the ginning roller of DR gin and are carried in between the fixed knife and the roller such that the fibres are partially gripped between them. The oscillating motion of the beater beats the seeds and separates the fibres. This process gets repeated for each individual locule thus ensuring the ginning of the cotton (**Fig. 1**)

Results and Discussion

Single locking cotton feeder cum cleaner (**Fig. 2**) was designed with an aim to maintain constant and optimum feeding rate of individual locules to ensure locule feeding exactly at the ginning point across the knife edges of double roller gin. The designed feeding mechanism replaces the micro-feeder and auto-feeder of conventional feeding system.

Design and Fabrication

Spike cylinder type single locking cotton feeder cum cleaner was designed and fabricated (**Fig. 3**). Feeding mechanism comprises of a pair of feed roller, pair of spiked cylinders and grid bar housed in a feeder hopper, chute for cotton distribution on either side of the beater of DR gin and power drive arrangement.

Feed Roller Assembly

The function of the feed roller assembly is to regulate the supply of seed cotton to the spike cylinders in a controlled manner at a rate in synchronization with the capacity of the DR gin. Feed roller assembly (**Fig. 4**) comprises of a pair of counter rotating fluted rollers with roller length of 1,283.5 mm. The main components of feed roller are shaft, flats, driving and driven pin. Six number of 40 × 3 mm M.S. flats are mounted on the periphery of the shaft at an equal angular spacing of 600. The overall diameter of the feed roller is 124.5 mm. The 16 mm clearance is maintained between the tips of the flats of two counter rotating feed rollers. The feed rollers are driven by 30W DC motor (24 V and 1.5 A). Variable frequency drive and voltage control drive is used to vary the speed of feed rollers.

Spike Cylinder Assembly

The primary function of the spike cylinders is to ensure the unlocking or single locking of the seed cotton bolls and the secondary function is to remove the foreign matter from the seed cotton. It consists of a pair of spiked cylinders. Each cylinder (**Fig. 5**) comprises of shaft, cylinder, spikes and centre plates. The cylinder with 1,283.5 mm length and 228.6 mm diameter is made out of sheet metal. The overall dimeter of the cylinder with the spikes is 279.4 mm. Altogether 200 spikes are mounted in zig zag pattern in eight rows over the periphery of cylinder. The spacing of 50 mm is maintained between the two spikes. The 10 mm clearance is maintained between the tips of spikes of two cylinders. The spike cylinders are driven by 2 hp, 1,440 rpm electric motor. Variable frequency drive is used to vary the speed of the cylinders.

Grid Assembly

The function of the grid is to ensure further unlocking of seed cotton by agitating and scrubbing action between spikes and its surface. The dislodged foreign matter falls through

Fig. 1 Schematic diagram of spike cylinder single locking cotton feeder with DR gin

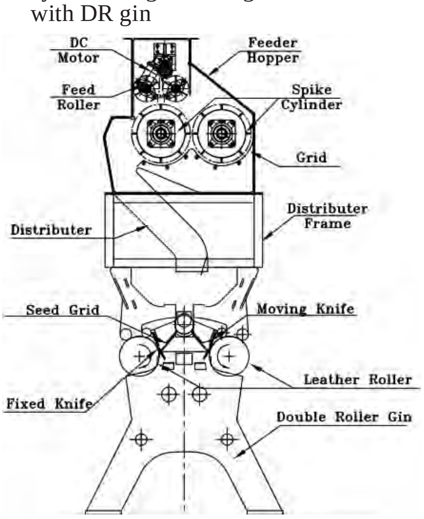

Fig. 2 Schematic diagram of spike cylinder single locking cotton feeder

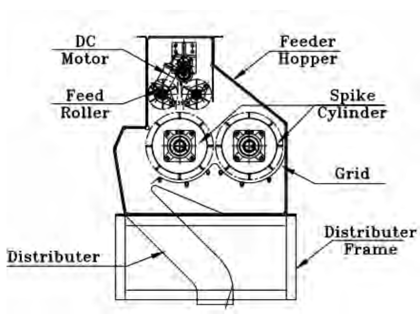

Fig. 3 Prototype of spike cylinder single locking cotton feeder

Fig. 4 Feed roller

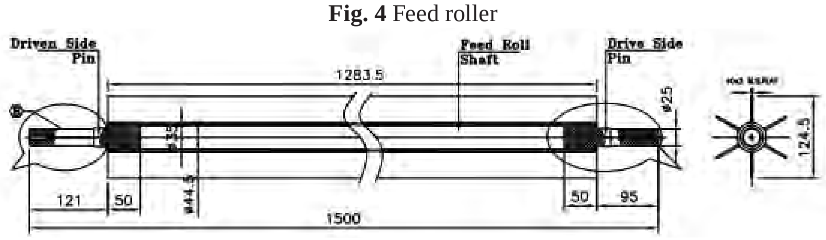

Table 1 Specifications of spike cylinder single locking cotton feeder

Particulars	Values
A. Feed roller assembly	
1. Length of feed roller (mm)	1,283.5
2. Number of flats on each feed roller	6
3. Feed roller diameter (mm)	124.5
4. DC motor power to drive feed rollers (W)	30
5. Feed roller speed (rpm)	1-5
B. Spike cylinder assembly	
1. Cylinder length (mm)	1,283.5
2. Spike length (mm)	25.0
3. Cylinder diameter with spikes (mm)	279.4
4. Number of spike rows on cylinder	8
5. Spike to spike distance in a row (mm)	50
6. Power to drive spike cylinder (hp)	2
7. Spike cylinder speed (rpm)	100-500
C. Grid assembly	
1. Sieve mesh size (mm)	11.2
2. Sieve wire diameter (mm)	1.6
3. Grid concave radius (mm)	150
D. Feeder hopper assembly	
1. Length (mm)	1,300
2. Top width (mm)	277
3. Bottom width (mm)	671
4. Height (mm)	739
E. Distributor chute assembly	
1. Distributor chute width (mm)	250
2. Distributor chute length (mm)	1,283.5
3. Frame Size (mm)	1,300 × 749 × 353

Table 2 Optimum setting and adjustments for spike cylinder single locking cotton feeder

Settings and adjustments	Values
1. Minimum tip to tip clearance between the flights of two feed rollers when diametrically aligned	16 mm
2. Maximum tip to tip clearance between the flights of two feed rollers while moving in opposite direction	31 mm
3. Tip to tip clearance between spikes of two spike cylinders when diametrically aligned	10 mm
4. Clearance between tip of feed roller flight and tip of spike cylinder	12 mm
5. Clearance between tip of spike cylinder and grid	12 mm

the grid openings. The concave shape grid assembly (**Fig. 6**) with radius of 150 mm is made out of a square wire mesh of sieve size 11.2 mm with sieve wire diameter of 1.6 mm. Grid assembly is mounted below the spike cylinder assembly. Provision is made to vary clearance between the tips of spike on cylinder and the grid in the range of 12-20 mm.

Fig. 5 Spike cylinder

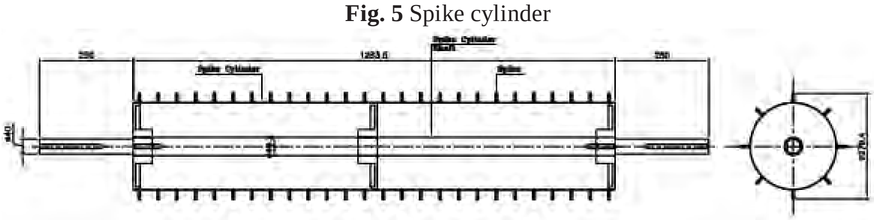

Fig. 6 Grid

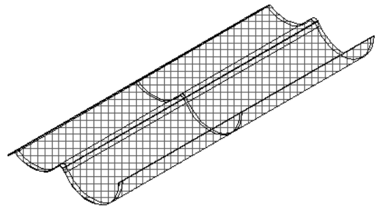

Feeder Hopper

The feeder hopper (**Fig. 7**) is designed to house all the three assemblies, namely, feed roller, spike cylinder and grid. The hopper is provided with suitable inlet to receive the seed cotton and an appropriate outlet to deliver the unlocked and cleaned seed cotton to the distributor mounted below it. The grid assembly is mounted underneath the spike cylinders. The trash chamber is provided below the grid to collect the trash obtained during cleaning operation. A sliding window is provided in the hopper to remove the trash manually. The overall dimensions of the feeder hopper are 1,300 × 671 × 739 mm.

Distributor Chute

It is designed to receive the unlocked cotton from the feeder hopper outlet to convey and drop it evenly along the length and on either side of the beater of DR gin. The distributor chute is attached to the outlet lower of the feeder hopper. It is fitted in a rectangular angle iron frame of size 1,300 × 749 × 353 mm.

The specifications of the developed prototype of the spike cylinder type of single locking feeder cum cleaner are shown in **Table 1**.

Fig. 7 Feeder hopper

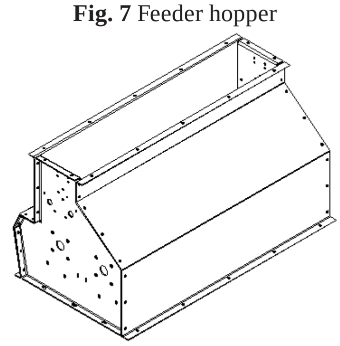

Performance Evaluation

The prototype of single locking feeder cum cleaner was set and adjusted to the settings as depicted in **Table 2**. A view of DR gin with single locking feeder cum cleaner in operation is shown in **Fig. 8**. The designed mechanism comprising of pair of feed rollers and spike cylinders and gird was found to unlock the cotton bolls to individual locules to the desired extent. The developed prototype successfully opened the lumps of seed cotton and unlocked bolls to individual locules. The principle on which the prototype was designed i.e. to ensure single locking of cotton bolls and to deliver the individual locules to the ginning point of DR gin was found to work satisfactorily. The desired unlocking of cotton bolls was obtained that resulted in efficient ginning on DR gin. Single locking was evidenced by decrease in bulk density of the cotton.

Bulk density was found to decrease with the increase in the speed of spike cylinders. Bulk density found to decrease by 10-30% with increase in cylinder speed from 200-400 rpm. Output of the DR gin was found to increase by 15-20% with use of single locking feeder cum cleaner as compared to the conventional feeding system comprising of auto-feeder and micro feeder. The increase in output may be attributed to opening of lumps of cotton, removal of entanglements within the boll and individualisation of fibres adhering the cottonseed. Unlocking increased the surface area of cotton thereby more number of fibres came in contact and adhered to the ginning roller in the given time. The energy consumption of the feeder was found to vary between 0.18-0.25 kW/h for the speeds ranging from 200-400 rpm (**Table 3**).

Cotton quality improved in terms of colour grade which is evidenced from the reduction in trash content, increase in degree of reflectance and reduction degree of yellowness. Improvement in colour grade may be due to unlocking of cotton bolls and removal of trashes. The prototype successfully removed fine trashes, leaf bits, dust etc. The cleaning efficiency was found to vary from 20-30 % depending on the initial condition of the cotton. The degree of whiteness was found to increase by 5-10% whereas the degree of yellowness found to decrease by 5-10%. The other quality parameters such as fibre length, strength and micronaire remain unaffected.

Table 3 Performance evaluation of spike cylinder single locking feeder in comparison to conventional feeder

Parameters	Values
1. Increase in capacity of double roller gin (%)	15-20
2. Degree of unlocking in terms of decrease in bulk density (%)	10-30
3. Cleaning efficiency (%)	20-30
4. Increase in energy consumption (%)	5-7
5. Increase in degree of whiteness (Rd) of lint (%)	5-10
6. Reduction in degree of yellowness (b+) (%)	5-10

Conclusions

Spike cylinder type single locking cotton feeder cum cleaner was observed to be successful for single locking of cotton bolls that resulted in enhancing the ginning efficiency of double roller gin. The output of the double roller gin with the use of single locking feeder was found to increase by 15-20%. The fibre quality of the cotton processed using feeder was improved in terms of reduction in trash, improved whiteness and reduction in degree of yellowness. With the above advantages, the single locking feeder would be highly useful for Indian cotton ginneries.

REFERENCES

Antony, W. S. 1994. Overview of ginning process. Cotton Ginners Handbook, United States Department of Agriculture (USDA), Agricultural Handbook, 503, 43-46.

Baker, R. V., W. S. Antony and R. M. Sutton. 1994. Seed cotton cleaning and extracting. Cotton Ginners Handbook, United States Department of Agriculture (USDA), Agricultural Handbook, 503, 69-71.

Lummus Corporation. 2003. Rotomatic roller gin feeder. Service Manual, M/s. Lummus Corporation. Savannah. (USA).

Patil, P. G. and P. M. Padole. 2003. Double roller cotton ginning machine, its drawback and possible modification. Proceedings of 11th National Conference on Machines and Mechanisms (NaCOMM-2003), IIT, Delhi, pp: 745-749.

Patil, P. G., P. M. Padole, J. F. Agrawal and A. B. Dahake. 2007. Effect of roller speed and moisture content of cotton on ginning rate, lint quality and electric energy consumption in double roller gins. Textile Research Journal, 77, 9, 635-644.

Sharma, M. K. 2014. Advances in cotton ginning technology in India during 2010-2013. Book of papers, National Seminar on "Advances in Cotton Ginning and Testing Technology" organized by Indian Fibre Society (IFS) and CIRCOT, Mumbai, India. ■■

Fig. 8 A view of DR gin with spike cylinder single cotton locking feeder in operation

Development and Testing of a Coconut Dehusking Machine

by
P. M. Chukwu
Department of Agricultural and
Bio-Resources Engineering,
Federal University of Agriculture Abeokuta,
Abeokuta, Ogun State, NIGERIA
promisechukwu3@gmail.com

B. A. Adewumi
Department of Agricultural and
Bio-Resources Engineering,
Federal University of Agriculture Abeokuta,
Abeokuta, Ogun State, NIGERIA

I. A. Ola
Department of Agricultural and
Bio-Resources Engineering,
Federal University of Agriculture Abeokuta,
Abeokuta, Ogun State, NIGERIA

O. D. Akinyemi
Department of Physics,
Federal University of Agriculture Abeokuta,
Abeokuta, Ogun State, NIGERIA

Abstract

Nigeria is well known for its annual production of coconut which amounts to over 265,000 tons/year. Dehusking of coconut has been done manually through the use of machete. Due to the difficulty involved in dehusking coconut using the manual method, there is the need to mechanize its operation by developing an indigenous coconut dehusking machine. The machine comprises of rollers with spikes, chain drive, gears, electric motor, bearings, shaft, speed reduction gear box and sprockets.The machine performed best using a local variety of coconut having an average moisture content of 5.08% (d.b.) to give an average machine capacity and percentage throughput of 175 coconut/h and 84%, respectively.

Keywords: Coconut, Moisture Content, Diameter, Dehusking, Capacity, Throughput

Fig. 1 Coconut and its parts

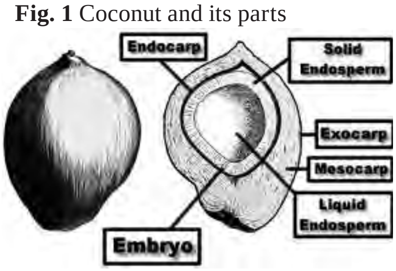

1. Introduction

Coconut is known widely for its culinary and non-culinary uses. Nigeria is the 19th largest coconut producer with an annual production of 265,000 tons and has room for great improvements on its productions due to the availability of vast lands and arable soils in the tropics (FAOSTAT, 2014). There are many methods of dehusking coconut (Abi and Jippu, 2014); manually, mechanically and sometimes with the use of automated machines. Manual dehusking with the use of machete is the most common method of dehusking coconut in Nigeria. There is need to improve on the method of dehusking coconut in Nigeria as the manual method mostly used is somehow unsafe, uncomfortable and uneconomical. Though, there exist some coconut dehusking machines that have been designed and developed in some Asian countries that are still facing one challenge or the other such as high cost of importing this machinery into the country, unreliability of these machines for use with our local variety of coconut, unavailability of these machines in the commercial market, etc. Based on these problems, there is need to design and develop an indigenous coconut dehusking machine that will easily dehusk coconut in order toincrease its productivity and encourage investment in this area. **Fig. 1** shows the pictorial view of the coconut and its parts.

2. Materials and Methods

2.1 Design of Machine Parts

2.1.1 Main Frame

The mainframe of the machine was made up of 50 mm by 50 mm mild steel angle iron. The length, width and height of the mainframe were 440 mm, 440 mm and 700 mm, respectively.

2.1.2 Diameter of Shaft

The shaft diameter was determined using the expression given by Khurmi and Gupta (2005) as:

$$d^3 = 5.1 / \tau_{max}\sqrt{(K_bM_b)^2 + (K_iT)^2} \quad (1)$$

where,

M_b = Maximum bending moment (Nm)

T = Torque (Nm)

τ_{max} = Maximum shear stress (N/m^2)

d = Diameter of shaft (m)

K_b = Bending moment factor

K_i = Torque factor

The shaft diameter was calculated to be 35 mm.

Table 1 Experimental design

Factor 1 (M)	Factor 2 (D)	Replicates				
M_1	D_1	$M_1D_1R_1$	$M_1D_1R_2$	$M_1D_1R_3$	$M_1D_1R_4$	$M_1D_1R_5$
M_1	D_2	$M_1D_2R_1$	$M_1D_2R_2$	$M_1D_2R_3$	$M_1D_2R_4$	$M_1D_2R_5$
M_1	D_3	$M_1D_3R_1$	$M_1D_3R_2$	$M_1D_3R_3$	$M_1D_3R_4$	$M_1D_3R_5$
M_2	D_1	$M_2D_1R_1$	$M_2D_1R_2$	$M_2D_1R_3$	$M_2D_1R_4$	$M_2D_1R_5$
M_2	D_2	$M_2D_2R_1$	$M_2D_2R_2$	$M_2D_2R_3$	$M_2D_2R_4$	$M_2D_2R_5$
M_2	D_3	$M_2D_3R_1$	$M_2D_3R_2$	$M_2D_3R_3$	$M_2D_3R_4$	$M_2D_3R_5$
M_3	D_1	$M_3D_1R_1$	$M_3D_1R_2$	$M_3D_1R_3$	$M_3D_1R_4$	$M_3D_1R_5$
M_3	D_2	$M_3D_2R_1$	$M_3D_2R_2$	$M_3D_2R_3$	$M_3D_2R_4$	$M_3D_2R_5$
M_3	D_3	$M_3D_3R_1$	$M_3D_3R_2$	$M_3D_3R_3$	$M_3D_3R_4$	$M_3D_3R_5$

Where,
M = moisture content of the husk, D = diameter of the coconut and R = replicates.
Likewise, M_1 = 60.40%, M_2 = 30.02%, M_3 = 5.08%; D_1 = 109.8 mm, D_2 = 159.0 mm and D_3 = 198.1 mm.

2.1.3 Drive Mechanism

The drive mechanism of the machineincludes electric motor, speed reduction gear, sprockets, chains and gears.

2.1.3.1 Electric Motor

A. Power Required to Dehusk Coconut

The power required to dehusk coconut is expressed as:

$$P = 2\pi NT / 60 \quad (2)$$

where,

P = Power generated (W)

N = Speed of rotation (rpm)

T = Torque (Nm)

The torque was further expressed as:

$$T = F \times r \quad (3)$$

where,

T = Torque required to dehusk coconut (Nm)

F = Force (N)

r = Perpendicular distance from force to the point of load (m)

The force required to dehusk coconut, according to Alonge and Adetunji (2011), is 6 kN. By considering a perpendicular distance of 0.1 m and an average speed of 20 rpm, therefore, the torque and power required to dehusk coconut can be calculated as follows:

$T = 6000\ N \times 0.1\ m = 600\ Nm$

$P = (2\pi \times 20 \times 600) / 60 \approx 1257\ W$ (1.68 hp)

B. Power Required to Rotate Mass (Transmission)

Total mass acting on the rotating shaft = Mass of gears + mass of cylinders and spikes + mass of sprocket = 5.64 kg + 17.72 kg + 3.02 kg = 26.38 kg

Force = mass × acceleration due to gravity = 26.38 × 10 = 263.8 N

Torque = Force × perpendicular distance from force to the point of load = 263.8 × 0.1 = 26.38 Nm

Power to rotate mass = $2\pi NT / 60 = (2\pi \times 20 \times 23.7) / 60 = 55.26$ W = 0.074 hp

Therefore, the total power required to operate the machine = 1.68 hp + 0.074 hp = 1.754 hp

A 2 hp electric motor is suitable to operate the machine.

C. Design for Speed of Sprockets

Velocity ratio = $N_1 / N_2 = T_2 / T_1$ (Khurmi and Gupta, 2005) (4)

where,

N_1 = Speed of the small sprocket (rpm)

N_2= Speed of the large sprocket (rpm)

T_1 = Number of teeth on the small sprocket

T_2 = Number of teeth on the large sprocket

Fig. 2 Orthographic projection of the machine (All dimensions in mm)

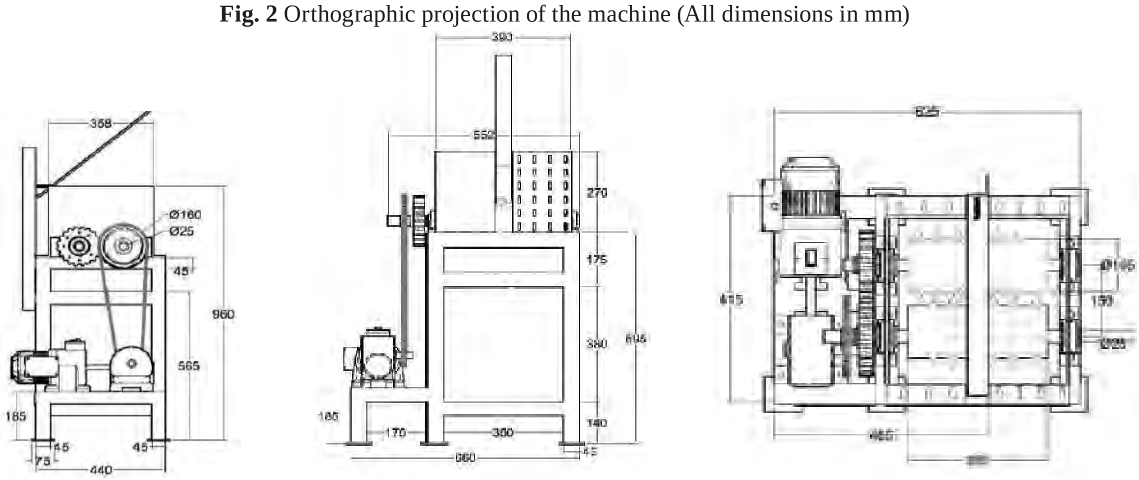

Table 2 Diameter of coconut

S/N	Small (mm)	Medium (mm)	Large (mm)
1	111.1	158.2	178.2
2	124.0	157.5	199.3
3	115.2	160.2	200.8
4	109.2	161.4	199.2
5	113.0	157.8	205.7
6	109.0	161.0	180.6
7	103.0	159.4	185.8
8	116.1	148.5	179.5
9	108.0	156.8	193.7
10	107.2	159.3	196.2
11	106.6	160.3	210.2
12	112.2	158.1	205.4
13	105.1	159.2	189.7
14	106.7	160.1	246.3
15	100.6	167.2	200.4
Av.	109.8	159.0	198.1
Std. dev	23.13	3.80	16.70

Table 3 Moisture content (d.b.) of coconut husk

Category	Replicates						
	*M.C.1 (%)	M.C.2 (%)	M.C.3 (%)	M.C.4 (%)	M.C.5 (%)	Avegare (%)	Standard deviation
Wet	60.3	63	58	61.2	59.5	60.40	1.87
Fairly Dry	30.8	35.4	29.1	30.5	24.3	30.02	3.91
Very Dry	8	5	1.5	4.5	6.2	5.08	2.45

* Moisture content

Substituting the values of T_1 = 19, T_2 = 39, N_1 = 40 rpm into (4), N_2 = 20 rpm

D. Length of Chain

The expression for thelength of chain is given by Khurmi and Gupta (2005) as:

$L = K \times P$ (5)

where,

L = Length of chain (mm)

K = Number of chain links

P = Pitch of the chains (mm)

But

$K = [(T_1 + T_2) / 2] + [2x / P] + [(T_2 - T_1) / 2\pi]^2 P / x$ (Khurmi and Gupta, 2005) (6)

where,

T_1 = Number of teeth on the small sprocket

T_2 = Number of teeth on the large sprocket

P = Pitch of the chain (mm)

x = Centre distance (mm)

Given T_1 = 19, T_2 = 39, N_1 = 40 rpm, N_2 = 20 rpm, x = 280 mm, P = 25 mm

By substituting into equation (6), K = 52.31

By substituting K into equation (5), L = 1307.8 mm = 1.3 m

2.1.3.2 Speed Reduction Gear Box

The gear box is made up of worm gears whose primary function is to reduce the speed from the electric motor. Its reduction ratio is 36: 1. Italso has chain and sprockets attached to it to further reduce its speed to 20 rpm. The selection of the motor is based on the speed the shaft is required to rotate. **Fig. 2** shows the orthographic view of the machine while **Fig. 3** shows the isometric view of the machine.

Fig. 3 Isometric view of the machine

2.2 Operation of the Machine

The machine is made up of rollers with spikes welded unto them. The speed of rotation is low in order to produce the desired torque needed to dehusk the coconut. A coconut is placed between the rollers when in operation. Once the coconut is in contact with the spikes, the spikes penetrate the husk of the coconut and tears it off thereby leaving the coconut. The machine is shut off in order to retrieve the coconut. This operation is carried out one after the other. The handle of the coconut is used to hold the coconut in place. The electric motor is provided with a switch that is usedfor controlling the on and off of the machine during operation. **Fig. 4** shows the pictorial view of the fabricated machine.

Fig. 4 The fabricated machine

2.3 Testing Procedures

Tall local coconut variety was harvested and used in testing the machine. The coconuts were categorized according to their average moisture content and diameter. The capacity and percentage throughput of the machine were used to evaluate the machine performance.

2.4 Experimental Design

Table 1 shows the experimental design of two factors at three levels each with five replicates.

3. Results and Discussion

3.1 Coconut Diameter and Husk Moisture Content

The average diameters obtained for small, medium and large size of un dehusked coconuts as shown in **Table 2** were 109.8 mm, 159.0 mm and 198.1 mm, respectively. The average moisture content (dry basis) obtained for wet, fairly dry and very dry coconut husk as shown in **Table 3** were 60.40%, 30.02% and 5.08%, respectively.

3.2 Machine Capacity and Percentage Throughput

It can be deduced from **Table 4** that the experiment which consist of two factors (moisture content and coconut diameter) at three levels eachwith five replicates, recorded an average machine capacity and percentage throughput of 45 coconut/h and 48%, respectively, when tested with coconut having an average moisture content of 60.40% (d.b.). When the machine was tested with coconut having an average moisture content of 30.02% (d.b.), the average machine capacity and percentage throughput obtained were 97 coconut/h and 64%, respectively. Likewise, when the machine was also tested with coconut having an average moisture content of 5.08% (d.b.), the average machine capacity and percentage throughput obtained were 175 coconut/h and 84%, respectively. The result obtained showed a sign of improvement over the machine developed by Nwankwojike et al. (2012) which gave a machine capacity of 79 coconut/h which could be as a result of the type of coconut variety used in testing the machine.

3.3 Effects of Moisture Content of Husk and Diameter of Coconut on Machine Capacity

The results obtained from the Analysis of Variance (ANOVA) are presented in **Table 5**. It can be deduced from **Table 5** that moisture content of husk had significant effect on the machinecapacity at $p \leq 0.05$ while the diameter of coconut had no significant effect on the machine capacity at $p \leq 0.05$. The interaction between the moisture content of huskand diameterof coconuthadsignificant effect on the machine capacity at $p \leq 0.05$.

3.4 Regression Analysis

Two models were developed using regression analysis to predict the capacityand percentage throughput of the machine. The twoequations generated were:

$$C = 0.18D - 2.34M + 151.72 \quad (7)$$

$$T = 0.92D - 6.45M + 71.77 \quad (8)$$

where,

M = Moisture content of the coconut husk (%)

D = Diameter of the coconut (mm)

C = Capacity of the machine (coconut/h)

T = Percentage throughput of the machine (%)

The model generated for predicting the capacity of the machine as shown in Equation (7) has a R-squared value of 0.774. Equation (7) simply shows that an increase in the diameter of coconut will increase the machine capacity. But an increase in the moisture content of the husk will decrease the machine capacity.

The model generated for predicting percentage throughput of the machine as shown in Equation (8) has a R-squared value of 0.978. In the case of Equation (8), an increase in the diameter of coconut will increase the percentage throughput of the machine whereas an increase in the moisture content of the coconut husk will decrease the percentage throughput of the machine. Having determined the value of the moisture content and diameter of the coconut, these equations can be used to predict the capacity and percentage throughput of the machine.

3.5 Effect of Moisture Content on the Throughput and Capacity of the Machine

During machine testing, the coconuts that were completely broken or shattered were mostly coconuts hav-

Table 4 Experimental results obtained with two factors and five replicates

Average moisture content (%)	Average diameter content (mm)	Replicates: Time taken (s) to dehusk the replicates					Average (s)	Capacity (coconuts/h)	Throughput (%)
60.40	109.8	45	47	39	49	60	48	56	43
60.40	159.0	80	70	72	90	60	74.4	43	48
60.40	198.0	90	120	85	70	60	85	38	54
							Average	45	48
							Std. dev	9.29	5.50
30.02	109.8	30	32	28	38	33	32.2	89	62
30.02	159.0	28	29	30	22	27	27.2	102	66
30.02	198.0	25	28	27	27	28	27	102	66
							Average	45	48
							Std. dev	9.29	5.50
5.08	109.8	18	19	17	17	16	17.4	141	78
5.08	159.0	10	11	13	10	9	10.6	193	87
5.08	198.0	11	13	10	11	8	10.6	193	87
							Average	45	48
							Std. dev	9.29	5.50

Table 5 ANOVA result for the effect of moisture content of husk and diameter of coconut on machine capacity

SV	SS	Df	MS	F	Sig.
M	25,232.933	2	12,616.467	152.803	.001
D	525.733	2	262.867	3.184	.053
M * D	3,345.733	4	836.433	10.130	.001
Error	2,972.400	36	82.567		
Total	32,076.800	44			

Key: M = Moisture content of husk, D = Diameter of coconut

ing the husk average moisture content values of 60.40% and 30.02% (d.b). These categories of coconuts fall under the small coconut size that had an average diameter of 109.8 mm. This led to the increase in the number of broken coconut as the machine was unable to dehusk the coconut fed into the machine. The percentage weight loss in throughput was mostly due to the breakages obtained.The percentage weight loss in throughput was also because some fibers were trapped in the machine and couldn't be recovered. The exocarp of the fairly dry coconut were not very strong to withstand the impact of the spikes when the husk have been removed. This also led to breakage of some of the coconuts. The electric motor had a switch in order to switch off the machine once a coconut is de-husked and retrieved. A delay in the switching off of the machine after dehusking of the coconut is another possible cause for the spikes on the rollers to penetrate the endocarp of the coconut, thereby causing the breakage of the coconut.

It is important as well to state that the space between the rollers played an important role in the dehusking of coconut as it was observed that the larger coconuts did not easily break because they had less space between the rollers compared to the coconuts of smaller sizes which easily got in between the rollers and were shattered during the process.

In order to obtain a good result, the machine needs to be operated with a very dry coconut that has an average moisture content of 5.08% (d.b.). This will improve the machine capacity and as well reduce the percentage loss in the throughput of the machine.

Fig. 5 shows the pictorial view of a broken coconut sample obtained during testing operationof the machine. **Fig. 6** shows the pictorial view of a completely de-husked coconut obtained from the machine during its performance evaluation as **Fig. 7** shows the pictorial view of the coconut husk.

4. Conclusions

A coconut dehusking machine was designed, constructed and evaluated. It was discovered during machine testing that the machine performed well when a coconut with an average moisture content of 5.08% was used for dehusking to give an average machine capacity and percentage throughput of 175 coconut/h and 84%, respectively. The machine was designed in a simple way such that it is made available to our local farmers in Nigeria at an affordable price. One person can easily operate the machine. This research work has been able to meet its objectives by reducing the energy expended during dehusking of coconut through the use of machete. This will definitely improve coconut production in Nigeria.

REFERENCES

Abi, V. and J. Jippu. 2014. A review of coconut husking machines. International Journal of Design and Manufacturing Technology. Volume 5, Issue 3, September - December (2014), pp 68-78.

Alonge, A. F. and Adetunji, W. B. 2011. Properties of Coconut (CocosnuciferaL.) Relevant to its Dehusking. Journal of Agricultural Science and Technology A 1 (2011) 1089-1094.

Food and Agriculture Organization, 2014. Nigeria: Coconuts, Production Quantity (tons) http://www.factfish.com/statistic-country/nigeria/coconuts,+production+quantity (Dec. 2014).

Khurmi, R. S. and J. K. Gupta. 2005. A Textbook of Machine Design (S.I. Units), Eurasiapublishing House (PVT) Ltd., Ram Nagar, New Delhi.

Nwankwojike B. N., O. Onuba and U. Ogbonna. 2012. Development of Coconut Dehusking Machine for Rural Small Scale Farm Holders. International Journal of Innovative Technology and Creative Engineering, 2(3): 1-7.

Fig. 5 Broken Coconut

Fig. 6 Completely De-husked coconut

Fig. 7 Coconut husk

Maize Ear Threshing - an Experimental Investigation

by
Yang Liquan
School of Mechanical and Electrical Engineering,
Henan Agricultural University,
(Collaborative Innovation Center of Henan Grain Crops)
Zhengzhou 450002, CHINA
lqyoung@henau.edu.cn

Wang Wanzhang*
School of Mechanical and Electrical Engineering,
Henan Agricultural University,
(Collaborative Innovation Center of Henan Grain Crops)
Zhengzhou 450002, CHINA
*Correspondence author: wangwz@henau.edu.cn

Zhang Hongmei
School of Mechanical and Electrical Engineering,
Henan Agricultural University,
Zhengzhou 450002, CHINA

Wang Meimei
School of Mechanical and Electrical Engineering,
Henan Agricultural University,
Zhengzhou 450002
(School of Mechanical Engineering, Anyang Institute of Technology, Anyang 455000)
CHINA

Hou Mingtao
School of Mechanical and Electrical Engineering,
Henan Agricultural University,
Zhengzhou 450002, CHINA

Abstract

Corn harvesting has been the bottleneck of maize scale production in the Huang-Huai-Hai Plane. The factors affecting the harvesting of maize grain are as follows: the biomechanical properties of maize and the technical parameters of harvesting machinery. In this study, it has been described that how a threshing system was established on a set of tangential flow-transverse axial flow. The grain damage rate was selected as the target of this experimental study, and the target's variations were investigated with respect to the biological characteristics of maize. The threshing tests were carried out to determine the effect of the main biological factor, that is, the moisture content of grains. Thereafter, the primary technical parameters were defined for the peripheral velocity of the threshing drum. The feed amount was kept economical at 2.6 kg·s^{-1}, while the threshing clearance was maintained 36 mm when corn ears with an average diameter in this study. When the moisture content was below 28%, the threshing capacity of the tangential flow drum was similar to that of the axial flow drum. When the moisture content was more than 28%, the threshing capacity of the tangential flow drum decreased significantly. When the moisture content was 24-26% and the peripheral velocity of the axial flow threshing drum was 17.28 m·s^{-1}, the minimum value of the grain broken rate of the threshing system was minimum, with an average value of 1.7%.

Keywords: maize ear, threshing system, grain damage rate, moisture content, drum peripheral velocity

Introduction

The Huang-Huai-Hai Plane is the main grain-producing area in China. The most farmers cultivate wheat and maize as rotational crops each year. During the corn harvest season, the corn matures but the water content remains higher in these grains. The grain damage rate is higher with mechanized harvesting. Climate, planting system, agronomic growth, etc. are some of the factors governing the efficiency of mechanized harvesting[1, 2], which in turn seriously impacts the quality and safety of the corn produce[3-5]. The harvesting process consists of three stages: picking, drying, and threshing. This approach of harvesting fails to adapt the developments of corn industry, because labor and economic costs are the primary reasons that are restricting the proliferation of conven-

Fig. 1 Maize threshing test system

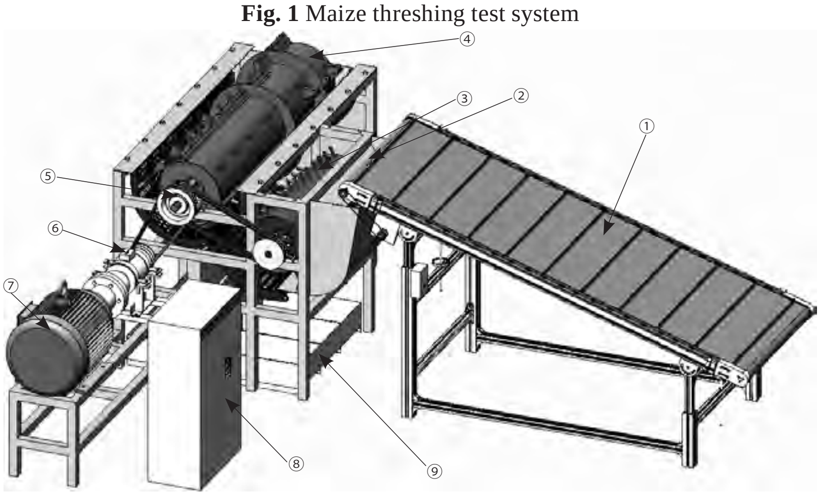

1. Feeding device, 2. Feeding port, 3. Tangential flow drum, 4. Axial flow drum, 5. Grid grating, 6. Torque speed sensor, 7. Motor, 8. Electrical control cabinet (inverter), 9. Grain collection box

tional harvesting. Recently, efforts have been made to ensure that the low corn damage rate is achieved despite carrying out mechanized grain harvest in the Huang-Huai-Hai area. The empirical model of these efforts has not yet been developed; therefore, it is needed to further investigate whether grain harvesting and collection of corn germplasm can be achieved with a heterosis model in this region [6].

With respect to the corn crop, the most important performance indicators of combine harvester threshing system are as follows: grain damage rate, threshing loss rate, and impurity rate; these parameters are affected by factors, such as bioaccumulation of grain, moisture content, feed amount of material, peripheral velocity of threshing drum, threshing clearance, etc. During the process of threshing, the machine has to overcome frictional forces between grains and the adhesion force between the cob and grains; the magnitude of the adhesion force depends on the moisture content and the position of the grain on the ear[7]. At the ear base, the corn kernels are attached very strongly to the cob. In contrast, the same corn kernels are weakly attached to the cob at the top end of the ear. Within a certain range of the moisture content, we notice that the adhesion force increases proportionately with the increasing moisture content[4, 8]. The interaction between the material and the threshing system is a very complex, dynamic process. To investigate the laws of maize threshing, researchers have developed a mathematical model of theoretical analysis[9-15]. Then, they have conducted both natural and simulation experiments of this model[16-19]. In some studies, researchers have used the discrete element method[20] to formulate the law of maize threshing[21-23].

Since the threshing process of corn ear is a complex process due to the biocomposite nature of corn ear, there are limitations in the various mathematical models proposed to develop the maize threshing theory. In this study, we established a maize threshing system based on a set of "tangential flow-transverse axis flow". The primary objective of our novel grain harvesting program was to reduce the corn damage rate.

Materials and Methods

Experiment Materials

The Henan Province Crop Variety Approval Committee has recommended the test corn varieties ‘QY8’ while carrying out analysis in the Huang-Huai-Hai Plane; the test varieties need to be checked both during sowing and harvesting seasons. To perform the test, we obtained bracts of maize ears in the ripening period of October 2016; the planting site was located on the Yellow River shore test field of Henan Liqi Seed Co., Ltd. The growth of field maize was monitored every day. As soon as the water content of maize grains was equal to test requirements, we carried out artificial harvesting of the quantity of ear produced at that stage. Then, we subjected the collected corn earns to testing procedures.

Using the five point sampling method, we measured the following parameters of maize: the length of each corn ear, the diameter of each corn ear, the number of rows in each ear, the number of core, and the diameter of the cob. Based on the data of various parameters, we adjusted the technical parameters of the test system. The statistical results are shown in **Table 1**.

Experiment System

In Huang-Huai-Hai Plane, 4YL-4/5 harvester threshing system is most commonly used in mechanical machines meant for harvesting corn grains. This threshing system adopts the “tangential flow + transverse axial flow” technology in its unit structure; it is driven by 37 kw power produced by the variable

Table 1 Statistical indices of biometrical traits of maize ears of variety ‘QY8’

Parameter	Unit	Range value	Average value.
Ear length (with bracts)	mm	250-270	260
Ear diameter (with bracts)	mm	50-60	55
Number in the vertical rows		35-40	37
Cob mass (moisture 26%)	g	45-60	51
Ear mass with bracts (moisture 26%)	g	290-350	320
Cob diameter	mm	20-30	25

frequency motor[24]. The threshing chamber consists of a grid concave plate screen; a fixed number of guide plates are set inside the cover. An intelligent instrument is used for torque/speed measurements; this instrument is arranged between the motor's output end and the threshing drum. It monitors the real-time changes in torque, rotational speed, and power of the system during the threshing process. The basic structure of the threshing system is shown in **Fig. 1**.

The design of the threshing system is explained as follows[25]: The structure of the threshing drum is illustrated in **Fig. 2a**. It consists of two components, namely tangential flow drum and axial flow drum. The tangential flow drum has a cylindrical tooth structure; the six rows of teeth have a spirally staggered arrangement to facilitate the propeller combing the corn ear. Then, the corn ear moves into the axial flow drum, as shown in **Fig. 2b**. At this stage, the corn ear is subjected to threshing strokes in the drum.. The structure of axial flow drum has a mixed arrangement of column tooth/plate tooth; the column has a strong ability to grasp the material, and it exerts a carding effect to strike off the right balance. The plate tooth strongly exudes adaptability by exerting a rubbing effect on the unevenly fed crop layers. The separation efficiency of threshing process is enhanced with the mixed arrangement of column teeth and plate teeth. The structure of the axial flow drum has three functional sections: threshing, sieving and discharging; these functions are carried out by the three sections of the ring baffle. The main objective of this assembly is to slow down the rapid flow of materials and to increase threshing time. Therefore, plate teeth are aligned into a certain angular arrangement, and they initiate the process by playing a pivotal role.

The feed conveyor transports corn ears to the hopper. After being subjected to threshing in the tangential flow drum, the corn ears are fed into the axial flow drum of the threshing chamber: the grains are shed under the action of the centrifugal force exerted by the concave plate sieve, driving the separated grains into the lower set of grain storage box. Following the separation of grains from the ear, the lighter but larger materials, such as bracts and shafts, are diverted into the straw separation area via the cover guide plate of the threshing chamber. Then, they are thrown out of the bench. To accurately analyze the threshing capabilities of the various functional sections in the threshing system, and to formulate the law of distribution of particles along the drum, we divided the threshing chamber is divided into three sections: (A) the tangential flow region, (B) an axial flow region, and (C) a sieve discharge region. To further determine the operating performance of the each zone in the threshing system, we divided each zone into three cells along the axial direction: In the sieve discharge region (C), the separation of grains was carried out, depending on whether they coerced into the straw or broken from corn cobs. Thus, entrainment loss was prevented in section (C). Based on the statistical data of previous threshing tests, the amount of grain sieved from the threshing total grain was 0.9 to 1.6% in section C; the data were accurate enough to avoid the need of a separate in-depth analysis.

Experimental Investigation

The principle of corn threshing primarily includes the threshing impact on corn ear as well as the knead and rub action existing among three entities: corn ears, threshing drum, and concave plate sieves; the concurrent actions of these entities ensure that the grain peels off[24]. In terms of efficiency and loss rate, the grain breaking rate primarily defines the performance of maize grain harvesting equipment. The quality of the commodity is severely hampered with an increase in the content of damaged grains; moreover, the respiration in damaged grain is much greater that in normal grains. Consequently, mildew forms at a much faster rate on damaged grains, seriously affecting the quality of commercial corn to such an extent that its food safety standards become questionable. In most cases, impurity rate and other similar indicators are not considered to be serious, but grain damage rate is a serious problem that is impacting the commercial prospects of corn grain harvest in the Huang-Huai-Hai Plane of China. In fact, the problem of damaged grains is so severe that it is now being considered as the only indicator of the

Fig. 2 Structure of threshing drum

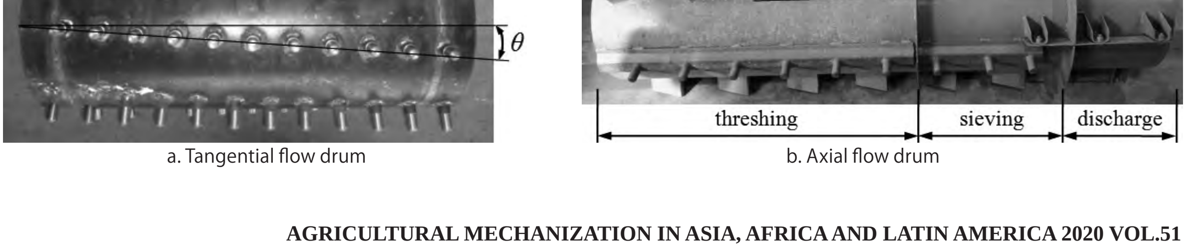

a. Tangential flow drum

b. Axial flow drum

performance of harvesters. In this paper, an experimental analysis was conducted to determine the factors affecting the grain damage rate of maize threshing process.

Determine Effect Factors

In threshing process, the factors affecting the fragmentation of grains were as follows: the moisture content of grains, the peripheral velocity of threshing drum, threshing clearance, and feedstock material. The factors mainly affecting the threshing process were analyzed to simplify the experiment, whereas the feeding amount and the threshing gap were simplified according to the situation prevailing during the threshing process; the feed amount corresponding to 2.6 kg·s^{-1} is used to perform threshing tests. The threshing clearance is the minimum distance between the top of column tooth or plate tooth and the concave transverse bars; the threshing clearance of the apparatus is dependent on the internal diameter of maize ears and cobs. According to the material movement direction, the beginning clearance is the concave clearance at the beginning; this parameter should be smaller than the average diameter of corn ear. The end clearance is the conclave clearance at the end; this parameter should be half of the cob diameter [18]. Based on the statistical results defining the biological traits of 'QY8'[18, 24], the beginning clearance is adjusted to 36 mm, whereas the end clearance is adjusted to 12 mm. This is because the beginning clearance includes the clearance of tangential flow drum. In totality, the threshing clearance lies in the range of 36-12 mm, with a clearance ratio of 3.

The threshing test measurements quantify the influence of grain moisture content and the peripheral velocity of threshing drum. The growth rate, dehydration rate, and the moisture content of different parts of corn ear were different. Furthermore, the structure and mechanical properties of keratinous endosperm, powdery endosperm, and the embryo of corn kernels were also different. All these features of maize grains were significantly affected by the water-bearing state of corn, because they were unstable composite biomaterials in that state. In contrast, the dehydration process was the result of internal pressure experienced by the grains apart from the external tensile stress, so the process of dehydration was completely opposite to the moisture absorption process. In the threshing test, it is not possible to determine the moisture content precisely as completely exact values cannot be obtained with the experimental measurements; the results are only in accordance with the moisture content range of fuzzy test and evaluation. The moisture content of maize ears was monitored in the experimental field. During the natural dehydration process, the moisture content range of 22-32% is an average range; this average range is further divided into five intervals for performing the threshing test. Based on the results of conventional threshing tests and the related threshing studies focusing on maize[18, 19, 24], we conclude that the peripheral velocity of threshing drum is generally between 15-22 m·s^{-1} while threshing corn ears with high moisture content. If the peripheral velocity of threshing drum is too high, then the impact is also too large on the grains. As a consequence, the grain damaged rate increases sharply; the amount of broken straw also increase tremendously, increasing the burden on the machine's cleaning mechanism. All these effects completely translate into higher power consumption by the harvesting machine. If the peripheral velocity of threshing drum is too low, then the impact is insufficient on the grain; therefore, the grain will not shed from its chaff. Moreover, because the material persistently resides for a long time to in the threshing room, the rubbing action is repeated several times on grains. The final result would be undesirable as the grain damage rate would increase sharply. In the threshing drum, the peripheral velocity of axial flow drum is chosen as 15.84 m·s^{-1}, 17.28 m·s^{-1}, 18.72 m·s^{-1}, 20.16 m·s^{-1}, and 21.6 m·s^{-1}, and the speed of the corresponding tangential-flow drum is 16.53 m·s^{-1}, 18.03 m·s^{-1}, 19.53 m·s^{-1}, 21.06 m·s^{-1}, and 22.56 m·s^{-1}.

Fig. 3 The collected grains are in the box

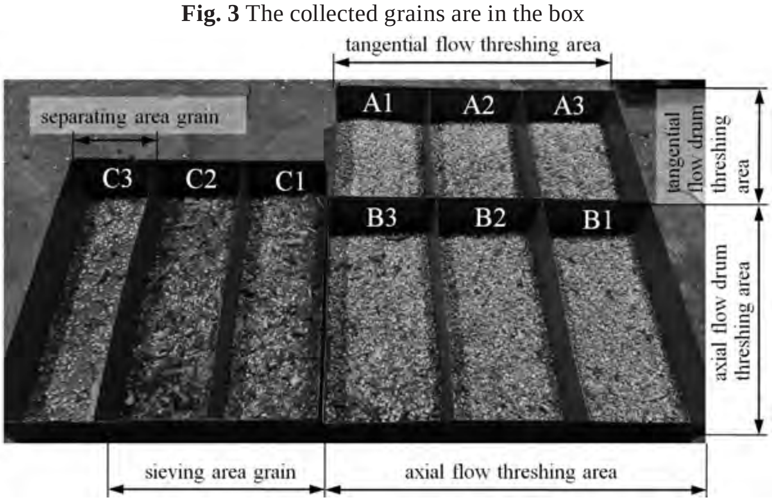

Experimental Results and Analysis

Based on the statistical data on damaged grain identification[26, 27], **Fig. 3** illustrates the effect of threshing test on grain collection process: An appropriate amount of threshing grains is sampled out from the grain collection box. After removing impurities, 200 g of the sample is weighed. From this proportion, the grains damaged by the machine are sorted out easily as they have an obvious crack. Then, we weighed the quantity of damaged grain and the total grain mass. With these parameters, we calculated the grain damage rate according to the following formula:

$$Z_s = (W_s / W_i) \times 100\ \% \qquad (1)$$

where, Z_s is the grain damage rate in terms of %; W_s is damaged grain weight expressed in g; W_i is the total weight of sampled grains, and it is expressed in g.

A comparison of the threshing amount between the tangential flow drum and the axial flow drum: To compare the threshing amount in the three areas, namely, (A) the tangential flow region, (B) the axial flow region, and (C) the sieve discharge region, we calculated the average threshing amount obtained during the threshing test of each threshing area. As shown in **Fig. 4**, the average threshing amount of the three regions in A, B, and C were 41.9%, 44.5%, and 13.6%, respectively.

Within the different ranges of moisture content, **Fig. 5** illustrates the relationship between the threshing amount of segments in the threshing system and the grain moisture content. When the moisture content is less than 28%, the threshing amount in the axial flow section and tangential flow section is almost same; the average difference between the two threshing amounts lies within 1%. When the average moisture content is 25%, the difference between the two threshing amounts is only 0.4%. With an increase in the moisture content of the material, threshing amount produced in the tangential flow drum decreased but that in the axial flow drum increased. Meanwhile, the threshing amount in region C also increased in a synchronous manner. The experimental results indicate that if the moisture content of grains is controlled below 28%, the threshing capacity of the tangential flow drum is almost equal to that of the axial flow drum. When the grain moisture content is greater than 28%, the threshing capacity of the tangential flow drum is significantly less than that of the axial flow drum. According to a previous study on the material properties of corn ears, the line clearance and ring gap of grains on corn ears increased obviously with the decrease in grain moisture content, provided the moisture content is less than 28%. This indicates that dehydration in grains causes the shrinking of grain volume[28], thereby decreasing the agglomeration of grains and reducing the difficulty of threshing.

Studies have shown that the action time of the material in the threshing system is about 2-3 s[24]. When the material is fed into the threshing room of axial flow drum, they are subjected to repeated combat. Consequently, they flip and squeeze with each other whilst rubbing against each other for a long time. Thus, the threshing effect is relatively complete on grains. During the threshing process in the tangential flow drum, the material from the feeding inlet compels the tangential flow drum to drive it out of the region A with high speed; the expended time length is only 0.021-0.029 s as per theoretical calculation. Within that moment, the corn ear strike with high speed and create an impressive impact on the concave plate sieve squeeze to achieve tangential threshing. The time of action is very short for achieving significant threshing of ears with high moisture content. Consequently, tangential flow drum pushes more material into the threshing room of axial flow drum. As a result, the threshing room of the axial flow drum witnesses a large amounts of material being subjected to retardation, and the risk of clogging increases tremendously with the amassed material.

Because our threshing system is based on “tangential flow + transverse axial flow”, we lay more emphasis on the structure and threshing function of the axial flow drum to optimize the grain harvest. Thus, we only pay attention to the feeding capability of the tangential flow drum whilst ignoring the threshing capacity of the same. This approach is adopted because the tangential flow drum does not perform much of the threshing action when corn ears are fed at once. Throughout the test, tangential flow drum is not only performing the feeding function, but it is also producing a significantly large threshing amount of more than 40%. Therefore, while optimizing the structure design of the threshing system based on “tangential flow + transverse axial flow” , manufacturers must pay equal attention to both components: tangential flow drum and axial flow drum. Only by modifying their approach

Fig. 4 Demineralization of each section of threshing flow drum

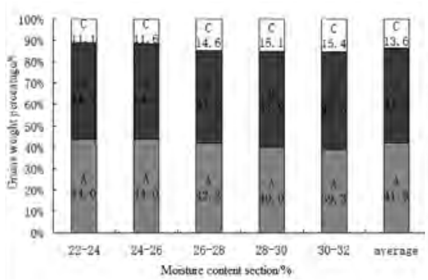

Fig. 5 The relationship between the threshing amount of segments and the grain moisture content

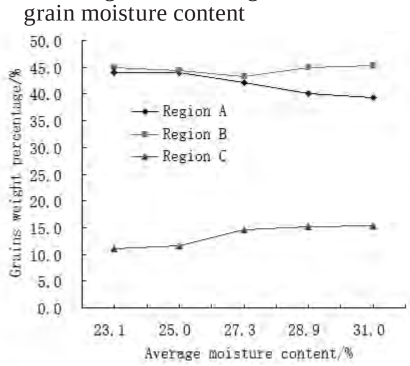

can they be able to effectively reduce the grain damage rate, improving the operational performance of harvest. Bearing in mind the threshing capacity of the tangential drum, we can try to develop the “double tangential flow + transverse axial flow” threshing system for corn grain harvester; however, further research studies must be conducted to fully explore the potential of models based on transverse axial flow.

The influence of moisture content on grain damage: Suitable moisture content is a prerequisite for performing mechanized harvest of corn grain[5]. In case of grains with high moisture content, the grain strength or the hardness of grains is too low; therefore, such grains gets easily damaged during the threshing process. In case of grains with very low moisture content, the hardness of grains would be significantly greater but these grains have poor toughness; therefore, these are the brittle grains susceptible to fracture when subjected to high impact stress during threshing process.

Fig. 6a show the relationship between grain damage rate and the moisture content of grains in the tangential flow drum. It can be seen that the grain damage rate increases rapidly with the increasing moisture content. While performing threshing test in the axial flow drum, it was found that the peripheral velocity of the axial flow drum was in the range 15.84-18.72 m·s^{-1}; moreover, the moisture content of grains was in the range 22-26%, with the grain damage rate being less than 5%. All these observations conform with the standard requirements of mechanized grain harvest[27]. When the moisture content was in the range 24-26%, the threshing damage grain rate was the lowest; therefore, it is obviously a turning point. Furthermore, when the drum speed was fixed at 17.28 m·s^{-1}, the grain damage rate was 1.5%. When the moisture content was 26-28%, the grain damage rate was about 5%, which is basically close to the national standard. In addition, when the moisture content is greater than 28%, the grain damage rate increases with an increase in moisture content; these values deviate from the national standard at this stage, and the adaptability of grain harvesting machine is reduced. When the speed range of the drum is between 20.16-21.60 m·s^{-1}, the grain damage rate is more than 6% in the total range of moisture content of the threshing test.

While performing the threshing test, it was realized that the relationship between the grain damage rate and the moisture content is almost same for both the tangential flow drum and the axial flow drum. As shown in **Fig. 6b**, when the moisture content of grains is in the range 24-26% and the drum peripheral velocity is 18.03 m·s^{-1}, the grain damage rate is the lowest at 1.9%. In the moisture content range 24-26%, the grain damage rate for the whole experimental system is 1.7%; it is the average damage rate of the values witnessed for the axial and tangential flow drums.

Fig. 6 Relationship between the grain damage rate and the moisture content

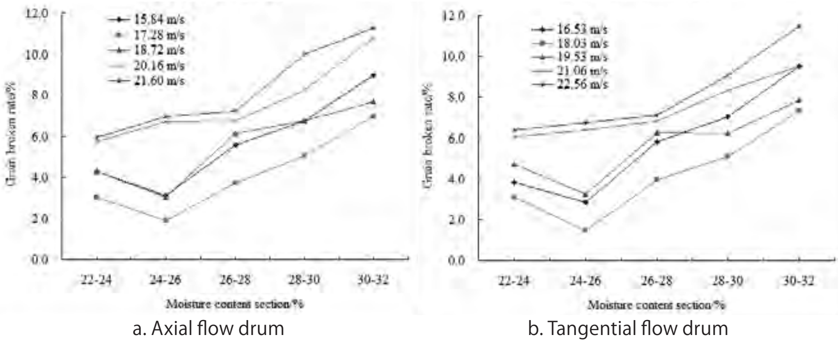

a. Axial flow drum b. Tangential flow drum

Based on the comprehensive test results, an appropriate amount of moisture content is a prerequisite for the accomplishing of corn grain harvest; it accelerates the dehydration rate of corn grain maturity. Therefore, it is important to control the grain moisture content while making concerted efforts to improving the efficiency of mechanized grain harvest, especially in the case of corn. By extending the harvest period to a later stage, the drying time can adequately be extended, Thus, it is also an effective way to reduce the grain damage rate in the current harvest.

Peripheral velocity of threshing drum: The peripheral velocity of threshing drum is the primary technical condition affecting the grain damage rate in the threshing process[3, 9]. When the threshing process in the axial drum is carried out at different linear speeds, it was observed that the minimum value of grain damage rate was 17.28 m·s^{-1} at each interval of moisture content. Among these, the minimum value of the grain damage rate occurred when the moisture content interval is 24-26%. When the peripheral velocity of the drum was reduced to 15.84 m·s^{-1}, both the damage rate and the grain broken rate increases. This is because when the drum velocity decreases, the drum’s threshing efficiency also reduces consequently. As the time of dwelling of the mixed material increases in the threshing room, the rubbing effect coupled with squeeze is enhanced for the material; however, the long period of squeeze can increase the grain damage rate. Therefore, it is essential to control the material’s threshing time so as to effectively improve the threshing quality and reduce the grain damage rate. As shown in **Fig. 7**, the influence of the peripheral velocity of tangential flow drum on the grain damage rate is similar to that witnessed with respect to the axial flow drum.

Conclusions

According to the results of statistics analysis of biometric trait indices of maize ears of variety ‘QY8’, the beginning clearance of the “tangential flow-transverse axial flow” was adjusted from the based threshing test system to 36 mm, whereas the end clearance was adjusted to 12 mm. The feed amount was set to 2.6 kg·s^{-1} according to the economic efficiency of the harvester. The corn ear threshing test was carried out on a sample containing grains with a moisture content of 22-32% at different values of the drum peripheral velocity. The conclusions obtained were as follows:

(1) The threshing capacity of tangential drum decreases with increasing moisture content. When the moisture content was below 28%, the threshing capacity of the tangential flow drum was almost equal to the B section of axial flow drum. The threshing capacity of the tangential flow drum decreased significantly when the moisture content was more than 28%.

(2) The threshing system is based on “tangential flow + transverse axial flow” principle, so it has a strong ability to adapt with the moisture content ranging between 24-26% of corn ears. When the average moisture content was 25%, the threshing amount of the tangential flow drum was only 0.4% smaller than the axial flow drum, and the threshing capacity of tangential and axial flow drums was deemed to be sufficient.

(3) When the moisture content was in the range 24-26%, the peripheral velocity of axial drum have inflection points about the grain damage rate, with minimum values occurring at 15.84 m·s^{-1}, 17.28 m·s^{-1}, and 18.72 m·s^{-1}. When the threshing speed of axial flow drum was 17.28 m·s^{-1}, the minimum value of grain damage rate was the smallest in the threshing system, with the average value being 1.7%.

With respect to the prevalent conditions of maize breeding and grain harvesting in Huang-Huai-Hai Plane, the grain damage rate can effectively be reduce and the threshing quality can be improved by delaying the harvest period slightly, thereby causing a timely extension of drying time and suitable working parameters for the threshing system. Given the threshing capacity of the tangential flow drum, it is further recommend that an innovative grain harvester must be designed such that the threshing system works on a “double tangential flow + transverse axial flow.” To fully exploit the potential of the innovative model, further research studies must be conducted.

Acknowledgments

This work is supported by the Earmarked Fund for Henan Agriculture Research System (Grant No.17S10-02-G07). We sincerely thank the Henan WODE Machinery Manufacturing Co., Ltd. for providing and technically guiding us with the operation of test equipment. We would also like to extend our vote of thanks to the Henan LIQI Seed Co., Ltd. for providing a mass of maize ears for the test.

REFERENCES

[1] Wang, K. R. and S. K. Li. 2017. Progresses in Research on Grain Broken Rate by Mechanical Grain Harvesting. Scientia Agricultura Sinica, 50(11): 2018-2026.

[2] Yang, L., T. Cui and Z. Qu et al. 2016. Development and application of mechanized maize harvesters. Int J Agric & Biol Eng, 9(3): 15-28.

[3] Li, S. K., K. R. Wang and R. Z. Xie et al. 2017. Grain Breakage Rate of Maize by Mechanical Harvesting in China. Crops, (02): 1-4.

[4] Waelti, H. and W. F. Buchele. 1969. Factors Affecting Corn Kernel Damage in Combine Cylinders. Transactions of ASAE, 12(1): 55-59.

[5] Li, S. F., C. X. Zhang, M. Lu et al. 2014. Research Development of Kernel Dehydration Rate in Maize. Molecular Plant Breeding, 12(04): 825-829.

[6] Guo, Q. C., H. R. Kang and L. E. Wang et al. 2016. Study on Standard and Breeding Pattern of Maize Produced by Grain Machine in Huanghuai Region. Bulletin of Agricultural Science and Technology, (1): 159-162.

[7] Petkevichius, S., L. Shpokas and H. D. Kutzbach. 2008. Investigation of the maize ear threshing process. Biosystems Engineering, 99(4): 532-539.

[8] Akubuo, C. O. 2002. Performance Evaluation of a Local Maize Sheller. Biosystems Engineering, 83(1): 77-83.

[9] Zhang, X. W., K. C. Yi and L. X. Gao. 2015. Contacting Mechanics

Fig. 7 Relationship between the drum peripheral velocity and the grain damage rate

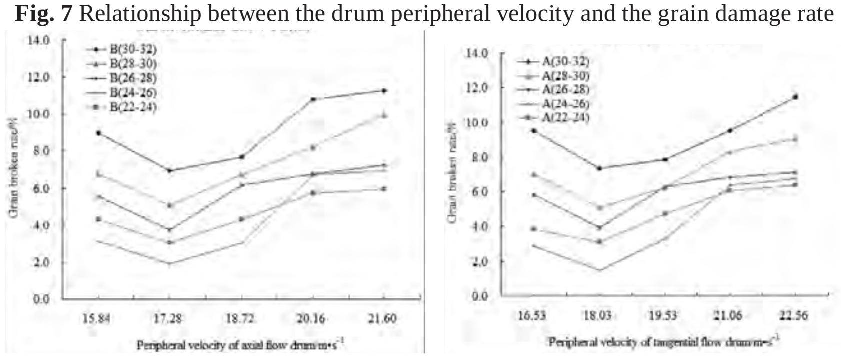

a. Axial flow drum　　b. Tangential flow drum

Analysis during Impact Process between Corn Seeds and Threshing Component. Chinese Agricultural Science Bulletin, 31(14): 285-290.
[10] Petre, M. 2016. Combine Harvesters Theory, Modeling and Design. Boca Raton: Taylor & Francis Group.
[11] Petre, I. M. and K. Heinz-Dieter. 2008. Modeling and simulation of grain threshing and separation in threshing units-Part I. Computers and Electronics in Agriculture, 60(1): 96-104.
[12] Petre, I. M. and K. Heinz-Dieter. 2008. Modeling and simulation of grain threshing and separation in axial threshing units-Part II. Computers and Electronics in Agriculture, 60(1): 105-109.
[13] Petre, I. M. and K. Heinz-Dieter. 2007. Mathematical model of material kinematics in an axial threshing unit. Computers and Electronics in Agriculture, 58(2): 93-99.
[14] Petre, I. M. 2002. Mathematical Model of Threshing Process in an Axial Unit with Tangential Feeding: AIC 2002 Meeting CSAE/SCGR Program. Saskatoon, Saskatchewan.
[15] Volkovas, V., S. Petkevičius and L. špokas. 2006. Establishment of maize grain elasticity on the basis of impact load. MECHANIKA, Nr.6(62): 64-67.
[16] Myhan, R. and E. Jachimczyk. 2016. Grain separation in a straw walker unit of a combine harvester: Process model. Biosystems Engineering, 145: 93-107.
[17] Steponavičius, D. and V. Butkus. 2012. The empirical model of grain separation on straw walker. Journal of Food, Agriculture & Environment, 10(3 & 4): 296-302.
[18] Petkevičius, S., L. špokas and D. Steponavičius. 2008. Substantiation of technological parameters of wet maize ear threshing. Agronomy Research, 6(S): 271-280.
[19] špokas, L., D. Steponavičius and S. Petkevičius. 2008. Impact of technological parameters of threshing apparatus on grain damage. Agronomy Research, 6(S): 367-376.
[20] Zhong, W. Q., A. B. Yu and X. J. Liu et al. 2016. DEM/CFD-DEM Modelling of Non-spherical Particulate Systems: Theoretical Developments and Applications. Powder Technology, 302: 108-152.
[21] Yu, Y. J., H. Fu and J. Q. Yu. 2015. DEM-based simulation of the corn threshing process. Advanced Powder Technology, 26(5): 1400-1409.
[22] Yu, Y. 2013. Research on analysis method of corn threshing based on 3D DEM. Dr. Jilin: Jilin University.
[23] Yu, J. Q., H. Fu and H. L. Zhou et al. 2012. Based on Discrete Element Method of the Analytical Method on Maize Threshing Process: China, CN102415243A, 2012-04-18.
[24] Chinese Academy of Agricultural Sciences. 2007. Agricultural machinery design manual. Beijing: China Agricultural Science and Technology Press, 1022.
[25] National Agricultural Machinery Standardization Committee. 1999. JB/T 9778.2-1999, Rasp-bar threshing drum-Types dimensions and specifications. Beijing.
[26] China Machinery Industry Federation. 2008. GB/T 21961-2008, Test methods for corn combine harvester. Beijing.
[27] China Machinery Industry Federation. 2008. GB/T 21962-2008, Technical requirements for corn combine harvester. Beijing.
[28] Gao, L. X., F. Li and X. W. Zhang et al. 2011. Mechanism of Moisture Content Affect on Corn Seed Threshing. Transactions of the Chinese Society for Agricultural Machinery, 42(12): 92-96, 42.

■■

Design, Development and Performance Evaluation of CIAE-Millet Mill

by
S. Balasubramanian*
Principal Scientist
ICAR-Central Institute of Agricultural Engineering
Regional Centre,
Coimbatore-641 003, Tamilnadu, INDIA
*Corresponding author: balaciphet@gmail.com

S. D. Deshpande
Ex-Principal Scientist
ICAR-Central Institute of Agricultural Engineering,
Bhopal-462 038, Madhya Pradesh, INDIA

I. R. Bothe
Assistant Professor
SP College of Food Technology,
Kharawate-Dahiwali Chiplun-415 606,
Maharashtra, INDIA

Abstract

An eco-friendly CIAE-Millet Mill integrated with pneumatic suction arrangement was designed and developed. It simultaneously dehulls minor millets and separates the husk from the dehulled mass. It is a power operated (1 HP, single phase motor) with a main shaft speed of 960 rpm (for dehulling) and blower shaft speed of 1920 rpm (for pneumatic suction). Its capacity is 100 kg/h for all minor millets at 10-12% mc (wb). The overall dimensions of the machine are 860 mm × 842 mm × 1460 mm. The performance of CIAE-Millet mill was evaluated by using various types of minor millets. The result showed that the co efficient of dehulling is in the range of 70-85 %.

Keywords: CIAE-Millet Mill, minor millet, dehulling, pneumatic suction arrangement, dehulling efficiency.

Introduction

Millets are small-seeded spices crops; grow around the world for food and fodder. The term millet includes a number of small grained cereal grasses. Its agricultural importance arises from their hardiness, tolerance to extreme weather and could be grown with low inputs in low rainfall areas. Finger millet/ Ragi (Eleusine coracana), Foxtail millet/ Navane (Setaria italica), Little millet/ Saamai (Panicum miliare), Kodo millet/ Haraka (Paspalum scrobiculatum), Proso millet/ Panivaragu (Panicum miliaceum), Barnyard millet/ Banti (Echinochloa frumentacea) are the important millets cultivated largely in the Asian and African countries. Fonio (Digitaria exilis) and Tef (Eragrostic tef) are specific to Nigeria and Ethiopia, respectively (Jaybhaye et al., 2014). Millets are nutritious food and they are rich in phytochemicals, fibre and minerals. There is an immense potential to process millet grains into value-added foods and beverages (Devi et al., 2011). Dehulling or decortication is the process of removing outer pericarp and hull (testa, seed coat) of cereal, legumes, and oilseeds. It plays most important role in utilizing the food grains in our daily diet. Although, dehulling although depends upon the methods and machinery used for the process; several factors such as environment agronomic aspects genotypes and pretreatment influence the dehulling process. Many reports has witnessed the drudgery involved in traditional dehulling method and emphasized as one of the major problems militating against the realization of the full potential of millets. The traditional way of dehulling millets in rural areas are by pounding the slightly moisturized millet grains in pestle and motor. Husk is not edible; therefore must be removed from the minor millets. Different types of dehulling equipment for cereals and legumes are available employing either abrasive, attrition, or roller-milling principles. The abrasive type machines employing carborundum stones or other abrasive devices have been tried mainly for millet dehulling by most researchers rather than other two types of mills. Therefore, there is a need for proper dehulling technique and machinery. Thus, the objective of this work is to design and develop an eco-friendly millet mill with improved efficiency involving less power with integrated actions of gentle attrition/abrasion and pneumatic suction arrangement.

Material and Methods

CIAE-Millet Mill of 100 kg/h capacity was designed and developed at ICAR-Central Institute of Agriculture Engineering, Bhopal, India. All the construction materials are locally sourced and the concepts and ideas are transformed to into useful machinery (Bernard et al., 1999). The principle and procedure in design and construction of millet mill machine are explained as below.

(i) Dehulling Operation

The dehulling operation of husk from kernel was performed with a gentle pressure (abrasion/attrition) exerted for the millet grain to dehull in a single pass and to increase the efficiency. The dehulling action and energy requirement were worked out using selected abrasive stone/grinding wheel by our laboratory set-up study. The concepts and ideas were imparted in design of each component and using CREO ELEMENTS / PRO, the model and detailed CAD were prepared.

(ii) Pneumatic Suction Arrangement

Pneumatic suction arrangement is effective for separation of lighter materials like husk and products in powdery form from small seeded minor millets (Balasubramanian, 2007). Due to lighter weight of millet husk, pneumatic system consisting of a fan with increased speed of air to suck the husk from the hulled mass was operated by taking power from main rotor shaft. The blower was positioned in the suitable place to suck the husk from the grain outlet chute. The suction air velocity was kept higher than the terminal velocity of the husk and powdery materials. The high speed air makes the product to flow in the air stream to grain outlet. The design of the pneumatic suction arrangement was based on the aerodynamic properties of the material velocity, determined by sucking the husk with suitable blower design and distance moved per unit time was determined. It becomes important to have efficient millet mill machine to ensure not only the processed millet availability but also in right quantity.

Fig. 1 Hopper

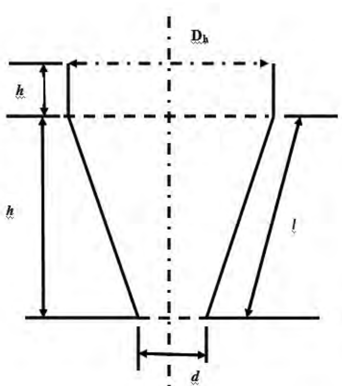

(iii) Design and Construction

A set number of design consideration points viz., cost of construction, power requirement of machine and operational labour requirement were carried out during the design of millet mill. Also, ease of design component parts and its replacement in case of damage or failure sufficiently rugged to function properly for a reasonably long period and cheap enough to be economically feasible were taken into consideration.

I. Theoretical Design and Material Selection

The materials for construction of millet mill are shaft, abrasive grinding wheel, pulley, belt, electric motor, bearing, and mild steel plates. These materials were selected based on the power requirement in dehulling of millets. Using the engineering properties data for all minor millets has various moisture content reported by Balasubramanian and Viswanathan (2010) and the laboratory data on power requirement for the dehulling was taken to design considerations.

(A) Electric Motor

An electric motor of the following specification was selected:

Power (P): 0.75 kW (1 hp)
Rotational speed (N): 1440 rpm
Phase: Single
Frequency: 50 Hz

(B) Hopper Design

Based on the angle of repose of different millets (Balasubramanian and Viswanathan, 2010) and on gravity discharge principle, volume of the hopper was estimated (Eq.1)

$$V_h = [\pi(D^2_h - d^2)h] / 12 \quad (1)$$

Where, $h = l \cos\varphi$ (see **Fig. 1**).

(C) Abrasive/Grinding Wheel

The abrasive grinding wheels of dimension 300 mm × 40 mm × 38.1 mm was selected with A 24 super-life V272 features.

(D) Selection of Transmission Drives

The power transmission drives used for the machine are belt and pulley (**Table 1** and **2**).

(i) Pulley or sheave

The rotor's pulley diameter was selected (Eq. 2) for required speed ratio as

$$D_r = (D_m\, N_m) / N_r \quad (2)$$

The speed of rotor (shaft) was chosen as 960 rpm for grinding wheel (dehulling operation) and was doubled as 1920 rpm (husk separation) to generate enough air velocity greater than the critical velocity of husk to be conveyed and discharged in cyclone separator.

(ii) Belt

Based on the power transmitted (0.75 kW) and according to Indian Standards (IS: 2494-1974), belt type B was selected (**Table 1**).

(iii) Calculation of Belt Length

The belt length was calculated (Eq. 3) according to Khurmi and Gupta (2004).

$$L = \pi/2\,(D_1 - D_2) + 2X + (D_1 + D_2)^2 / 4x \quad (3)$$

These parameters are represented in **Fig. 2**.

(iv) Arc of Contact

The arc of contact, β, is given by (Eq. 4) as suggested by Anon (1994)

$$\beta = 180° - 60°\,[(D_1 - D_2) / x] \quad (4)$$

(v) Shaft

The shaft of millet mill rotates the bottom grinding wheel (960 rpm) and through another belt arrangement, a van blades of blower (1920 rpm) extended to a cyclone separator was designed. For a shaft subjected to twisting moment only, diameter of shaft can be obtained by using torsion equation (Eq. 5)

$$T = (\pi / 16)\tau d^3 \quad (5)$$

$$T = (T_1 - T_2)R \quad (6)$$

Where,

$$T_1 = T_m - T_c \quad (7)$$

$$T_m = \sigma a \quad (8)$$

(vi) Determination of belts cross-sectional area

The cross-sectional area of belt was calculated (**Fig. 3**) from **Table 3**, top width (b = 17 mm), thickness (t = 11 mm) and by calculation, bottom width (x) was obtained as 8 mm. Thus,

(Area of triangle 1) + (Area of triangle 2) + (Area of triange 3) (9)

$$a = t/2[(b - x) / 2) + xt + t/2[(b - x) / 2] \quad (10)$$

$$a = [(b - x) / 2]t + xt \quad (11)$$

Also, centrifugal tension, T_c was determined (Eq. 12)

$$T_c = mV_l^2 \quad (12)$$

$$m = \rho a \quad (13)$$

From **Table 4**, density was found to be 1140 kg/m^3.

$$V_l = (\pi DN) / 60 \quad (14)$$

For a V-belt drive, tension ratio is given (Eq. 15) as

$$(T_1 - T_c) / (T_2 - T_c) = e^{\mu\theta \operatorname{cosec}\alpha / 2} \quad (15)$$

From **Table 3**, coefficient of friction between belt (rubber) and pulley (dry cast iron) was taken as 0.30. By considering the small pulley, θ was calculated (Eq. 16) as

$$\theta = [180 - 2 \sin^{-1}((D_1 - D_2) / 2x)] \pi/180 \text{ rad} \quad (16)$$

Fig. 2 Open belt drive

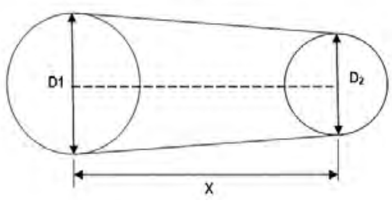

(vii) Power Transmission by Belt

The power transmitted by belt was calculated (Eq. 17) as

$$P_b = (T_1 - T_2)V \quad (17)$$

(E) Bearing

Based on type of load, the bearing support (static & dynamic) and shaft diameter, the ball rolling contact bearing of standard designation 307 was selected. It is a medium series bearing with bore (inside diameter) of 35 mm (Khurmi and Gupta, 2004)

(F) Power Requirement

The power requirement millet mill was obtained as (Eq. 22)

$$P = Qg\,Hf \quad (18)$$

II. Performance Evaluation of Millets

A. Preparation of Raw Material

The contaminants for millets may be sand (soil), small stones, leaves, shrivelled seeds, off-type seeds, broken seeds, glumes, sticks, chaff, parts of stem, insects, animal hair, animal excreta (e.g. rat and insect faeces) and more annoyingly, metal pieces. Metal pieces, if not removed, may damage the sieves of milling machines if mechanized grinding is used.

Fig. 3 Cross-section of V-belt

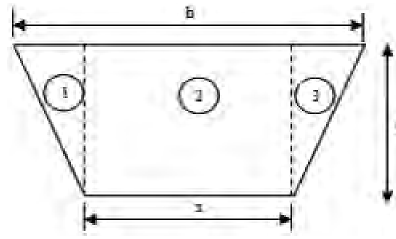

(i) Raw Millets

The Cleaning is done by destoner-cleaner-grader for the raw millets.

(ii) Parboiled Millets

For parboiled millets, boiler was filled with water to a level just above its bottom, and on top of the water, a wire net was placed to raise the samples above the water. The samples were then placed on the muslin cloth and the boiler was closed for steam-heating, and the boiler was connected to the power source. The steaming was done for 15 min, samples were taken out and allowed to temper for 24 h (**Fig. 5**).

Table 1 Dimensions of standard V-belts

Types of belt	Power ranges (kw)	Minimum pitch diameter of pulley (D, mm)	Top width (b, mm)	Thickness (t, mm)
A	0.7 - 3.7	75	13	8
B	2 - 15	125	17	11
C	7.5 - 75	200	22	14
D	20 - 150	355	32	19
E	30 - 350	500	38	23

Table 2 Density of belt materials

Material of belt	Mass density (kg/m^3)
Leather	1,000
Double woven belt	1,250
Rubber	1,140
Canvass	1,220
Balata	1,110
Single woven belt	1,170

Table 3 Coefficient of friction between belt and pulley

Belt material	Pulley material						
	Dry	Wet	Greasy	Wood	Compressed paper	Leather face	Rubber face
Leather oak tanned	0.25	0.2	0.15	0.3	0.33	0.38	0.40
Leather chrome tanned	0.35	0.32	0.22	0.4	0.45	0.48	0.50
Convass-stitched	0.20	0.15	0.12	0.23	0.25	0.27	0.30
Cotton woven	0.22	0.15	0.12	0.25	0.28	0.27	0.30
Rubber	0.30	0.18	-	0.32	0.35	0.40	0.42
Balata	0.32	0.20	-	0.35	0.38	0.40	0.42

Fig. 4 Plan and elevation of CIAE-Millet Mill

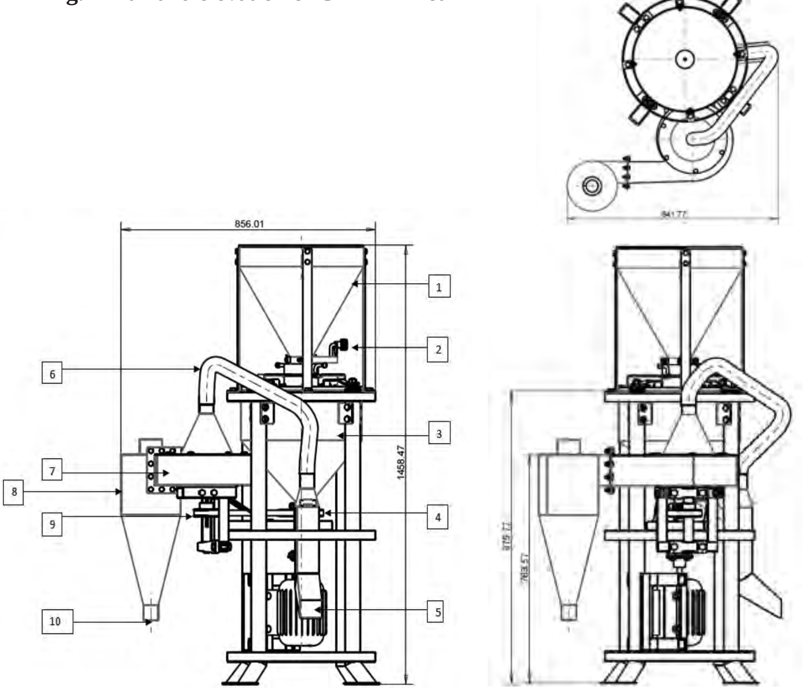

C. Determination of moisture content

The key to post-production of operations, grain moisture content is determined on wet basis as (Balasubramanian and Viswanathan, 2010).

$$m = (w_i - w_f) / W_i \times 100 \quad (19)$$

D. Testing of machine

The test carried out on millet mill to prove the conformity with requirement of relevant standard. The tests are checking of specifications, checking of materials and visual observation and provision for adjustment (NCAM, 1990).

E. Test at Load

Test under load was conducted to get the following data: dehulling index, degree of dehulling, effectiveness of dehulling, yield of the broken, yield of fine, quality of dehulling, coefficient of dehulling, overall dehulling efficiency and cleaning efficiency. The sample is analyzed for cracked and broken grains, undehulled grains, and clean grains. Analysis for cracked grains and broken grains is only made from the sample were taken at the specified grain outlet.

(i) Dehulling Index (η)

The dehulling index was calculated using the following equation:

$$\eta = [(m_k + m_h) - (m_{ud} + m_b)] / m_i \quad (20)$$

The dehulling index may vary from a maximum value of +1 to a minimum of −1. A value of +1 indicates that the entire original grain sample is completely dehulled into two fractions of grain (m_b) and husk (m_h) with no fines and undehulled grains. A value of −1 indicates that the dehulling is not complete, thus the broken grains (m_f) and /or not dehulled (m_{uh}) at all (Ikebudu et al., 2000).

(ii) Degree of dehulling (M_h)

The degree of hull removal is the ratio of mass of hull removed during dehulling to the initial mass of sample used for the dehulling process.

$$M_h = m_h / m_i \quad (21)$$

(iii) Effectiveness of dehulling (E_d)

Effectiveness of dehulling is the ratio between the mass of the material remaining undehulled and the initial mass of material taken for dehulling.

$$E_d = m_{ud} / m_i \quad (22)$$

(iv) Yield of broken (Y_b)

It is the ratio between the mass of broken generated during dehulling and the initial mass of sample used for dehulling.

$$Y_b = m_b / m_i \quad (23)$$

(v) Yield of fine (Y_f)

It is the ratio between the mass of fine generated during dehulling and the initial mass of sample used for dehulling.

$$Y_f = m_f / m_i \quad (24)$$

(vi) Quality of dehulling (Q_d)

It can be calculated as ratio between the weight of dehulled kernel (both broken and whole) and initial weight of material taken for dehulling.

$$Q_d = m_k / m_i \quad (25)$$

(vii) Coefficient of dehulling (C_{dh})

This can be calculated using the following equation:

$$Cdh = 100[1 - (Y_b + E_d + Y_f)] \quad (26)$$

(viii) Overall Dehulling Efficiency (η_o)

This is calculated using the following relationship:

$$\eta_o = (M_h + Q_d) \times C_{dh} \quad (27)$$

Fig. 5 Flowchart for experimental dehulling study

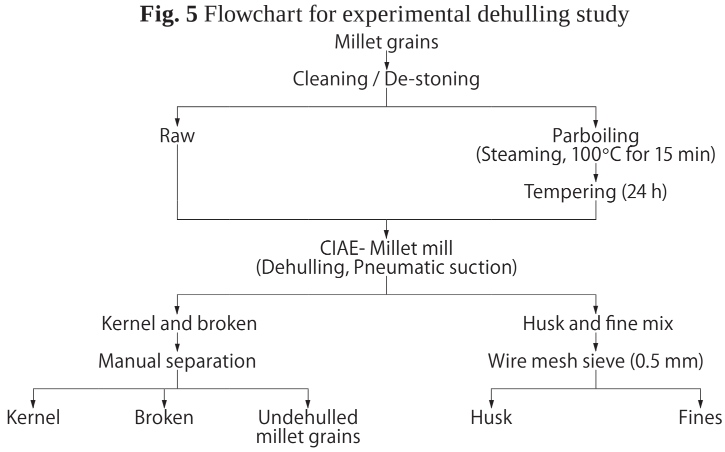

(ix) Cleaning Efficiency (C_e)

This can be calculated using the following equation:

$$C_e = m_w / m_k \quad (28)$$

Result and Discussion

The design parameters viz., assumed parameters and designed parameters of CIAE millet mill are shown in **Table 4**. The motor was selected on the basis of dehulling capacity and its power requirement. The shaft of millet mill rotates the bottom grinding wheel and through another belt arrangement, a van blades of blower extended to a cyclone separator was designed. The length and diameter of the shaft is 536 mm and 34 mm, respectively. The speed of rotor (shaft) was chosen as 960 rpm for grinding wheel and was doubled as 1920 rpm to generate enough air velocity greater than the critical velocity of husk to be conveyed and discharged at cyclone separator. The diameter of main shaft pulley is 150 mm and blower shaft pulley is 84.5 mm. The hopper was designed based on the dehulling capacity and bulk density of different millets. The volume of hopper is 3.7 × 105 mm^3 (**Table 4**). The ball rolling contact bearing of standard designation 307 was selected. Thus, the designed millet mill requires floor area of 860 × 842 mm and having 112 kg weight (excluding motor).

The machine was designed as a vertical frame work assembly, a vertical rotary shaft extending in the vertical axis in the framework assembly and abrasive grinding wheel mounted on the shaft for rotation there with, a face to face mounted upper abrasive grinding wheel with fine turner to adjust the clearance between the pair of grinding wheel, to define in a dehulling chamber there between a hopper at the top of the framework assembly and a dividing part at the bottom of the dehulling chamber. The upper grinding wheel with spring suspension mechanism provide and the bottom rotary grinding wheel is fixed with the shaft the clearance in between the grinding wheel adjust with the help of spring by the upper grinding wheel, and it possible to dehull all minor millets with theoretical uniform. The dehulled grain and husk is pass through the discharge pipe and hence passes to outlet chute, where the suction output high. The husk from the kernel, then discharge cleaned kernel out from the grain outlet and the husk is transfer toward the cyclone by the pneumatic suction as shown in **Fig. 4**.

The machine was found to be dust free. The grinding wheel and other parts do not wear and runs smoothly. This machine can dehull the millets with and without bran layers, thus judicious dehulling operations be achieved by setting the clearance of grinding wheel to suit different millets by coarse and fine adjustments. The rotor shaft was checked for torsion and bending and found safe. The driving mechanism of rotor was designed in such a way that the v-belt was safe and was able to transmit required speed to the rotor from the motor. A pair of abrasive stone (grinding wheel) were provided, thus permitting a much broader range of application for millet grain size accommodation for dehulling and size reduction operations. The millet grain is fed between the grinding wheels and dehulling operation taken place in the horizontal plane. Thus, the exact clearance setting reduces the excessive heat generation during gentle abrasion/attrition requiring low power. Also, less time is required for the dehulling and due to the air-tight nature, dust spillage is minimized. An average dehulling efficiency of designed millet mill was obtained 80% with different minor millet. The design parameters of the millet mill are summarized in **Table 4**. The overall specifications of the millet mill are shown in **Table 5**.

Table 4 Design specification/parameter

Component	Assumed parameters	Designed parameters
Electric motor	From shaft, pulley and capacity design	1,440 rpm, 1.0 Hp
Pulley		
Pulley (large)	OD = 150 mm, ID = 110 mm	OD = 150 mm, ID= 110 mm
Pulley (small)	OD = 84.5 mm, ID = 44.5 mm	OD = 84.5 mm, ID =44.5 mm
Hopper	h = 487.71 mm, D_h = 412mm	V = 3.715 × 10 5 mm^3
Speed ratio		
Main shaft	N = 1,440 rpm, D = 34 mm	N_r = 960 rpm, D= 34 mm.
Blower shaft	Double the rotation of the main shaft, 30 mm diameter	1,920 rpm, d = 30 mm
Diameter of shaft	T= 323 Nm	T = 323 N_m, D = 34 mm
Centre distance between pulley	D = 150, d = 84.5	x = 320 mm
Belt	D = 150, d = 84.5, x = 320.	L= 1,110 mm
Processing chamber	Dia. =407 mm, h = 366 mm	V = 6.23 × 106 mm^3
Grinding wheel (upper)	D = 300 mm	V = 2.668 × 106 mm^3
Grinding wheel (lower)	D = 300 mm	V = 2.838 × 106 mm^3
Arc of contact	D = 150, d = 84.5, x = 320	β = 167.7°
Power requirement	240 V, I = 2.5	460 watt

Table 5 Specification of CIAE-Millet Mill

Name of the machine	CIAE-MILLET MILL
Mode of operation	Continuous type
Overall dimension (mm)	860 × 842 × 1,460
Feed hopper	
Top (mm)	421
Base (mm)	75
Height (mm)	420.71
Emptying angle (°)	34.88
Grinding wheel	
Upper wheel diameter (mm)	300 × 40 × 38.1
Lower wheel diameter (mm)	300 × 40 × 38.1
Power unit (Electric motor)	
Power rating, (HP)	1 hp, single phase motor
Working speed (rpm)	960
Suction/blower speed (rpm)	1,920
Capacity (kg/h)	100-110
Weight (kg)	112 (excluding motor)
Floor area (mm)	860 × 842
Purpose	Dehulling of minor millets (with or without bran)
Working principle	Gentle abrasion & (aerodynamic) cyclone separator
Coefficient of dehulling (%)	70-85
Feed moisture (% wb)	10-12

coefficient of dehulling followed by little millet, proso millet, kodo millet and banyard millet, respectively. Similarly, the coefficient of dehulling was the highest in foxtail millet followd by proso millet, kodo millet and barnyard millets. Despande and Khan (2007) reported that pre milling treatments (soy oil water and microbial consortium) play an important role in improving the dhal recovery by loosening the husk from the cotyledons. Nwaigwe et al. (2012) designed the cassava milling machine at a power of 3.7 kW, rotor speed of 1080 rpm, tested and found to have a milling efficiency of 82.3%. Opokul et al. (2003) stated that dehulling characteristics of pigeon pea and mung bean in abrasion type of dehulling increased the yield of dehulled cotyledons.

Regarding the performance evaluation of designed mill at no load condition there was no marked oscillation during operation and presence of rattling sound is due to the contact of grain to the surface of the grinding wheel. During the test at load carried out to the different type of millets (100 kg) at different conditions (raw and parboiling) at constant rotation speed of grinding wheel. Different dehulling efficiencies were obtained from each type of millets at different condition and the averages of the efficiencies obtained are presented in **Table 6**. The moisture content of raw and parboiled millets ranged between 9.25-11.06% and 10.79-13.28% respectively. The overall dehulling efficiency of raw millet ranged from 83.95-69.76% and parboiled millets 85.15-72.07% and cleaning efficiencies higher in parboiled millets (84.83-62.75%) compared to raw millets (81.01-60.21%). Among the raw millet foxtail millet recorded highest

Conclusion

The CIAE-millet mill has been designed, fabricated, tested with a coefficient of dehulling as 70-85%. It operates with a 1 hp single phase electric motor. The integral suction arrangement provides the simultaneous separation of husk and dust particles from the dehulled mass from the grinding zone. The cyclone component provides a dust free i.e. eco-friendly environment during

Table 6 Performance of dehuller on raw and parboiled millets

Millet	Moisture content at dehulling (%, w.b.)	Dehulling index (η)	Degree of dehulling (M_h)	Effectiveness of dehulling (E_d)	Yield of broken (Y_b)	Yield of fine (Y_f)	Quality of dehulling (Q_d)	Overall dehulling efficiency (η_o)	Cleaning efficiency (C_e. %)	Coefficient of dehulling (C_{dh})
Raw										
Foxtail millet	9.30	0.840	21.800	0.001	0.146	0.003	76.867	83.95	81.01	85.083
Little millet	11.06	0.799	30.733	0.001	0.147	0.032	63.967	77.67	77.02	82.013
Kodo millet	9.25	0.753	31.333	0.007	0.227	0.003	66.667	75.42	66.00	76.960
Proso millet	10.83	0.785	23.967	0.005	0.213	0.008	76.333	77.70	72.14	77.470
Barnyard millet	9.85	0.711	30.733	0.004	0.269	0.018	67.600	69.76	60.21	70.943
Parboiled										
Foxtail millet	12.18	0.851	22.800	0.003	0.129	0.003	75.233	85.15	82.90	86.857
Little millet	13.28	0.794	27.567	0.001	0.173	0.013	69.200	78.68	75.05	81.313
Kodo millet	10.79	0.793	31.900	0.002	0.189	0.003	66.533	79.30	71.54	80.563
Proso millet	12.02	0.847	21.800	0.013	0.115	0.004	75.600	84.58	84.83	86.837
Barnyard millet	11.11	0.728	31.433	0.003	0.247	0.013	66.400	72.07	62.75	73.667

dehulling the small seeded minor millets. This machine has a provision for dehulling the millet with bran layer also. Thus, the millet mill when operated within the designed parameters will process 100 kg raw materials in an hour with judicious dehulling operations. The rate of dehulling of the machine was efficient compared to the traditional methods. This machine is able to dehull all types of minor millets irrespective of their sizes and shapes. However, the effectiveness of the machine is said to be dependent on the uniformity, size and moisture content of the millet grains.

Nomenclature

a: Area of belt
d: Diameter of shaft (mm)
D: Diameter of processing chamber
d_1: Diameter of disk
D_1: Larger sheave diameter
D_2: Smaller sheave diameter
D_h: Diameter of the upper opening of hopper
D_m: Measure diameter of motor's pulley
D_r: Rotor's pulley diameter
h: Vertical height of hopper
H: Height of lift
l: Slant height of hopper
L: Length of belt (in)
m: Mass of belt per unit length
N_m: Rotational speed of electric motor (1,440 rpm)
N_r: Rotational speed of rotor (rpm)
R: Radius of pulley (mm)
T: Twisting moment (Nm)
t: Thickness of hammer
T_1: Tight side tension (N)
T_2 : Slack side tension (N)
T_c: Centrifugal tension (applicable for belt running at high speed)
T_m: Maximum tension in belt (N)
V: Velocity of air (m/s)
V_l: linear speed of belt
Vh: Volume of hopper (mm^3)
X : Centre distance of pulleys (mm)
x: bottom width of the belt
α: Groove angle (34°)
θ: Angle of wrap (radian)
μ: Coefficient of friction between belt and pulley
ρ: Density of belt material (rubber, kg/m^3)
φ: Angle of repose
β: Arc of contact
τ: Torsional shear stress (42 MPa)
σ: Maximum allowable stress of belt (2.8 MPa)
Q_g: Gravimetric throughput capacity
f: Power factor
m_h: Mass of hull (kg)
m_{ud}: Mass of undehulled kernel (kg)
m_b: Mass of broken (kg)
m_i: Initial weight of sample taken for dehulling (kg)
m_w: Mass of whole grain (kg)
m_f: mass of fine (kg)
M_h: Degree of dehulling
E_d: Effectiveness of dehulling
Y_b: Yield of broken
Y_f: Yield of fine

REFERENCES

Anon. 1994. Design data. Complied by Faculty of Mechanical Engineering, PSG College of Technology, M/S. DPV printers. Coimbatore, India.

Anon. 2013. Policy paper: Role of millet in nutritional security of India. National Academy of Agricultural Sciences, New Delhi.

Balasubramanian, S. 2007. Studies on pearling and development of pasta from selected minor millets. PhD Thesis, Tamilnadu Agricultural University, Coimbatore, India.

Balasubramanian, S. and R. Viswanathan. 2010. Influence of moisture content on physical properties of minor millets. Journal of Food Science and Technology. 47(3): 279-284.

Bernard, J. H., S. R. Schmid and B. O. Jacobson. 1999. Fundamentals of machine elements. McGraw-Hill International Publishers, New York, p: 3.

Deshpande, S. S. and S. Khan. 2007. Influence of premilling treatments on dhal recovery cooking characteriticsof pigeon pea. Journal of Agricultural Engineering. 44(1): 53-56.

Devi, P. B., R. Vijayabharathi, S. Sathyabama, N. G. Malleshi and V. B. Priyadarisini. 2011. Health benefits of finger millet (*Eleusine coracana L.*) polyphenols and dietary fiber: a review. Journal of Food Science Technology. DOI 10.1007/s13197-011-0584-9. for dehulling of canola. Canadian Agricultural Engineering 42(1): 27-32.

Ikebudu, J. A., S. Sokhansanj R. T. Tyler, B. J. Milne and N. S. Thakor. 2000. Grain conditioning.

Jaybhaye, R. V., I. L. Pardeshi, P. C. Vengaiah and P. P. Srivastav. 2014. Processing and technology for millet based food products: a review. Journal of Ready to Eat Food. (2): 32-48.

Khurmi, R. S. and J. K. Gupta. 2004. Shaft, V-belt and Rope Drives: A Textbook of Machine Design. 13th Edn., S. Chand and Co. Ltd., New Delhi, pp: 456-498, 657-659.

Kundgol, N. G., B. Kasturiba and K. K. Math. 2014. Antioxidant Activity of Value Added Ready to Eat Millet Based Food Products. International Journal of Science and Research. 3(8):474- 476.

NCAM. 1990. Test code for power maize shellers. Draft Nigerian industrial standard. Prepared by the National Center for Agricultural Mechanization 1, 1-10.

Nwaigwe, K. N., C. Nzdiegwn and P. E. Ugwnoke. 2012. Design, construction and performance evaluation of a modified cassava milling machine. Research Journal of Apllied sciences, Engineering and Technology. 4(18):3354-3362.

Opoku, A., L. Tabil, J. Sundarami, W. J. Crerar and S. J. Park. 2003. Conditioning and dehulling of pigeon peas and mung beans paper presented at the CSAE/SCGR 2003 meeting paper No. 03-347.

■■

Development of a Front Mounted Cultivator for Power Tiller

by

Sourav Srichandan Das
Graduate Student
Agricultural and Food Engineering Department
Indian Institute of Technology,
Kharagpur, INDIA

Hifjur Raheman*
Professor
Agricultural and Food Engineering Department
ndian Institute of Technology,
Kharagpur, INDIA
*Corresponding author: hifjur@agfe.iitkgp.ernet.in

Abstract

A front mounted hydraulically operated cultivator was designed and developed considering the draft ability of the power tiller and negative draft developed by the rotary tiller. A proper linkage system was designed to mount the cultivator to the front of the power tiller. Field performance of the power tiller was measured with both front mounted cultivator and rotary tiller and with only rotary tiller. Results indicate a significant decrease 50% and 13% in clod size and fuel consumption respectively with improvement in tillage performance index by 50%, when the power tiller was operated with front mounted cultivator and rotary tiller in combination as compared to when it was operated with rotary tiller alone.

Introduction

For dry land cultivation, power tiller is not very commonly used for primary tillage operation due to its low draftability which increases the completion time for field preparation. Use of rotary tiller is advantages over the conventional implements as the working blades in contact with soil are active hence it achieves both cutting and pulverising actions in a single pass of machine in the field. There is a reduction in traction demand of power tiller driving wheels due to ability of the soil working blades to provide some thrust (Sirisak et al., 2008). But use of rotary tiller for primary tillage is limited due to high power requirement and excessive soil pulverization (Kepner et al., 1978).

Adamu et al. (2014) evaluated the performance of a power tiller in the Savanna agro-ecological zone of Nigeria. The field work and laboratory experiment showed that the field efficiency, effective field capacity and fuel consumption obtained were 47% and 48%; 0.04 ha/h and 0.06 ha/h; 1.3 l/h and 1.6 l/h for ploughing and rotovating, respectively. The ploughing and rotovating were done at a depth of 9 cm and 5.5 cm when soil moisture contents were 6.3% and 8%, respectively. Tiwari et al. (1997) evaluated a 7.5 kW rotary type power tiller fitted with seated attachment for rota-puddling and roto-tilling operations. For dry roto-tilling the effective field capacities of the power tiller with and without seat attachment were 0.097 ha/h and 0.099 ha/h, respectively. Similarly, field operations were carried out for ploughing (with disc and mould board), cultivation, cultivation cum planting and harvesting using a 9 kW two-wheel tractor. Field efficiencies reported were: 53.98% for disc ploughing, 88.30% for mould board ploughing, 66.63% for cultivation, 81.26% for cultivation cum planting and 72.88% for harvesting with a reaper (Ademiluyi et al., 2007).

Generally, primary tillage operation with power tiller is cumbersome and tedious and it requires number of passes for making the field ready for sowing. So, with the use of front mounted cultivator in power tiller which can act as combination tillage implement with rotary tiller when operated together may result in reducing soil clods with less number of passes. This arrangement may also utilize the negative draft power of the rotary tiller to meet the full or part of the power requirement of cultivator.

Keeping the above facts in mind, a study was carried out to develop a front mounted cultivator for power tiller and to provide a suitable mechanism for its lifting and lowering. Performance of the developed front mounted cultivator when operated along with rotary tiller was evaluated in the field and compared with the performance of the rotary tiller alone and the results obtained are discussed in this paper.

Materials and Methods

Design of Prototype Front Mounted Cultivator System

The cultivator was designed based on the draft ability of the power tiller and also by taking negative draft developed by the rotary tiller into consideration. A proper linkage system was designed to mount the cultivator to the front chassis of the power tiller. To ensure proper manoeuvrability of the power tiller when fitted with front mounted cultivator and to operate the cultivator at proper depth in the field, a hydraulic system powered by the power tiller engine was designed and developed. The schematic view of the power tiller with front mounted cultivator is shown in **Fig. 1** along with the forces acting on it.

At balanced condition of power tiller with front mounted cultivator during tillage work, balancing all the vertical forces , we get

$$R_1 + R_2 + R_3 = W_t + W_i \quad (1)$$

Balancing all the horizontal forces, we get

$$D + F_1 + F_2 = P + T \quad (2)$$

Where, W_t = weight of power tiller, W_i = weight of implement system (cultivator, cylinder and lifting arms), R_1 and R_3 = reaction of net dynamic load on gauge wheel and power tiller wheel, respectively, F_1 and F_2 = rolling resistance of power tiller wheel and gauge wheel, respectively, R_2 = vertical forces acting on rotary tiller, D = Draught developed by the power tiller, P = thrust developed by the rotary tiller, T = thrust developed by the power tiller wheels.

Table 1 Design dimensions of the developed cultivator

Sl. No.	Particulars	Details
1	Overall Dimension (L × W × H), mm	600 × 160 × 220
2	Tines (width × thickness), mm	30 × 10
3	No. of Furrow openers	5
4	Furrow opener type	Shovel
5	Shovel (width × thickness), mm	40 × 4
6	Penetration angle	40º
7	Cross-section of Frame	Hollow rectangular
8	Height of frame cross-section, mm	45
9	Width of frame cross-section, mm	26
10	Weight of cultivator, kg	26.5

Design of Front Mounted Cultivator

A 5 × 12 cm two row cultivator was designed and developed to match the cutting width of rotary tiller (**Table 1**). The cultivator is supposed to perform tillage operation up to a maximum depth of 10 cm in a medium soil. The negative draft from rotary tiller was also considered while designing the cultivator. The draft of the cultivator was predicted using ASAE draft equation (ASAE D497.4 MAR 99).

Design of Front Linkages for Cultivator

Lifting system for the front cultivator mainly consisted of side brackets (side arms), lower link, middle link and a double acting hydraulic cylinder. The side brackets attached to the chassis of power tiller were used to mount cultivator using lower links and middle link (**Fig. 2**). Lower link was designed in such a way as to decrease the horizontal distance between two hitch points of the lower link in order to minimise the moment arm. Lower link was also given a vertical bend of 15 cm to accommodate the cultivator at a lesser horizontal distance from the front end of the chassis of power tiller and also to decrease the distance between front axle centre and centre of resistance of the front implements. At first, the shape of the brackets was decided and then their thicknesses were decided according to the maximum force acting on it and material used. The forces acting in different links are shown in **Fig. 2**.

Taking moment about lower link hitch point of the cultivator at point O, we get

$$F_t \sin\theta_t \times w + W_i \times x = D \times Y + Fc \times x \quad (3)$$

On balancing forces in horizontal and vertical direction, we get

$$F_h + F_t \cos\theta_t = D \quad (4)$$

$$W_i + F_t \sin\theta_t = F_v + F_c \quad (5)$$

Where, F_t = force acting in the middle link, F_v = vertical force acting in the lower link, F_h = force act-

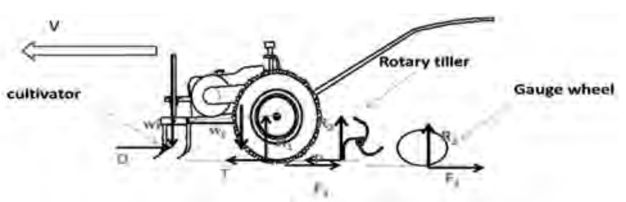

Fig. 1 Free body diagram of power tiller with front mounted cultivator

Fig. 2 Schematic diagram of prototype front mounted cultivator

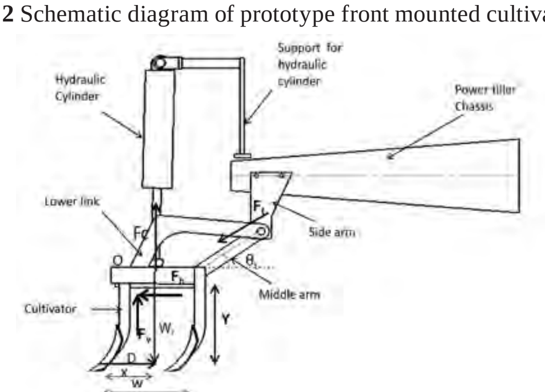

ing in the lower link in horizontal direction along the direction of motion, F_c = force acing on the hydraulic cylinder, W_i = weight of the front mounted implement, x = moment arm of resultant vertical soil and gravitational force on the implement about the lower link hitch point, Y = height of cross-shaft from centre of resistance, w = width of cultivator, θ_t = angle of middle link with the horizontal.

The design of front linkage system was done for both the conditions i.e. working with cultivator at maximum depth and when the implement was lifted to the maximum height. Forces acting on the lower links, middle link and side brackets were calculated using Eqns. 3, 4 and 5. Lower links and middle link were designed based on the forces acting on it. The lower link having width and thickness as 4 cm and 1.2 cm, respectively was selected. One side of the lower link was attached to the side bracket and other side was connected to the cultivator hitch point. Side brackets were given to provide space for the free vertical movement of the front mounted cultivator. The shape of the side bracket as shown in **Fig. 2** was optimised in order to reduce weight. The side arm selected was having thickness as 1.4 cm. The middle link was provided at the centre of the cultivator frame to restrict the free movement of the cultivator. A common shaft with diameter 2.2 cm was provided to connect the two lower links and middle link to the side bracket of the front linkage system. All the links were checked for its design stress such that it should remain below maximum permissible stress of links with a factor of safety equal to three. As the design was found to be safe so linkages were fabricated.

Hydraulic System and Its Associate Parts

To operate the front mounted cultivator, a hydraulic system powered by the engine of the power tiller was designed. The components of hydraulic system were hydraulic cylinder, gear pump, mono block directional control valve (DCV), reservoir and hose pipes. The hydraulic system design included the dimensions of actuator size (i.e. stroke length, bore diameter and rod diameter), capacity of reservoir and type and size of hydraulic pump. The design of hydraulic cylinder was done for both the conditions i.e. working with cultivator at maximum depth and the implement when lifted to the maximum height. Stoke length was decided based on the maximum raised height of cultivator and the maximum depth of operation i.e. 10 cm. So, a double acting cylinder with bore diameter 50 mm, rod diameter 25 mm, and stroke length 150 mm was used in this study. The double acting hydraulic cylinder was controlled by a four port, three-position, spring centred, hand lever operated DCV. The hydraulic system was operated at 1500 rpm of flywheel. The hydraulic circuit for the developed hydraulic system for lifting and lowering the front mounted cultivator is shown in **Fig. 3**.

Considering the time of lowering the implement as 5 s and dimensions of hydraulic cylinder, the design pump capacity was found to be 4.69 l/min. The pump selected was of gear type with fixed displacement and with pump size of 6.4 cubic centimetres per revolution. The hydraulic gear pump was powered from engine using a pulley and belt. As the pump was of fixed displacement type, so the revolution per minute requirement of pump was calculated from the flow requirement of the hydraulic cylinder and capacity of pump. An intermediate pulley of 7 cm diameter was provided at the driven pulley end of the power tiller. The intermediate pulley was connected to the pulley of diameter 9 cm attached to the gear pump through a V-belt of length 1030 mm.

An oil tank was used which acted as a reservoir for oil, as a cooler, coarse strainer, sedimentation unit for the impurities and acted as both air and water separator. The general thumb rule for the capacity of the reservoir is three times the pump flow rate. According to this, the reservoir capacity required was 3 × 9 = 27 l/min. This value multiplied with the time required to complete the

Fig. 3 Schematic diagram of hydraulic circuit for lifting arms

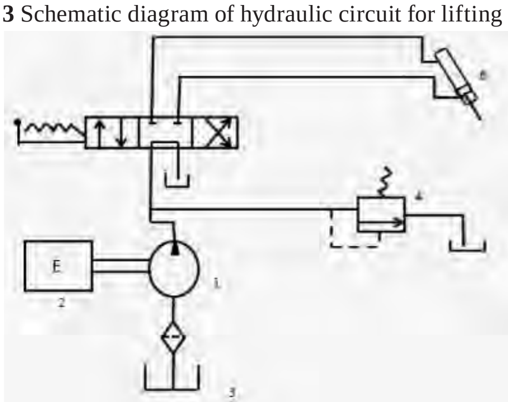

1. Pump, 2. Engine, 3. Reservoir, 4. Pressure relief valve, 5. 4/3 spring centered manually operated, DCV 6. Actuator

Fig. 4 Power tiller with front mounted cultivator assembly

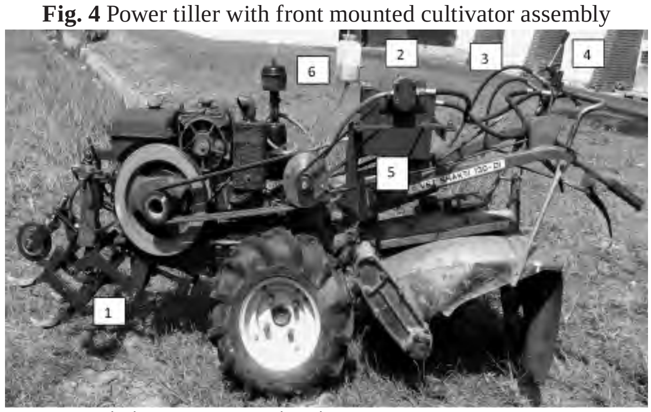

1. Front linkage system with cultivator,2. Gear pump, 3. Pressure pipe, 4. Monoblock DCV, 5. Hydraulic oil tank, 6. Auxiliary Fuel tank

extend stroke, i.e. 5 s then reservoir capacity required was 27 × 5/60 = 2.25 l. The tank selected was of size 15 × 15 × 30 cm.

Available Rotary Tiller

The specifications of the power tiller are given in **Table 2**. The rotary tiller available with the power tiller was having 18 nos. of C-typed blades and the speed available at the rotary shaft of the power tiller was 180 ±20 rpm and 240 ±30 rpm with rotary (low) and rotary (high), respectively, at the engine speed of 1600 ±100 rpm. This was powered by taking power from the engine in two steps.

Field Testing of Power Tiller-Operated Prototype Front Mounted Cultivator

Field testing of prototype front mounted cultivator was carried out to evaluate the performance of both rotary tiller and front cultivator operated simultaneously, and only with rota tiller for comparison. Soil in the test field was sandy clay loam soil with an average moisture content and cone index in the range of 9±1 per cent dry basis; 700±100 kPa, respectively. The tillage tool was set to operate at maximum tillage depth of 10 cm. The engine speed was kept at 1600 ±100 rpm. Tests were carried out at 2nd (low) and 3rd (low) gears of the power tiller to evaluate its performance in terms of field capacity, soil pulverisation, travel speed, fuel consumption and tillage depth.

Performance Parameters Considered for Field Evaluation

The performance of a tillage implement was expressed in terms of tillage performance index (TPI), which is considered to be directly proportional to volume of soil handle per time (V_s) and inversely proportional to fuel energy (Fe) and mean weight diameter of soil (MWD).

Mathematically it could be expressed as:

$$TPI = KV_s / (MWD \times Fe) \qquad (6)$$

Here, K is proportionality constant. While comparing different tillage implements in same soil condition, K could be absorbed in the equation.

Sieve analysis was carried out to find mean weight diameter (MWD) of the clods which represents the soil pulverization. Sieve of sizes 60, 40, 26, 17, 11.2, 8, 5.6, 4, 2.8 and 2 mm was used for the test. MWD was calculated using the following equation:

$$MWD = \sum\nolimits^{n}_{i=1} w_i M_i / \sum\nolimits^{n}_{i=1} w_i \qquad (7)$$

Where, MWD = mean weight diameter of soil aggregates, mm; w_i = weight of soil sample retained over i^{th} sieve, g; M_i = class of mean size for ith sieve, mm.

The volume of soil handled per unit time (Vs) is expressed as:

$$Vs = FC \times d \times 100 \qquad (8)$$

Where, Vs = volume of soil handle in m^3/h; FC = actual field capacity in ha/h; d is the depth of operation in cm.

The fuel energy input to carry out a tillage operation could be expressed as:

$$Fe = FC \times CV \qquad (9)$$

Where, Fe = fuel energy input, MJ/ha; FC = fuel consumption, l/h; CV = calorific value of diesel, MJ/l.

Results and Discussion

Power Tiller with Prototype Front Mounted Cultivator

The power tiller with prototype front mounted cultivator assembly is shown in **Fig. 4**. Its component includes cultivator, front lifting linage system and hydraulic system. The cultivator at the front of power tiller is to be carried to the field. For this, it has to be raised so that there is no hindrance to transportation of power tiller due to mounting of cultivator at the front. With the selected pump for the hydraulic system i.e. with a pump flow rate of 6.4 cm^3 per revolution, the cultivator could be raised up to 18 cm from ground surface. However, in the field the cultivator could be raised to a height more than this as it was mounted to the chassis of the power tiller (with more depth of the rotary tiller, front portion of the power tiller chassis was raised hence the cultivator was raised to a higher height).

The performance of the developed hydraulic system was evaluated in terms of time required to lower and raise the cultivator. At different rpm

Table 2 The specifications of the power tiller

Sl. No.	Particulars	Technical details
1	Make	VST
2	Model	VST 130 DI
3	Overall Dimensions (L × W × H), mm	2360 × 900 × 1210
4	Type	Horizontal 4 stroke single cylinder water cooled diesel engine /OHV
5	Combustion Chamber	Direct Injection (DI)
6	Max. HP as per IS 13539 1996	13.0HP@2400 rpm
7	SFC (specific fuel Consumption), g/hp-h	195
8	Stroke, mm	95
9	Bore, mm	95
10	Cooling System	Condenser Type Thermo siphon cooling system
11	Transmission From engine to main shaft	 V belts
12	From first shaft to rotary shaft	Chain and Sprocket
13	Size of pneumatic wheel, cm (inch	15.2-30.5 (6.00-12.0)
14	Rotavator, number of tines	18
15	Weight of power tiller (dry weight, kg)	436

of the power tiller engine, time required to raise or lower the cultivator were measured using stop watch. The time required for lowering and lifting at 1800 rpm were 6.06 s and 2.53 s, respectively as compared to 6.87 s and 4.41 s at an engine speed of 1000 rpm.

Field Performance of Power Tiller When Operated with Front Mounted Cultivator and Rotary Tiller Simultaneously

Field performance of the power tiller was evaluated with both front mounted cultivator and rotary tiller operated simultaneously and with only rotary tiller. When field tests with both rotary tiller and cultivator were carried out, cultivator was given more tillage depth compared to the rotary tiller in order to get more tillage depth with higher pulverisation and lower fuel consumption. Similarly, the tillage depth for only rotary tiller was kept same as that used for implements when operated in combination. Performance parameters such as fuel consumption, field capacity, wheel slip, soil pulverization and travel speed for both the implements in gears L2 and L3 were measured and are summarized in **Table 3**.

The average speed of operation with rotary tiller and cultivator in combination was 1.37 kmph which was lower compared to rotary tiller only (i.e. 1.44 kmph in L2). The difference in travel speed of operation with both the implements in combination and with rotary tiller alone is quite marginal in second (low) gear as compared to third (low) gear. This could be due to lesser draft requirement of the cultivator at lower speed (i.e. second (low)) of operation. However, draft requirement of cultivator increased at higher speed (third (low)) of operation and the power tiller could produce required draft to pull the cultivator at higher wheel slip. The effective field capacity of rotary tiller and cultivator in combination in L2 gear is 0.072 ha/h which is lower than L3 gear i.e. 0.099 ha/h due to higher travel speed of power tiller in L3 gear.

Mean weight diameter (MWD) of soil aggregates was found from sieve analysis of soil samples collected after tillage operation and was calculated using Eqn. 7. Tillage with only rotary tiller implement produced larger soil aggregates than with both rotary tiller and cultivator (**Table 3**). When front mounted cultivator was used it opens up the soil which was pulverised further by the rotary tiller. The largest clod size obtained was of 13.11 mm with rotary tiller alone and smallest clod size of 6.94 mm with both cultivator and rotary tiller.

Table 3 Comparison of test results of power tiller with both cultivator and rotary tiller and with only rotary tiller in L2 and L3 gear

Parameters	With both cultivator and rotary tiller		With rotary tiller alone	
	L2 Gear	L3 Gear	L2 Gear	L3 Gear
Average Speed (km/h)	1.37	2.27	1.44	2.70
Average tillage depth (cm)	8.50	8.95	8.23	8.70
Theoretical Field capacity (ha/h)	0.098	0.18	0.098	0.18
Effective Field capacity (ha/h)	0.072	0.099	0.074	0.115
Field Efficiency (%)	73.46	55.00	75.55	63.80
Volume of soil handled (m^3/h)	61.20	88.60	60.86	100.05
Wheel slip (%)	16.20	25.80	11.90	11.70
Fuel consumption (l/h)	0.72	1.02	0.83	1.36
Mean weight diameter (mm)	6.94	8.35	11.96	13.11
Specific energy requirement (kJ/m^3)*	423.36	413.22	488.16	490.68
Tillage performance index (TPI)*	0.34	0.28	0.17	0.15

*Calorific value of the diesel taken for calculation is 36 MJ/l

Fuel consumption of the rotary tiller and cultivator combination was lower i.e. 0.72 l/h compared to the rotary tiller alone i.e. 0.83 l/h in L2 gear. Tillage operation with rotary tiller and cultivator in combination consumed less engine power as the rotary tiller at the back pulverised the soil loosened by the front cultivator. Whereas with rotary tiller alone, fuel consumption was found to be higher due to cutting of the hard soil surface which produced high peak torque of the rotary shaft. However, tillage operation with third gear increased the fuel consumption due to increase in the power requirement. Similarly, the specific energy requirement for rotary tiller and cultivator in combination was found to be 423.36 kJ/m^3 which is lower in comparison to rotary tiller alone i.e. 488.16 kJ/m^3.

The TPI, calculated using Eq. 6 was lesser for tillage operation with rotary tiller alone (i.e. 0.17) compared to both front mounted cultivator with rotary tiller (i.e. 0.34). This improvement in tillage with both tillage implements operating simultaneously was due to the smaller size of soil aggregates and lesser fuel consumption.

Conclusions

This study was carried out to increase the tilling ability of power tiller with front mounted cultivator. Field performance of the power tiller was evaluated with both front mounted cultivator and rotary tiller and comparison were made with rotary tiller alone. The field experiment data showed that the field capacity and field efficiency of power tiller with front mounted implement and with only rotary is 0.072 ha/h and 0.074 ha/h; 73.46 and 75.55 percent when it was operated with second (low) gear. The volume of soil handled by rotary tiller alone is 60.86 m^3/h compared to 61.2 m^3/h for both the implements operated simultaneously. The mean weighted diameter of soil clods obtained with both cultivator and rotary tiller is 6.94 mm as compared to 11.96 mm with only rotary tiller. Similarly, fuel consumption obtained are 0.825 ha/h and 0.72 ha/h for only rotary tiller and both cultivator and rotary tiller. The TPI of front mounted cultivator with rotary tiller is 0.34 compared to 0.17 for rotary tiller alone. This was possible due to the soil opened by the cultivator and which was further reduced to smaller aggregates due to rotary tiller. From the results of performance evaluation of the front mounted cultivator it can be concluded that there was significant improvement in the power tiller tilling ability in dry land.

REFERENCES

Adamu, F. A., B. G. Jahun and B. Babangida. 2014. Performance Evaluation of Power Tiller in Bauchi State Nigeria.Journal of Biology, Agriculture and Healthcare. 4(9): 10-14.

Ademiluyi, Y. S., A. O. Ani, B. O. Ugwuishiwu and O. A. Oyelade. 2007. Performance Assessments of Two-Wheel Tractors on Loamy Sand Soil of Ilorin. Nigerian Journal of Technology (NIJOTECH). 26 (1): 59-66.

ASAE D497.4: 1999 Agricultural Machinery Management Data .ASABE St. Joseph, Mirch.

Kepner, R A, R. Bainer and E. L. Barger. 1978. Principle of Farm Machinery (3rd Edition). The AVI Publishing Company, Inc., USA.

Sirisak, C., T. Niyampa, W, Jantaraduch and K. Saensuwan. 2009. The performance of rotary tiller using prototype rotary blade in dry land field. Mj. Int. Sci. Tech.:17-26.

Tiwari, P. S., A. C. Varshney and C. R. Mehta. 1997. Field evaluation of power tiller rotavator with seating attachment. Indian Journal of Agriculture Science. 67(9): 414-417.

■■

EVENT CALENDAR

2020

◆ EUBCE 2020
April 27-30, Marseille, INDIA
www.eubce.com/eubce-2020.html

◆ 5th CIGR International Conference 2020
June 14-18, Quebec, CANADA
www.cigr2020.ca/

◆ ASAEB 2020 Annual International Meeting
July 12-15, Omaha, Nebraska 68102, USA
www.asaeb.org/

◆ SIMA
November 8-12, Paris (Nord Villepinte), FRANCE

◆ EIMA International
November 11-15, Bologna, ITALY
www.eima.it

■■

Development of Mathematical Model for Predirecting Peel Mass of Cassava Tubers

by
John C. Edeh
Department of Mechanical Engineering,
College of Engineering and Engineering Technology,
Michael Okpara University of Agriculture,
Umudike, NIGERIA
engredehjohnc@gmail.com

Abstract

The peel masses of cassava varieties required in the evaluation of tuber flesh loss and peeling efficiency of mechanized cassava peeling machine were studied based on their moisture contents. Five improved cassava varieties.UMUCAS 36, UMUCAS 37, UMUCAS 38, TME 419, and TMS 30572 were considered with the developed mechanistic and regression mass models compared with actual peel mass. Results obtained showed that TME 419 at moisture content of 63.33% had average mass of 585.6 g, percentage mass of peel of 19.13%, and average peel thickness of 2.33 mm; TMS 30572,at 63.5% moisture content recorded 499.24 g, 23%, and 2.3 mm for average mass, mass of peel and average peel thickness respectively; UMUCAS 36 had average mass of 357.48 g, 21.90% mass of peel and average peel thickness of 1.6 mm at 72.69% moisture content; while UMUCAS37at 84% moisture content recorded 16.97% mass of peel, 2.4 mm average peel thickness and 430.24 g average mass; and UMUCAS 38 had average mass of 497.96 g, average peel thickness of 2.44 mm and 19.77% mass of peel at 73.83% moisture content. ANOVA result revealed that the mass of peel models can approximate the actual response (mass of peel) of the cassava varieties above 97% prediction accuracy. These eliminated drudgery and rigors associated with determining actual peel mass hence relieving researchers of the ambiguities in evaluating flesh loss and peeling efficiency in cassava processing systems.

Keywords: Cassava tuber, variety, peel mass, moisture content, flesh loss, peeling efficiency

Introduction

Cassava (Manihot esculenta) is a perennial root tuber crop which grows in the tropical and subtropical areas of the world. It is the third largest source of food carbohydrates in the tropics after rice and maize and it belongs to the family of Euphrobbiaceae (FAO, 1990). In Nigeria, cassava referred as Rogo orkaraza in Hausa, gbaguda or ege in Yoruba, Akpu or Egburu in Igbo is cultivated virtually in most regions and across various vegetation belts. It is propagated by stem cutting and after a period of eight months to one year, it gets ready for harvesting and processing depending on the variety (Stephen, 1998). This and other characteristics attributes of cassava informed the classification of cassava based on variety. Cassava varieties grown in Nigeria include Oloronto 53101, Oloronto 6044, Oloronto 60447, Oloronto 60506, TMS 30211, TMS 30001, TMS 30572, TMS 30555, etc. Recently, the International Institute of Tropical Agriculture (IITA), Ibadan, Nigeria in collaboration with National Root Crop Research Institute (NRCRI), Umudike, produced cassava varieties that are resistant to major

Fig. 1 Cassava Tuber Section

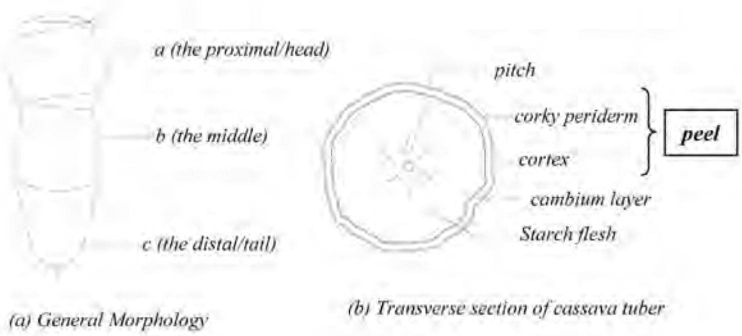

pests and diseases, compatible with intercrops as legumes, cereals, and vegetables, have extended ground storage and early maturity. These varieties contain the popular vitamin A among others hence referred to as improved varieties. Generally, cassava tubers when cut through as shown in **Fig. 1** consist of three regions, namely, the periderm which is the outermost layer, brown in colour and consists of dead cells which covers the surface of the tuber, the cortex that lies below the periderm and is usually about 1.5-2.5 mm thick and white in colour, then the central portion of the tuber, which makes up the greater bulk of the cassava tuber and is composed of essentially starch (Abdukadir, 2012). The size of the root depends on the fertility of the soil and the cassava variety.

Cassava is converted during its processing stage to useful products such as starch, garri, fufu, feed, tapioca, flour, starch used in paper industries as form of adhesives, and in textile industries for strengthening clothes, etc; the peels are mostly used for animal feed.However, its food security, economic and industrialization potentials are currently underutilized due to inadequate mechanization of the processing operation.

The need for mechanizing the processes involved in cassava production spurs the engineer into action of producing machines for the unit operations in the processing of cassava such as peeling, grating, boiling/ par boiling, drying, milling, sifting, extrusion, frying, etc. Several processes such as grating, drying, milling, pressing, sieving, frying and extrusion have been mechanized successfully, however, cassava peeling remains a serious global problem to design engineers (Olukunle et al., 2006; Abdukadir, 2012). Peeling involves the removal of a thin layer (the peel) from cassava roots as it contains the highest concentration of cyanogenic glucoside responsible for cassava toxicity and also for end product quality. Cassava tubers' size and shape variations caused peeling to be the most difficult unit operation in the entire processing operations (Olukunle and Akinnuli, 2013). Over the years, manual method which involves using knife or other sharp objects remains the most used method due to the fact that mechanical methods developed have been less efficient in the peeling process of cassava. This manual method is time consuming, full of drudgery, inefficient for commercial production and requires much man-power which increases the cost of production. Many machines have been developed for the mechanical method of peeling, yet

Table 1 UMUCAS 36 Variety

Sample	L (mm)	M_c (g)	V_c (cm^3)	ρ_s (g/cm^3)	R_{th} (mm)			GMD (mm)	Sphericity ϕ	Sa (mm^2)	P_{th} (mm)	V_p (mm^3)	M_{Pt} (g)	M_{Pa} (g)
					a	b	c							
1	385	610	565	1.08	63	60	29	47.86	0.76	7,198.98	1.71	12,310.25	104.37	99.44
2	437	920	1,035	0.89	83	72	46	65.02	0.78	13,287.91	1.84	24,449.75	136.38	125.19
3	358	675	624	1.08	80	63	37	57.13	0.71	10,258.86	3.16	32,452.20	196.59	186.05
4	315	365	349	1.05	58	50	33	45.74	0.79	6,575.86	3.07	20,165.96	135.22	121.78
5	366	565	472	1.20	73	62	32	52.52	0.72	8,668.04	2.95	25,570.71	197.24	182.23
6	340	345	305	1.13	66	42	32	44.60	0.68	6,251.34	1.54	9,627.07	67.92	64.72
7	311	510	498	1.02	60	61	22	43.18	0.72	5,860.66	3.39	19,848.12	147.61	117.73
8	259	365	349	1.05	55	52	39	48.14	0.88	7,282.80	1.83	13,327.52	72.95	73.87
9	315	245	214	1.14	47	36	31	37.43	0.80	4,404.05	1.43	6,297.79	53.57	49.21
10	398	315	285	1.11	51	44	22	36.68	0.72	4,229.69	2.13	8,995.13	100.46	87.69
11	226	382	352	1.09	74	60	22	46.05	0.62	6,666.25	1.45	9,666.06	46.61	45.60
12	294	300	258	1.16	52	47	32	42.76	0.82	5,747.93	1.35	7,740.55	58.90	47.70
13	218	485	453	1.07	74	67	30	52.98	0.72	8,823.27	3.05	26,910.97	112.93	112.70
14	328	250	186	1.34	57	40	43	46.11	0.81	6,682.62	1.33	8,910.16	72.48	63.47
15	296	285	213	1.34	54	47	22	38.22	0.71	4,591.49	1.47	6,734.19	65.26	57.76
16	224	375	314	1.19	66	54	23	43.44	0.66	5,930.91	1.33	7,907.88	44.27	42.05
17	211	295	281	1.05	61	48	28	43.44	0.71	5,931.49	1.40	8,304.09	37.83	36.20
18	198	195	140	1.39	51	40	28	38.51	0.76	4,661.62	1.46	6,805.96	43.48	41.24
19	227	225	235	0.96	54	45	35	43.98	0.81	6,078.47	1.43	8,692.21	39.38	44.11
20	218	195	166	1.17	53	44	25	38.78	0.73	4,725.60	1.28	6,064.52	36.65	37.76
21	195	225	196	1.15	55	45	23	38.47	0.70	4,651.00	1.26	5,844.76	30.92	30.56
22	205	165	152	1.09	49	37	22	34.17	0.70	3,669.09	1.81	6,628.82	37.89	38.14
23	184	195	220	0.89	51	58	20	38.97	0.76	4,771.96	2.07	9,877.95	44.18	44.40
24	201	170	112	1.52	53	41	31	40.69	0.77	5,203.46	1.44	7,510.32	49.94	50.42
25	194	280	258	1.09	62	49	22	40.58	0.65	5,176.28	1.42	7,333.07	34.05	32.18
Av	276.12	357.48	329.28	1.13	60.08	50.56	29.16	44.22	0.74	6,293.18	1.86	12,319.04	78.68	71.77

they have low efficiency and high flesh loss. Effective peeling, according to Adetan et al. (2003), is dependent on the proper application of the engineering properties in the development of the processing machines. Peel thickness, geometric mean diameter and sphericity are among the properties of cassava that vary across cassava varieties as functions of mass of peel. Theoretical determination of mass of peel of cassava varieties became imperative as this formed the basis for the evaluation of the flesh loss and peeling efficiency. Determination of mass of peel has been challenging. Most researchers in their works assumed mass of peel by manual method to be ideal with no flesh loss hence the yardstick for comparison of mass of peel by any peeling machine. The ratio of this mass of peel to the total mass of cassava tuber gives proportion by weight (ppw- percentage peeling weight). Oluwole and Adio (2013) obtained a value of 0.163 (16.3%). However, Adetan et al. (2003) observed that the percentage by weight of peel ranged from 10.6-21.5%, Kazeen et al.(2013) had 17.36-24.09 % and Ademosun et al. (2012) ranged from 13.12-20.06%. These varying PPW necessitated the need to establish and validate a theoretical mass of peel in the evaluation of machine performance parameters.

The objective of this study is to determine physical properties of five varieties of cassava roots, namely: Umudike Cassava (UMUCAS) 36, UMUCAS 37 and UMUCAS 38) also known as Tropical Manihot specie (TMS) 01/1368, TMS 01/1412, TMS 01/1371, respectively. Likewise TME 419 and TMS 30572 were also part of the five cassava varieties considered which were all used for establishing percentage peel mass of each cassava variety as it affects peeling mechanization, applicable in the subsequent designs of cassava peeling machines to increase efficiency and reduce tuber flesh losses.

Materials and Mthods

The tuber samples were accessed from National Root Crop Research Institute Umudike (NRCRI). They were randomly harvested 12 months after planting, sorted and cleaned from dirt. Twenty five (25) samples each of the varieties (marked 1-25) were selected randomly for the experiment. The experiment was conducted at the post-harvest Laboratory of Agricultural and Bio-Resources Engineering Department, College of Engineering and Engineering Technology (CEET), Michael Okpara University of Agri-

Table 2 UMUCAS 37 Variety

Sample	L (mm)	M_c (g)	V_c (cm^3)	ρ_s (g/cm^3)	R_{th} (mm)			GMD (mm)	Sphericity ϕ	Sa (mm^2)	P_{th} (mm)	V_p (mm^3)	M_{Pt} (g)	M_{Pa} (g)
					a	b	c							
1	490	326	346	0.94	78	63	28	51.63	0.66	8,376.32	2.92	24,458.86	157.97	89.88
2	401	1,666	1683	0.98	83	61	39	58.23	0.70	10,657.12	2.87	30,550.40	151.52	116.76
3	320	423	486	0.87	79	71	48	64.57	0.82	13,104.16	2.75	35,992.75	129.70	122.18
4	336	458	476	0.96	66	45	28	43.65	0.66	5,987.80	3.18	19,021.26	98.90	71.38
5	355	420	490	0.85	74	56	29	49.35	0.67	7,653.67	2.50	19,159.69	83.91	63.51
6	325	1,212	1,309	0.93	84	66	33	56.77	0.68	10,128.60	1.83	18,569.10	71.48	67.05
7	245	1,140	1,148	0.99	73	70	41	59.39	0.81	11,086.50	2.43	26,903.24	92.59	94.19
8	298	519	600	0.87	40	47	31	38.77	0.97	4,724.30	1.82	8,598.23	56.21	39.01
9	266	1,008	1,017	0.99	69	63	44	57.62	0.84	10,433.25	2.56	26,743.89	104.05	103.38
10	271	1,395	1,421	0.98	43	37	30	36.27	0.84	4,135.41	3.50	14,473.95	90.52	75.42
11	220	1,215	1,200	1.01	56	60	28	45.48	0.81	6,501.14	2.33	15,147.66	63.59	59.81
12	348	910	930	0.97	33	30	16	25.11	0.76	1,982.26	2.32	4,592.24	49.25	22.37
13	297	699	687	1.01	40	47	31	38.77	0.97	4,724.30	1.95	9,196.64	69.97	56.23
14	255	201	247	0.81	75	72	34	56.84	0.76	10,152.50	2.00	20,271.16	59.54	54.33
15	310	1,070	1,086	0.98	49	48	16	33.51	0.68	3,529.36	2.20	7,776.36	54.19	29.72
16	396	479	491	0.96	83	73	29	56.01	0.67	9,859.55	2.54	25,043.27	126.29	93.76
17	305	135	153	0.89	66	36	27	40.03	0.61	5,036.53	2.00	10,073.06	44.50	34.96
18	155	114	127	0.86	72	64	36	54.95	0.76	9,488.58	2.35	22,329.79	43.14	44.89
19	167	395	457	0.86	48	44	28	38.96	0.81	4,770.45	2.94	14,025.12	43.30	42.28
20	198	135	154	0.88	36	34	13	25.15	0.70	1,988.27	2.92	5,812.36	30.83	29.87
21	167	251	282	0.89	30	27	17	23.97	0.80	1,805.57	2.34	4,219.01	21.51	18.65
22	228	175	207	0.85	74	64	42	58.37	0.79	10,709.40	1.93	20,669.15	55.34	54.15
23	308	340	374	0.91	68	34	20	35.89	0.53	4,048.90	2.05	8,300.23	38.72	29.43
24	236	965	1004	0.96	69	60	20	43.59	0.63	5,970.51	1.89	11,284.27	42.27	42.30
25	230	445	532	0.83	67	63	32	51.31	0.77	8,273.73	1.87	15,444.30	46.31	49.99
Av	285.08	430.24	467.65	0.92	62.20	53.40	29.60	45.77	0.75	7,005.13	2.40	16,746.24	73.02	65.79

culture, Umudike. Moisture content was determined by randomly selecting 3 samples of each cassava tuber variety. The cleaned tuber samples were sliced transversely with a knife to a thickness of 5mm and set on the sliding plate. The sample was weighed using a sensitive weighing balance of 0.0l g accuracy. The moisture content was determined by dehydrating the samples at 105 °C for 24 hrs in a drying oven (AOAC, 2005). After which the samples were taken out, cooled in a desiccator, and then weighed again. The loss of weight in the sample was used to calculate the moisture content using the expression given by Del Nobile et al. (2007) as shown in Equation (1). Three replications of this process were carried out and the average was taken to be the moisture content of the variety.

$$M_c\% = [(W_w - W_d)] / W_w \times (100 / 1) \quad (1)$$

where,

W_w = weight of wet sample (g)

W_d = weight of dried sample (g)

M_c = moisture content on wet basis (%)

The length of tuber used in grading of the samples were measured using a measuring tape; size and thickness (measured at three parts of the tuber: the major diameter, a, the intermediate diameter, b, and the minor diameter, c) of cassava tuber was determined using a Vernier caliper. These measurements were taken for the unpeeled cassava after which the cassava was peeled carefully and the corky periderm together with the cortex (the peel) dimensions were measured and recorded. Then, the geometric mean diameter of the cassava was calculated using the expression given in Equation (2) as given by (Mohsenin, 1980; Simonyan and Ehiem,2012; Nwachukwu and Simonyan, 2015). This has been investigated by Nwachukwu et al. (2015) to be a characteristic property of cassava tuber variety. Mean value of GMD accounts for the morphological disparities in cassava tuber during evaluation.

$$GMD = (a \times b \times c)^{1/3} \quad (2)$$

where,

GMD= Geometric Mean Diameter, mm

a = major diameter (head), mm

b = intermediate diameter (middle), mm

c = minor diameter (tail), mm

Shape and sphericity which evaluates the degree of roundness of the cassava tubers was determined using the expression given by Koocheki et al. (2007) as:

$$\text{Sphericity}, \varphi = GMD / a \quad (3)$$

Thereafter, the surface area of the tubers was calculated using the expression given by Nwachukwu and Simonyan (2015) as:

$$S_a = \pi \times GMD^2 \quad (4)$$

Table 3 UMUCAS 38 Variety

Sample	L (mm)	M_c (g)	V_c (cm^3)	ρ_s (g/cm^3)	R_{th} (mm)			GMD (mm)	Sphericity ϕ	Sa (mm^2)	P_{th} (mm)	V_p (mm^3)	M_{Pt} (g)	M_{Pa} (g)
					a	b	c							
1	243	388	388	1.00	51	60	33	46.57	0.91	6,815.56	2.43	17,720.45	81.23	82.40
2	259	480	474	1.01	41	38	34	37.56	0.92	4,433.11	2.47	11,526.09	70.25	64.27
3	478	256	238	1.08	74	66	42	58.98	0.80	10,931.87	3.06	39,573.36	238.81	197.93
4	457	615	510	1.21	73	47	24	43.51	0.60	5,948.84	2.71	16,716.24	134.10	123.73
5	216	2,033	1,960	1.04	63	61	58	60.63	0.96	11,554.29	2.37	31,312.13	97.30	93.60
6	598	758	770	0.98	80	54	28	49.46	0.62	7,687.27	2.38	20,448.14	146.99	141.02
7	314	416	246	1.69	56	48	24	40.11	0.72	5,055.58	2.52	14,509.53	128.34	124.09
8	250	189	151	1.25	51	42	24	37.18	0.73	4,345.42	2.92	15,817.32	81.56	82.06
9	339	473	443	1.07	63	46	26	42.24	0.67	5,606.94	2.36	13,849.13	80.88	78.76
10	263	409	346	1.18	71	62	38	55.10	0.78	9,541.87	2.27	29,007.28	98.11	101.49
11	444	1,018	979	1.04	62	62	32	49.73	0.80	7,773.80	2.52	20,989.26	152.32	159.44
12	186	302	348	0.87	49	40	25	36.59	0.75	4,208.64	3.27	14,141.03	47.08	47.06
13	353	392	367	1.07	51	46	25	38.85	0.76	4,744.49	2.43	13,426.91	89.33	86.69
14	200	404	375	1.08	48	43	23	36.21	0.75	4,120.68	1.76	8,076.54	34.10	40.46
15	378	977	805	1.21	52	46	32	42.46	0.82	5,666.11	2.07	13,655.33	105.43	109.27
16	195	934	868	1.08	68	58	31	49.63	0.73	7,742.42	2.58	25,162.87	65.07	70.90
17	205	686	625	1.10	58	57	41	51.37	0.89	8,293.46	2.02	17,499.19	65.79	79.31
18	360	1,226	1,112	1.10	50	38	22	34.71	0.69	3,785.55	1.99	7,381.82	63.07	57.84
19	267	333	374	0.89	86	75	43	65.21	0.76	13,366.87	1.85	28,337.77	71.27	71.33
20	321	786	708	1.11	83	74	46	65.62	0.79	13,532.86	2.37	36,538.71	141.80	138.48
21	210	615	510	1.21	46	43	25	36.70	0.80	4,234.37	2.63	11,940.92	63.55	66.96
22	276	807	778	1.04	78	62	37	56.35	0.72	9,980.13	2.11	22,654.91	80.79	77.06
23	537	974	911	1.07	67	57	24	45.09	0.67	6,389.28	3.23	23,832.00	193.69	188.62
24	243	337	312	1.08	53	42	28	39.65	0.75	4,940.83	2.02	10,276.92	51.11	51.62
25	410	541	549	0.99	58	43	21	37.41	0.65	4,399.68	2.39	11,747.16	79.50	78.83
Av	320.08	497..96	452.69	1.10	61.28	52.40	31.44	46.28	0.76	7,004.00	2.43	19,045.64	98.46	96.37

Fig. 2 Cylindrical Model

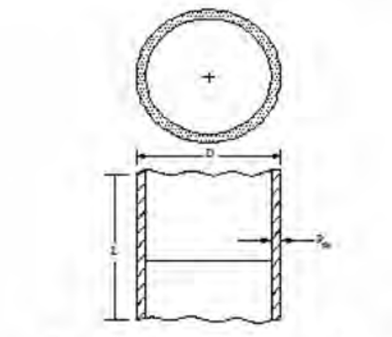

where,

S_a = Surface area, mm^2

The mass of individual sample for both the peeled and the unpeeled cassava tuber was determined using sensitive weighing balance of 0.0lg accuracy. The volume of each tuber was determined experimentally using water displacement method as given by Hughes (2005). A displacement device with a flow path created closer to the top was used. Water was poured into the device until it reaches the flow point. The excess water was allowed to flow out until it stopped. The cassava tuber was put inside water proof nylon and placed in the displacement device. An amount of water displaced was collected and its value read from a measuring cylinder. The volume of displaced water was taken as the volume of the tuber. The average volume used was determined from 25 replications. The ratio of mass to the volume was used to determine the true density for each of the 25 samples of the cassava tubers (varieties) as shown in Equation (6).

$$\rho_s = M_c / v_c \qquad (6)$$

where,

ρ_s = True density, g/cm^3

M_c = mass of tuber, g

v_c = volume of tuber, cm^3

The theoretical mass of peel was developed from basic mass as shown in Equation (7) for a cylindrical configuration modeled with D as diameter; L as length of tuber and Pth as peel thickness (**Fig. 2**).

$$m = \rho v \qquad (7)$$

where,

m = mass of peel, g

ρ = density of peel, g/cm^3

v = volume of peel, cm^3

$$v = S_a \times P_{th} = \pi D L P_{th} \qquad (8)$$

Taking, D, as Geometric mean diameter (GMD), Dg, expressed in Equation (2), which is a dimensional property that takes care of the variation in the tuber thickness along the full length. Assuming ρ, density of peel = ρ_s, density of cassava (Equation 6) and since cassava tuber is not perfectly round as projected by the model, the shape factor known as sphericity expressed in Equation (3) was introduced. Integrating all these, the theoretical mass of peel was therefore, formulated mechanistically from Equation (7) as:

$$m_p = \pi \varphi \rho_s D_g L P_{th} \qquad (9)$$

Table 4 TMS 30572 Variety

Sample	L (mm)	M_c (g)	V_c (cm^3)	ρ_s (g/cm^3)	R_{th} (mm)			GMD (mm)	Sphericity ϕ	Sa (mm^2)	P_{th} (mm)	V_p (mm^3)	M_{Pt} (g)	M_{Pa} (g)
					a	b	c							
1	340	250	186	1.34	85	81	55	72.35	0.85	16,450.87	1.87	30,817.96	168.70	157.40
2	314	285	245	1.16	65	63	51	59.33	0.91	11,063.53	2.12	23,491.56	132.75	103.84
3	290	375	247	1.52	47	44	19	34.00	0.72	3,632.57	2.43	8,815.03	89.06	50.86
4	461	295	273	1.08	79	67	60	68.23	0.86	14,630.07	2.28	33,356.57	211.68	136.97
5	220	195	140	1.39	47	44	31	40.02	0.85	5,034.46	2.17	10,924.77	72.37	57.82
6	460	225	196	1.15	66	66	53	61.35	0.93	11,828.24	2.36	27,954.08	224.82	121.94
7	355	280	258	1.09	67	67	47	59.53	0.89	11,138.91	2.02	22,537.73	131.34	92.95
8	263	610	565	1.08	62	54	43	52.41	0.85	8,633.37	2.76	23,856.88	110.48	97.88
9	298	305	273	1.12	51	48	24	38.88	0.76	4,749.99	2.26	10,719.15	73.80	55.51
10	286	645	575	1.12	53	53	43	49.43	0.93	7,679.94	2.76	21,222.24	129.07	90.46
11	265	410	396	1.04	66	63	43	56.34	0.85	9,975.00	2.47	24,671.51	104.37	97.07
12	225	921	1,035	0.89	57	45	44	48.33	0.85	7,340.14	2.22	16,270.65	57.55	55.02
13	198	820	806	1.02	63	64	43	55.76	0.89	9,772.46	2.05	20,033.53	65.09	67.45
14	258	575	500	1.15	63	68	48	59.02	0.94	10,949.77	2.64	28,943.88	137.79	126.48
15	322	545	534	1.02	56	58	44	52.28	0.93	8,591.26	2.23	19,187.15	113.42	74.41
16	354	480	356	1.35	73	69	47	61.86	0.85	12,027.93	2.26	27,143.03	180.73	139.07
17	365	240	190	1.26	83	75	37	61.30	0.74	11,809.69	1.73	20,391.40	120.11	97.88
18	240	545	405	1.35	65	64	41	55.46	0.85	9,666.35	2.18	21,040.42	106.82	107.59
19	263	435	382	1.14	62	54	43	52.41	0.85	8,633.37	2.12	18,331.52	89.54	79.32
20	235	340	270	1.26	67	63	32	51.31	0.77	8,274.11	3.07	25,401.52	118.07	121.55
21	275	580	491	1.18	59	54	28	44.68	0.76	6,275.00	2.36	14,829.91	85.88	66.57
22	366	1,790	1,685	1.06	54	51	28	42.56	0.79	5,694.11	2.37	13,476.06	101.06	54.40
23	363	425	300	1.42	53	52	46	50.24	0.95	7,931.75	1.97	15,651.99	152.16	84.26
24	349	410	272	1.51	54	51	20	38.05	0.70	4,549.95	2.36	10,753.06	114.71	61.59
25	230	500	514	0.97	58	57	38	50.08	0.86	7,883.80	2.31	18,185.29	71.43	67.22
Av	303.80	499.24	419.76	1.19	62.20	59.00	40.32	52.61	0.85	8,968.67	2.30	20,320.27	118.51	98.62

Therefore, Equation (9) is the theoretical mass of peel model while the percentage mass of peel is given as:

$$\%M_{pt} = (M_{pt} / M_c) \times 100 \qquad (10)$$

Analysis Procedure

In order to understand the contributions of the physical parameters of the various cassava tubers to the mass of peel, a statistical modelling technique known as linear regression was employed. Aanalysis of variance was employed in testing the adequacy of the fitted models to be true approximations of the measured data.

Results and Discussion

Moisture content of the test varieties determined from Equation (1) are 72.69%, 84%, 73.83%, 63.5% and 63.33%, for UMUCAS 36,UMUCAS 37, UMUCAS 38 TMS 30572 and TME 419 respectively. Experimental results of the measured and determined physical properties of cassava tuber varieties were tabulated in **Tables 1-5**. From these tables, UMUCAS 36 had 21.90% mass of peel and an average peel thickness of 1.6 mm; UMUCAS 37 recorded 16.97% mass of peel and an average peel thickness of 2.4 mm; UMUCAS 38 had an average peel thickness of 2.44 mm and 19.77% mass of peel. TME 419 had percentage mass of peel of 19.13% and an average peel thickness of 2.33 mm while TMS 30572 recorded high peel mass of 23% and 2.3 mm for average peel thickness. TMS30572, therefore, is suitable for animal production.

Theoretical mass of peel, M_{pt} in column 14 of **Tables 1-5** for the evaluation of the cassava attrition peeling machine was determined from the developed model expressed in Equation (9) while the actual mass of peel M_{pa} (column 15) was measured directly after carefully removing cassava peel by manual method. Ratio of its average value to the average mass of unpeeled cassava gives the percentage peel mass (determine from Equation 10). Tuber mass, length, volume, root and peel thickness were measured while geometric mean diameter, sphericity and surface area were determined from Equations 2 to 4, respectively. The generated data was subjected to regression analysis and fitted linear regression models was established as shown in Equations (11) to (15) for predicting the mass of peel for UMUCAS 36, UMUCAS 37, UMUCAS 38, TME 419, TMS 30572 and Mixed variety, respectively. These model predicted the mass of peel by relating it to the length of cassava tubers (L), mass of cassava tubers

Table 5 TME 419 Variety

Sample	L (mm)	M_c (g)	V_c (cm^3)	ρ_s (g/cm^3)	R_{th} (mm)			GMD (mm)	Sphericity ϕ	Sa (mm^2)	P_{th} (mm)	V_p (mm^3)	M_{Pt} (g)	M_{Pa} (g)
					a	b	c							
1	329	830	721	1.15	69	63	30	50.71	0.73	8,082.61	2.66	21,472.80	125.50	106.79
2	278	545	507	1.07	67	50	25	43.75	0.65	6,016.37	2.85	17,146.64	82.74	79.63
3	390	1000	916	1.09	80	70	27	53.27	0.67	8,920.29	3.33	29,674.83	174.90	139.95
4	371	715	662	1.08	68	60	32	50.73	0.75	8,088.81	3.74	30,225.18	187.24	184.03
5	282	835	726	1.15	74	67	42	59.27	0.80	11,042.01	3.37	37,174.78	167.68	146.71
6	409	630	567	1.11	54	46	24	39.06	0.72	4,796.45	3.28	15,748.33	140.22	125.59
7	240	565	225	2.51	63	54	33	48.24	0.77	7,314.36	2.83	20,724.03	205.47	204.81
8	317	620	560	1.11	58	54	32	46.45	0.80	6,781.50	2.57	17,428.45	108.97	93.36
9	260	445	413	1.08	58	51	22	40.22	0.69	5,085.01	2.86	14,543.12	76.26	67.69
10	228	630	547	1.15	67	70	50	61.67	0.92	11,951.97	3.31	39,521.19	156.57	156.64
11	276	470	428	1.10	65	48	22	40.94	0.63	5,269.01	2.90	15,280.14	78.30	72.49
12	255	380	298	1.28	52	49	24	39.40	0.76	4,878.48	2.42	11,822.19	78.18	65.13
13	356	645	600	1.08	58	47	30	43.41	0.75	5,921.65	3.23	19,107.18	130.70	113.73
14	251	495	388	1.28	61	55	32	47.53	0.78	7,099.69	2.87	20,399.78	111.15	112.43
15	290	665	598	1.11	69	64	35	53.67	0.78	9,051.96	3.18	28,785.22	140.38	138.28
16	162	340	305	1.11	61	55	25	43.77	0.72	6,022.35	2.44	14,714.61	46.77	45.86
17	325	485	378	1.28	54	47	23	38.79	0.72	4,729.60	2.73	12,911.80	106.23	79.57
18	236	475	427	1.11	64	63	26	47.15	0.74	6,987.80	2.58	18,051.81	80.09	81.75
19	221	455	374	1.22	53	63	31	46.95	0.89	6,928.88	2.67	18,523.21	98.06	97.35
20	267	535	459	1.17	70	51	32	48.52	0.69	7,399.85	2.94	21,780.24	101.77	101.67
21	298	740	685	1.08	76	63	22	47.23	0.62	7,010.18	3.62	25,400.20	122.26	118.54
22	295	755	700	1.08	64	60	35	51.22	0.80	8,246.64	2.96	24,437.55	125.70	113.87
23	193	320	278	1.15	55	53	40	48.85	0.89	7,501.42	2.58	19,378.67	79.04	76.36
24	295	290	268	1.08	50	35	20	32.71	0.65	3,362.97	2.12	7,118.29	48.62	43.28
25	217	275	214	1.29	50	44	31	40.86	0.82	5,246.47	2.46	12,888.83	73.30	71.55
Av	281.64	565.60	471.76	1.20	62.40	55.28	29.80	46.58	0.75	6,949.45	2.90	20,570.36	113.84	105.88

(M), true density (ρ), geometric mean diameter of the tubers (GMD), surface area (SA), peel thickness (P_{th}) and sphericity of the tubers (φ) above 98% interval.

$$M_{p(UMUCAS\ 36)} = -68.86 + 17.84\rho + 0.9088D_g + 10.338P_{th} \quad (11)$$

$$M_{p(UMUCAS\ 37)} = -25.40 + 0.00845L + 9.52\rho + 0.002205SA + 5.930P_{th} \quad (12)$$

$$M_{p(UMUCAS\ 38)} = -62.61 + 19.20\rho + 0.9099D_g + 8.25P_{th} \quad (13)$$

$$M_{p(TMS\ 30572)} = -43.54 + 12.38\rho + 0.6409Dg + 7.918Pth \quad (14)$$

$$M_{p(TME\ 419)} = 11.48 + 20.611\rho - 1.324D_g + 0.008010SA + 7.055P_{th} - 4.20\varphi \quad (15)$$

$$M_{p(MIXED)} = -143.6 + 21.35P_{th(TMS\ 30572)} - 0.02042M_{(UMU\text{-}36)} + 1.997D_{g(UMU\text{-}36)} - 0.00354SA_{(UMU\text{-}36)} + 17.35P_{th(UMU\text{-}36)} + 8.09\rho_{(UMU\text{-}37)} - 3.242D_{g(UMU\text{-}37)} + 0.01401SA_{(UMU\text{-}37)} - 0.02430L_{(UMU\text{-}38)} + 4.389D_{g(UMU\text{-}38)} - 0.01160SA_{(UMU\text{-}38)} + 1.723D_{g(TME\ 419)} - 9.04P_{th(TME\ 419)} - 35.3\varphi_{(TME\ 419)} \quad (16)$$

Inspection of the regression models developed, it can be seen that the true density, geometric mean diameter and peel thickness are main determinant for the mass of peel of all the cassava varieties while the significant contributions of length of cassava, surface area and sphericity impact on the mass of peel obtained for TME 419 and UMUCAS 37 cassava varieties. Also analysis of variance of the regression models shows that the predictability of the reduced models is within 95% confidence interval with the residual sum of squares (R^2 and R^2adj) so close to 100%.

Table 6 present the results of the mean values of theoretical, actual mass of peel and regression model prediction of mass of peel of cassava varieties under study. It is evident from the Analysis of Variance result as shown in **Table 7**, that there is no significant variation in predicted, theoretical and actual values of mass of peel across the cassava varieties since the respective P-value for the cassava varieties and percentage mass of peel are 8.96E-06 and 0.017225, respectively, which are less than the α-value of 0.05.

Table 6 Predicted, theoretical and actual peel mass for the test varieties

Sl. No.	Cassava variety	Percentage Mass of peel (%)		
		Predicted	Theoretical	Actual
1	UMUCAS 36	21.85	21.90	20.31
2	UMUCAS 37	15.07	16.97	15.29
3	UMUCAS 38	20.72	19.77	19.35
4	TMS 30572	23.51	23.73	22.75
5	TME 419	20.54	19.13	18.92

Table 7 ANOVA of predicted, theoretical and actual peel mass

	Count	Sum	Average	Variance
UMUCAS 36	3	64.06	21.35333	0.817033
UMUCAS 37	3	47.33	15.77667	1.080133
UMUCAS 38	3	59.84	19.94667	0.492633
TMS 30572	3	69.99	23.33	0.2644
TME 419	3	58.59	19.53	0.7761
Predicted	5	101.69	20.338	10.07157
Theoretical	5	101.5	20.3	6.7659
Actual	5	96.62	19.324	7.28668

ANOVA

Source of variation	SS	df	MS	Fcal	P-value	F_{tab}
Cassava Varieties	92.93969	4	23.23492	52.25872	8.96E-06	3.837853
% Mass of peel	3.303693	2	1.651847	7.715243	0.017225	4.45897
Error	3.556907	8	0.444613			
Total	99.80029	14				

Conclusions

Physical properties of five cassava varieties were studied. The results obtained were used to evaluate mass of peel required in the performance evaluation of cassava processing machines, especially cassava peeling machines, as it regards selection of peeling method, materials, time and cost. Results obtained showed that TME 419 cassava variety at 63.33% moisture content had an average mass of 585.6 g, percentage mass of peel of 19.13%, and average peel thickness of 2.33 mm. TMS 30572 cassava variety at 63.5% moisture content recorded 499.24 g, 23% and 2.3 mm for average mass, mass of peel and average peel thickness, respectively; UMUCAS 36 had average mass of 357.48 g, 21.90% mass of peel and average peel thickness of 1.6 mm at 72.69% moisture content; while UMUCAS 37 at 84% moisture content recorded 16.97% mass of peel, 2.4mm average peel thickness and 4303.24 g average mass; and UMUCAS 38 had average mass of 497.96 g, average peel thickness of 2.44 mm and 19.77% mass of peel at 73.83% moisture content. ANOVA result revealed that the models can approximate the actual response (mass of peel) of the cassava varieties within an acceptable error of ±5%. This, therefore, would possibly make the cassava peeling system designs accommodate different cassava varieties and tuber sizes by just adjusting some necessary parameters.

REFERENCES

A. O. A. C. 2005. Official Methods of Analysis. Association of Official Analytical Chemists, Washington DC, USA, 2005, 18th edition.

Abdulkadir, B. H. C. 2012. Design and Fabrication of a Cassava Peeling Machine”. IOSR Journal of Engineering (IOSRJEN) ISSN: 2250-3021 Vol. 2, Issue 6, pp. 01-08.

Ademosun, O. C., M. O. Jimoh and O. J. Olukunle. 2012. Effect of physical and mechanical properties of cassava tubers on theperformance of an automated peelingmachine International Journal of Development and Sustainability Volume 1 Number 3 (2012): Pages 810-822.

Adetan, D. A., L. O. Adekoya and O. L. Aluko. 2003. Characterization of some properties of cassava root tubers. Journal of Food Engineering. 59: 349-353.

Del Nobile, M. A., S. Chillo, P. M. Falcone, J. Laverse, S. Pati and A. Baiano. 2007. Textural Changes of CanestrelloPugliese Measured During Storage” J. F. ENG, 83: 621-628.

Food and Agriculture Organization. 1990. “Toxic Substances and Ant nutritional Factors of Roots, Tuber, Plantains and Banana in Human Nutrition”. Rome, United Nations, Ch.7 http://www.fao.org/docrep/t0207e/T0207E08.htm#Cassava%20toxicity. Retrieved 25th June, 2011.

Hughes, S. W. 2005. Archimedes Revisited: A Faster, Better, Cheer Model of Accurately Measuring the Volume of Small Objects”. Physics Education 40(5): 468-474. Bibcode: 2005PhyEd.$0..46811. DOI: 10.1088/0031-9120/40/008.

Koocheki, A., S. M. A. Razari, E. Milani, T. M. Moghadam, M. Abedini, S. Alamatiyan and S. Izadikhah. 2007. Physical Properties of Water Melon Seed as a function of Moisture Content and Variety”. International Agro Physics, 21: 349-359.

Mohsenin, N. N. 1980. “Physical Properties of Plants and Animal Materials”. Gordon Breach Science Publishers. New York, USA.

Nwachukwu, I. D. and K. J. Simonyan. 2015. Some Engineering Properties of Cassava Tuber related to its peeling Mechanization. Umudike Journal of Engineering and Technology (JET), Vl/ 1.No.1.pp 12-24.

Olukunle, O. J. and B. O. Akinnuli. 2013. “Theory of an Automated Cassava Peeling System”. International Journal of Engineering and Innovation Technology (Ijeit) Vol. 2, Issue 8, ISSN: 2277-3754 ISO 9001:2008 Certified.

Olukunle, O. J., O. C. Ademosun, A. S. Ogunlowo, A. S. Agbetoye and A. Adesina. 2006. Development of a double action cassava peeling machine. International Conference on prosperity and poverty in globalised world: challenges for agricultural research (www.twopentag.com).

Oluwole, O. O. and M. A. Adio. 2013. Design and Construction of a Batch Cassava Peeling Machine. Journal of Mechanical Engineering and Automation, 3(1): 16-21.

Simonyan, K. J. and J. C. Ehiem. 2012. Physical Properties of Wild Mango Fruit and Nut”. International Agrophys, 26, 95-98 DOI: 10.2478/v10247-012-0014-x.

Stephen, K. O. 1998. “Cassava”. Tropical Research and Education Centre, University of Florida. Revised Edition. Pp. 25-30.

■■

Design Modification and Comparative Analysis of Cassava Attrition Peeling Machine

by
J. C. Edeh*
Department of Mechanical Engineering,
Michael Okpara University of Agriculture,
Umudike, NIGERIA
*Corresponding author:
engredehjohnc@gmail.com

B. N. Nwankwojike
Department of Mechanical Engineering,
Michael Okpara University of Agriculture,
Umudike, NIGERIA

F. I. Abam
Department of Mechanical Engineering,
Michael Okpara University of Agriculture,
Umudike, NIGERIA

Abstract

An improved cassava attrition peeling machine was developed by modifying an existing cassava peeler. Comparative analysis was carried out on the test result which showed significant differences in the quantity and quality of peeled cassava in the existing attrition peeling methods and the modified technique. The results revealed that the modified machine performed well by giving an efficiency of 75.4%, throughput of 119 kg/h, tuber flesh loss of 5.88% and specific energy consumption of 57.1 kJ/kg. The average processing time of 17.5 min/batch and cost of N6.25/kg (1$ US ≈ 360 N) resulted in 42.3% and 25% improvement respectively. This improved technique eliminated pre-operational activities of trimming, sorting and grading of cassava tubers that characterised other techniques. Its operation was made simple requiring little or no skills from the operator while all materials used for fabrication were sourced locally to make the machine affordable for small scale processing industry

Keywords: Attrition peeling, cassava tuber, efficiency, flesh loss, pre-operational activity

Introduction

Cassava is the third-largest source of carbohydrates for meals in the world and Nigeria is one of the largest producers with over 34 million tonnes of tubers produced annually (Ajibola, 2000; Echebiri and Edaba, 2008; Kolawole et al, 2010). However, its food security, economic and industrialization potentials are underutilized in Nigeria due to inadequate mechanization of the processing operation, its perishable nature and high content of toxic cyanogenic glucoside especially in the peels. Adequate mechanised processing minimises or eliminates the drudgery associated with the post-harvest processing operations

Several unit operations as shown in **Fig. 1** are involved in the processing of cassava into various desired products (Odigbo, 1983a), and these according to Kolawole et al. (2010), Igbeka et al. (1992), Jimoh and Olukunle (2012) depending on the end product include peeling, washing, grating, boiling, parboiling, drying, milling, pressing, sieving, extrusion and frying.

Meanwhile, other cassava processing operations have been commercially mechanized successfully but cassava peeling which obviously from the flow diagram above is the first post-harvest processing operation has remained according to Olukunle and Jimoh (2012) and Egbeocha et al. (2016) a serious global challenge to the sector as it is yet to be successfully mechanised. The major problem associated with the peeling operation of cassava is that cassava roots exhibit appreciable differences in weight, size and shape (dimensional disparities across varieties) and this limits its mechanical peeling efficiency.

The efforts made by (Ezekwe, 1979; Nwokedi, 1984; Odigboh, 1983b; Ohwovoriole et al., 1988; Ejovo et al., 1988; Igbeka, et al., 1992; IITA, 2006; Olukunle et al., 2006; Adetan et al., 2006; Oluwole and Adio, 2013) towards mechanizing the cassava peeling process were acknowledged. The works of (Ejovo et al., 1988; Adetan et al., 2006; Jimoh and Olukunle, 2012) were based on knife edge peeling mechanism as most of the research efforts at developing a suitable cassava peeling machine have concentrated on the use of abrasive mechanism to achieve peeling (Ezekwe, 1979; Odigboh, 1983b; Nwokedi, 1984; Akintunde, 2005; IITA, 2006; Olukunle et al., 2006; Oluwole and Adio, 2013; Ugwu and Ozioko, 2015). The methods of mechanized knife edge for cassava peeling are adversely characterised by pre-operational activities which is associated with high tuber flesh loss. Egbeocha et al. (2016) in their study on performance of cassava peeling machines in Nigeria reported high tuber flesh losses (25-42 %) for knife-edge operated peelers due to the high speed, design and positioning of the knives in addition to preoperational activities but further confirmed attrition peeling to be more promising with great attention to its inherent advantage of improved efficiency at low speed of 60 rpm and improved abrasive surface. Though, common problem with these attrition machines is low output. In addition to this, tuber may be reduced to a uniform cylinder with considerable wastage of useful flesh before satisfactory peeling could be achieved. Among the outstanding of these attrition based innovations is the cassava attrition peeling machine developed by Projects Development Institute (PRODA), Enugu. This existing cassava attrition peeling machine consist of the peeling unit, discharge unit, washing unit, prime mover (electric motor), rounded cylindrical shaped peeling/nibbling balls was developed as an attempt to address the problem of pre-operational treatments and reduction in tuber flesh loss during mechanized peeling of cassava. The peeling balls together with the expanded metal lining of the drum provide the rough surfaces to effect peeling as the cylindrical peeling drums impacts rotational motion on the balls freely mixed with the cassava and consequently creating tumbling effect in the drum that gives random relative motion thereby causing the shredding of the cassava peels. The rounded cylindrical shape of the balls makes it possible for depressions on the surface of the cassava to be engaged.

However, problems with the PRODA developed cassava peeling machine are high peel retention especially with irregular shaped tubers; low operating speed (25 rpm) and poor frictional peeling drum surface resulting in more processing time for a batch. These shortcomings are attributed to insufficient design analysis stemming from inability to determine the appropriate shape (and number) of balls based on corresponding geometric attribute of tubers, frictional characteristics of the peeling surface, effect of speed variation on the performance indicator and failure to consider crop and operational parameters in the development of attrition peeling machine. For example, sphericity is a property of cassava that determines its degree of roundness (Koocheki et al., 2007) and for cassava tubers is usually less than one, this simply reveals that cylindrical shaped balls will not be suitable to effectively engaged recessed regions of tubers.

To address these deficiencies noticed in other types of cassava peeling machines available in the country, a modified cassava attrition peeling machine with appropriate shape of peeling balls, increased agitation by increasing peeling speed and improved peeling drum surface is needed.

Materials and Methods

Description of the Modified Machine

The machine comprises the frame, peeling unit, electric motor, water trough (bath) and peeled cassava discharging chute (**Fig. 2**). The frame is formed from 5 mm thick angle iron and served as the main supporting structure for mounting of other component parts of the machine. The peeling drum chamber consist mainly of a rolled perforated aluminum plate of 2,482 × 400 × 10 mm formed into a cylindrical drum and centrally mounted on a mild steel shaft which is 1,100 mm long by 45 mm diameter with three 400 mm long angular aluminum bars of 10 mm thickness welded to the inner

Fig. 1 Flow diagram of Unit Operations in Processing Cassava into Different Productsl

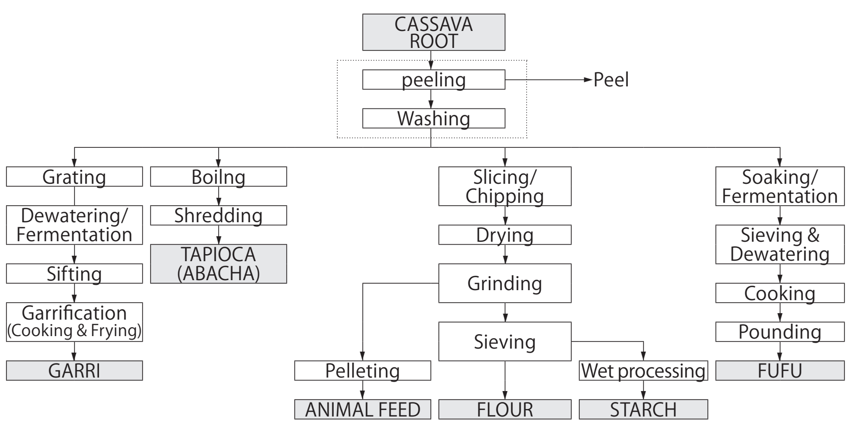

Sources: (Onwualu et al., 2006; Igbeka et al., 1992; Odigboh, 1983a) surface. The bars are equidistantly spaced acting as breaker baffles to check centrifugal effect thereby extending sticking speed. The perforations (6 mm hole) were made at regular interval of 4 hole/cm^2 such that the embossments inside enhance the frictional characteristics of the inner drum surface.

Design Concept of Modification

The identified design shortcomings for poor performance of an existing cassava peeler brought about the following modifications:

1 Replacing cylindrical rounded end peeling balls with egg shaped balls to provide more contact surface and easy access to the pronounced bend and recessed regions of cassava tubers
2. Introducing breaker baffles (3 inverted angular bars) equidistantly spaced in the inner walls of the peeling drum to enhance agitations and extend the sticking speed.
3. Improved inner peeling drum surface of embossed projections created by perforating regular 4 holes per cm^2 as peeling tools instead of expanded metal inner drum lining in the existing.

The design considerations upon the improvement were based on good abrasive surface for removal of the peel; uniform peeling at minimal useful tuber flesh loss; insensitivity and versatility to the size of tubers of different varieties, age, toughness and the thickness, accepting all sizes of tuber and peeling them to the economical depth thereby eliminating pre operational treatment; and capacity for high economic value of having a large throughput of peeled tubers which a batch machine achieve either by peeling small quantities very quickly or by accepting large quantity at a time or by both. In addition, simplicity of design, adequate automation and safety of operation since peeling machine will usually be manned by low grade labour were considered and the machine was fabricated with standard components (locally sourced without undermining the functional and environmental requirements) to ensure low cost of production and easy maintenance.

Design Analysis

Determination of Volume and Weight Capacity of the Peeling Drum

The volume capacity of the peeling unit, Vd depends on the radius of the drum which is limited by the sticking speed condition, quantity of cassava to be loaded per batch considering head space and as well the volume occupied by the shaft. Thus with head space of 20%, the volume capacity of the drum is calculated to be 0.18 m^3 using Equation (1).

$$V_d = \pi l\,(0.8r_d^2 - r_s^2) \quad (1)$$

where,
l = length of drum, m
rd = radius of drum, m
rs = radius of shaft, m

The effective weight capacity of the peeling unit, WT, was approximated to be 1500 N which was determined from the addition of maximum weight of cassava per batch (1000 N), weight of drum, W_d, (405 N) and estimated weight of peeling balls (0.5 N each) of 75 N.

Mass of the drum is given as:

$$Md = 2\pi r_d l t \rho_a \quad (2)$$

where,
t = thickness of drum, mm
ρ_a = density of aluminum, kg/m^3

In order to obtain 405 N as weight of drum, t = 10 mm, ρ_a = 2,830 kg/m^3

Selection of Pulleys and Belts

In peeling systems, increase in speed increases peeling efficiency but also increases tuber flesh loss and mechanical damage. According to Ezekwe (1979) and Odigboh (1983a), speed not more than 50 rpm is required in abrasive peeling of cassava and therefore maximum speed required is restricted by the sticking speed. Thus, the maximum speed of drum, Nd, selected for the design of the peeler was determined to be 49 rpm from sticking speed given by Ezekwe (1979) as:

$$\omega^2 r_d = g \quad (3)$$

where,
ω = angular velocity of the drum, rads^{-1}
r_d = radius of the peeling drum, m
g = acceleration due to gravity, 10 m/s^2

A gear electric motor of 1,440 rpm input speed rating having a reduction ratio of 1:8 together with 50 mm and 184 mm diameter pulleys were selected. Equation (4) given by Sharma and Aggarwal (2006) and

Fig. 2 Modified cassava attrition peeling machine

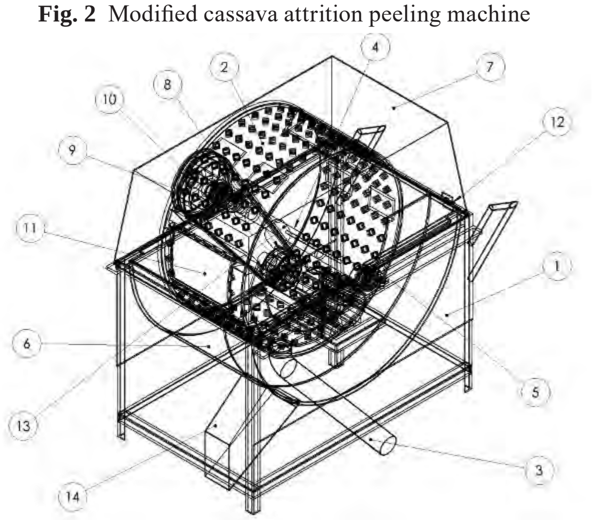

1. Structural Frame, 2. Peeling drum, 3. Discharge pipe, 4. Shaft, 5. Bearing, 6. Water bath (trough), 7. Covering hood, 8. Electric motor, 9. pulley, 10. Motor shaft, 11. Loading cover, 12. Hinges, 13.Belt, 14. Discharge spout

Khurmi and Gupta (2005) was used for obtaining the required speed of the peeling drum. Pulleys of larger diameters are required by this machine to obtain lower speeds during test run. Due to its availability, cost and performance, mild steel pulleys were selected

$$VR = N_1 / N_2 = D_2 / D_1 \quad (4)$$

where,

N_1 = speed of the driving pulley, rpm

N_2 = speed of the driven pulley, rpm

D_1 = diameter of the driving pulley, mm

D_2 = diameter of the driven pulley, mm

The design centre distance C, between the pulleys of the drive (electric motor/ drive shaft) is determined from the formula given by (Sharma et al., 2006; Khurmi et al., 2005) as:

$$C = (D_1 + D_2) / 2 + D_1 \quad (5)$$

C was obtained as 260 mm using Equation (5).

Thus the design length of the belt was computed as 905mm from the formula given by (Sharma and Aggarwal, 2006; Khurmi and Gupta, 2005) as:

$$L = 2C + 1.57(D_2 + D_1) + (D_2 - D_1)^2 / 4C \quad (6)$$

Since it is assumed that the drive transmits more than 3.75 kW, a type "B" V-belt was selected for the drive. According to IS: 2494-1974 standards, a V-belt of standard pitch length of 925 mm was selected as the minimum belt length for the drive. Consequently, the exact center distance between the pulleys in the drive was determined as 266 mm using Equation (6).

The angle of lap, (θ), of the drive was computed as 150° (2.62 rad) using Equation (7).

$$\theta = 180 - [2\sin^{-1}(D_2 - D_1) / 2C)] \quad (7)$$

The belt speed was determined as 0.47 m/s using Equation (8)

$$V = \pi (N_2D_2) / 60 \quad (8)$$

The coefficient of friction, μ, between the belt and pulley, maximum safe stress, σ, mass per unit length, m and the cross sectional area, a, of the belts were obtained from IS: 2494-1974 standards (Khurmi and Gupta, 2005) as 0.3, 2.1 N/mm², 0.144 kg/m and 140 mm² respectively.

Tension on the tight side, T_1 of the belt was determined as 294 N using Equation (9).

$$T_1 = T_{max} - T_c \quad (9)$$

$$T_{max} = \sigma a \quad (10)$$

$$T_c = mv^2 \quad (11)$$

where,

T_{max} = maximum tension of the belts, N

T_c = centrifugal tension, N

Thereafter, the slack side tension, T_2 was determined as 26.22 N using the expression given by Khurmi and Gupta (2005) as:

$$2.3\log (T_1 / T_2) = \mu\theta \operatorname{cosec} \beta \quad (12)$$

where,

2β = the groove angle 38°, β = 19°

Selection of Drive Shaft

The shaft diameter, d of the peeling drum, was determined using the expression given by (Sharma and Aggarwal (2006); Khurmi and Gupta, 2005) as:

$$d = [16/\pi\tau (\sqrt{((K_bM_b)^2 + (K_tM_t)^2)}]^{1/3} \quad (13)$$

where;

τ = Allowable Shear Stress for steel shaft with provision for key ways, 42 MPa

M_b = Maximum bending moment on the shaft, N-m

M_t = Maximum Twisting Moment on the shaft, N-m.

K_b = Combined shock and fatigue factor for bending (= 2).

K_t = Combined shock and fatigue factor for twisting (= 1.5).

Equation (13) is also known as ASME CODE for determination of standard shaft diameter.

The maximum twisting moment, M_t was determined as 24.64 N-m using Equation (14) given by Khurmi and Gupta (2005).

$$M_t = (T_1 - T_2) (D_2 / 2) \quad (14)$$

where,

T_1 = Tension on the tight side, N

T_2 = Tension on the slack side, N

D_2 = diameter of the driven pulley, m.

Bending moments occur on the shafts as a result of applied loads and belt tension. Thus, evaluation of the shear force, maximum bending moment and shaft selection was carried out using Beamboy software. **Figs. 3** and **4** show the free body diagram of the applied loads and belt tensions on the peeling drum shaft and bending moment diagram, respectively.

Maximum Bending moment as revealed from the plots was found to

Fig. 3 Free body diagram of applied loads and belt tension

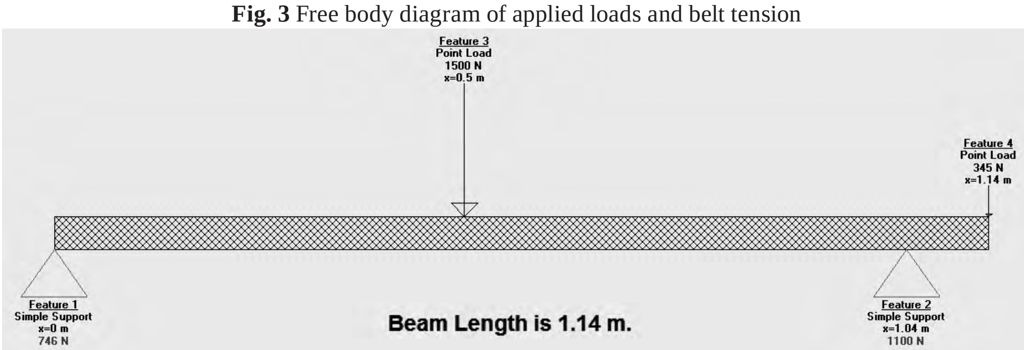

be 373 Nm at 0.51 m from left support. Shaft diameter was determined as 44.91 mm using Equation (14). Hence standard shaft diameter of 45 mm and the corresponding bearing number of 409 were selected.

Determination of Power Consumption and Selection of Prime Mover

The total power, P_T, required in powering the modified cassava attrition peeler as given by Equation (15), comprises of the power at no load, P_1, power at maximum load, P_2 and power consumed by the wave motion of water in the bath, P_3. P_1 was determined as 251.71 W from Equation (16), P_2 as 705 W from Equation (17) and P_3 as 599.25 W (assumed to be 85% of P_2).

$$P_T = P_1 + P_2 + P_3 \quad (15)$$

$$P_1 = (T_1 - T_2)\ v \times n \quad (16)$$

where,

n is number of v-belt used = 2,

$$P_2 = W_T v \quad (17)$$

Therefore, the power required to drive this machine at maximum capacity and factor of safety of 1.5 was determined to be 2.23 kW (2.99 hp). Hence, a gear electric motor of 3 hp will be suitable to power the cassava peeler.

Determination of Surface Area of the Peeling Ball

In attrition peeling, inner surface of the drum and the surface presented by the balls constitute the abrasive surfaces for the removal of the softer material (cassava peels). Shape of the ball was investigated to be a critical factor for effective peeling. Egg shaped balls were designed to replace the spherical balls previously used in the existing machine. The surface area of an egg shaped peeling ball (**Fig. 5**) was approximated as 0.21 m^2 using the expression given by *www.had2know.com* as:

$$S_{ab} = 2\pi A^2 + \pi A\ [B^2 / \sqrt{(B^2 - A^2)}\ \cos^{-1}(A/B) + (C^2/\sqrt{C^2 - A^2})\ \cos^{-1}(A/C)\ ] \quad (18)$$

where, A, B and C are the equatorial, short polar and long polar radius, respectively. Given that A = 2 cm, B = 2.2 cm and C = 3.2 cm. For number of peeling balls n_b Equation (18) is multiplied by n_b.

Operation of the Machine

The peeling drum of the modified machine was provided with a hinged feeding gate of 400 mm × 300 mm along the length and discharge gate (slit) at one end. To provide mechanical strength against the twisting moment, the drum was reinforced outside with mild steel webbed plate and the whole assembly mounted with two outboard bearings on the structural frame. The peeling unit is partially submerged in a semi-cylindrical tank (serving as water bath and discharge unit) of diameter 500 mm and length 1,050 mm welded to a structural stand, both made from 3 mm and 5 mm thick mild steel sheet and angular bar, respectively. The trough/housing is partitioned into two such that one partition serves as water bath during peeling operation and with a blow hole beneath discharges water and cassava peels (flake) after peeling while the other partition serves as peeled cassava evacuation chamber and discharge spout. The scooping mechanism provided on the shaft helps to scoop the cassava from the evacuation chamber through the discharge spout thereby eliminating the human intervention in evacuation. A 5 hp gear electric motor is mounted beneath the housing. The motor drives the peeling unit by means of a belt and pulley drive. The speed of the machine is varied by changing the pulley size. In the attrition peeler, peeling effects is enhanced by the introduction of peeling balls of high frictional properties. Shape of the ball was investigated to be a critical factor for effective peeling. Egg shaped balls were designed to replace the rounded cylindrical balls previously used in the existing machine. By carrying out a simple test

Fig. 4 Bending moment diagram

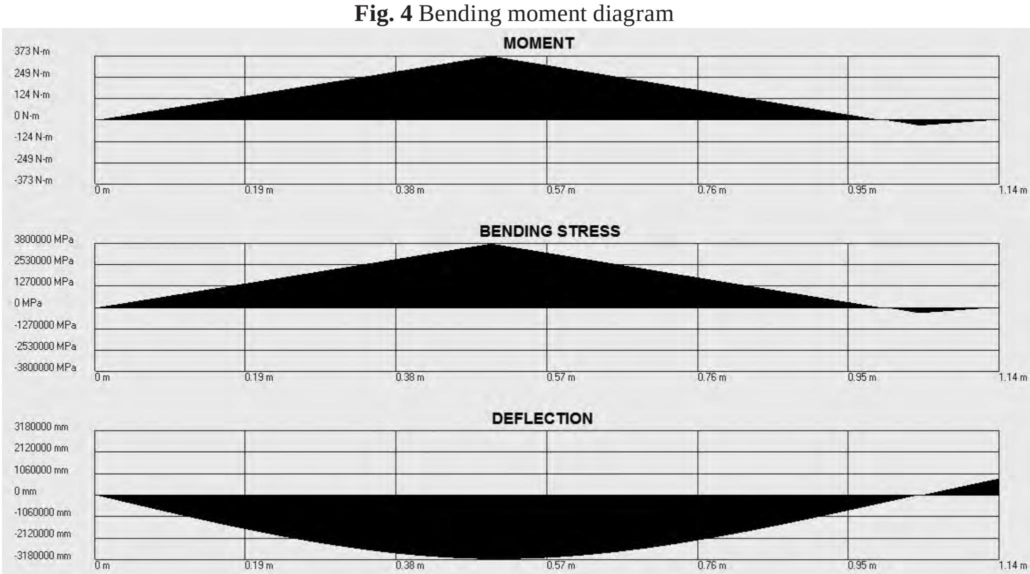

on the two different shapes of balls using the same operating condition, results revealed a slight higher peeling efficiency. The implication was that the narrower (needle like) ends of the balls made better contacts with the pronounced recessed portion of the cassava tubers. The peeling balls were produced from expanded mild steel sheet.

When the machine is on operation a known mass of cassava of precise weight are loaded into the machine through the gate into the peeling drum. The machine is energized through the prime mover causing a rotational motion of the drum. The egg shaped peeling balls together with the embossed inner surface of the drum causes the uniform wearing of the cassava peel. Being a batch process operation, the cylindrical peeling drums impacts rotational motion on the balls freely mixed with the cassava and consequently creating tumbling effect in the drum that gives random relative motion hence affecting the peeling process. The egg shape of the balls make it possible for depressions on the surface of the cassava to be engaged while the breaker baffles breaks the uniform angular speed which the loaded cassava attains at critical speed and this increases agitation, extending critical speed hence more peeling effect. Material removed from the surface of the cassava by abrasion, which has the form of flake and also tiny particles in pulpy matter, sinks through the perforation of the drum to the bottom of the housing trough serving as water bath and also prevents the clogging of nibbler balls. At the end of each peeling operation, the peeled cassava and peeling balls were evacuated into the evacuation chamber where the peeled cassava tubers are collected while the balls are recovered for next batch operation.

Performance Evaluation

The modified cassava attrition peeling machine was evaluated and had its result compared with an existing machine. Three cassava varieties, UMUCAS 36, TMS 30572 and TME 419 used were procured from National Root Crop Research Institute farm, Umudike, Abia State of Nigeria. In the experimental plan, the throughput, TP (kg/h) and efficiency, η (%) of the machine were studied using five experimental runs for freshly harvested cassava varieties having moisture content ranging from 60 to 85% w.b with the peeling drum speed for both machines maintained at 40 rpm. The peeling balls of the existing version was spherical while the peeling balls for the modified version was egg shaped and the number of peeling balls was kept constant at 250. In each of the test trial, a stop watch was used to monitor the time of peeling 20-50 kg of cassava tubers, after which the output (peeled cassava) were weighed and recorded. Thereafter, tuber flesh loss (the amount of starchy flesh removed alongside the peels during peeling), the throughput (total mass of cassava peeled and discharged by the machine per unit time), TP (kg/h) and efficiency (the ratio of the total mass of peel by the machine to mass of manual peel), η (%) of the machine were determined from the data obtained using the following expressions:

$$F_l = M_c - (m_{cp} + m_{pt}) \quad (19)$$

$$\eta_p = M_{Pc} / (M_{pr} + M_{pc}) \times 100/1 \quad (20)$$

$$TP = M_c / t \quad (21)$$

where, M_c is the mass of the loaded cassava (kg), m_{cp} is the mass of the peeled cassava (kg), $m_{pt} = (\pi\phi (m/v) D_g^2 P_{th})$ is the theoretical mass of peel (kg), P_{th} is the peel thickness of the cassava (m) and D_g is the geometric mean diameter (m), ϕ is the sphericity, M_{pc} and M_{pr} are the weight of peel (kg) collected through the peel outlet of machine and weight of peel removed by hand after machine peeling (kg), t is Time taken (s).

Specific energy of consumption of the modified machine which is quantity of energy used to peel a unit mass of cassava fed into it was also determined using Equation (22).

$$SE = P_t / M_c \quad (22)$$

where, P is Power consumed by the electric motor in kW

Data obtained were comparatively analyzed using Analysis of Variance (ANOVA)

Finally, the benefits in adopting the improved cassava attrition peeling machine was also evaluated using the time taken to complete batch peeling process, amount charged for peeling in the various techniques, the average price per kg for peeling batch cassava mass, throughput capacity for the various batch mass of cassava and the total energy cost. Energy cost savings was evaluated using Equation (23).

Table 1 Results of performance test of modified cassava attrition peeling machine

S/N Exp. Runs	Mass of unpeeled cassava (kg)	Peeling time (mins)	Mass of peeled cassava (kg)	Mass of peel (kg)	Percentage tuber flesh loss (%)	Throughput Capacity (kg/h)	Peeling Efficiency (%)
1	25	15	18.56	5.32	4.5	100	78
2	30	15	21.09	7.20	5.7	120	73
3	35	18	26.71	7.31	2.8	116.7	80
4	40	20	27.76	9.12	7.8	120	71
5	45	21	33.81	11.89	8.6	142	75
Mean	36	17.5	25.59	8.17	5.88	119	75.4

Fig. 5 Peeling ball profile

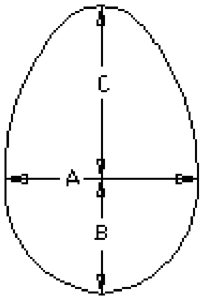

$$ECS = (TEC_{proda/Manual} - TEC_{MCAPM}) / TEC_{proda/Manual} \times 100 \quad (23)$$

where, TEC = Total energy cost

Results and Discussion

The results of the performance test (**Table 1**) showed that the machine performed above 75% efficiency. The results also indicated 119 kg/h as the average throughput of the modified cassava attrition peeling machine at 5.88% tuber flesh loss.

The results of the comparative evaluation of the modified machine, existing machine and manual method in cassava peeling is shown in **Table 2**. Evident from this table, it can be deduced that there was an improvement in the modified cassava attrition peeling machine as compared to the existing version. The average peeling efficiency of the modified machine increased to 75.4% as compared to the existing version which recorded an average peeling efficiency of 62%. However this peeling efficiency falls short when compared to the manual peeling process which has remained most efficient based on the expertise of the manual peeler.

The increase in the efficiency of the modified machine was attributed to the optimal design settings used in its fabrication and the use of egg shaped peeling/ nibbling balls which is in contrast with the spherical balls used in the existing machine. The irregularities in shape of the cassava varieties necessitated the design of an egg shaped peeling/nibbling balls. These nibbling balls increased the attrition force on the surface of the cassava peel especially in the recessed regions enhancing peeling action. Also, the manual peeling process is constrained to the expertise of the operator (peeler) and the modified machine ability to peel cassava of different physical composition without initial sorting and/or cutting to size is a great advantage over existing cassava peeling technologies. The manual peeling process had the least mass of peel as compared to the attrition machines. Increase in the mass of peel of the attrition machines can be attributed to the presence of cassava flesh in the peel mass and this is evident in the percentage increase in tuber flesh loss using the attrition peeling machines. Yet the modified machine performed better and reduced percentage tuber flesh loss associated with the existing machine significantly from 16.66% to 5.88%. Although Oluwole and Adio (2013), Ukenna and Okechukwu (2014) reported lower tuber flesh loss of 5.09% and 5%, respectively. These lower tuber flesh losses were of no significant difference with that of the modified machine compared to huge advantage of pre-operational treatment eliminated.

Table 3 shows the relationship between throughput in the manual peeling process and the mechanized process. Irrespective of the high peeling efficiency of the manual process as shown in **Table 2**, it was observed in **Table 3** that the throughput capacity for the manual peeling process was very low when compared to the machines owing to much processing time required. It was also observed from **Table 3** that as the mass of cassava increased, the throughput of the manual peeling process reduced. This can be attributed to the fact that the time taken in the manual peeling process increased as the mass of cassava increased. Also, drudgery sets in when the person handling the manual peeler gradually gets exhausted in the peeling process, due to tiredness and muscle cramps. Intermittently, the peeler takes some time to relax and regain its strength before continuing the peeling process. All these period of exhaustion non-productively reduces the throughput capacity of the peeler. Hence, for large scale process, the use of the modified machine is recommended as there is no drudgery associated with it and also, the modified machine has a throughput capacity greater than the existing machine. This improvement was as a result of the less processing time from 30.6 minutes/batch associated with existing machine to 17.5 minutes/batch (42.3% peeling time recovery) occasioned

Table 2 Evaluation result of modified machine with existing technologies

S/N Exp. Runs	Mass of cassava (kg)	MANUAL			EXISTING MACHINE			MODIFIED MACHINE		
		Mass of cassava (kg)	Percentage tuber flesh loss (%)	Peeling Efficiency (%)	Mass of cassava (kg)	Percentage tuber flesh loss (%)	Peeling Efficiency (%)	Mass of cassava (kg)	Percentage tuber flesh loss (%)	Peeling Efficiency (%)
1	25	4.20	2	98	7.50	13	63	5.32	4.5	70
2	30	5.49	3	99	11.20	19	65	7.20	5.7	73
3	35	6.44	0.8	98	13.10	19.2	60	7.31	2,8	80
4	40	9.55	4	97	13.94	19.8	62	9.12	7.8	71
5	45	6.34	2	99	15.70	12.3	60	11.89	8.6	75
Mean	36	6.34	0.8	98.2	12.29	16.66	62	8.17	5.88	75.4

by the modifications considered in the deign process.

Table 4 shows the cost benefit evaluation at ₦6.25/kg, ₦8.33/kg and ₦25/kg as prevalent processing cost for modified cassava attrition peeling machine, existing machine and manual peeling process, respectively. Specific energy consumption of the existing and modified cassava attrition peeling machine were also determined as 65 kJ/kg and 57 kJ/kg, respectively.

Since the peeling machines are both powered by an electric motor, the cost of generated electricity must be taken into consideration to determine the energy cost of using the machines. Electrical cost from the national grid used to power the machines at the rate of ₦43 per kWh while energy cost for the manual peeler was considered as his wages per batch mass of cassava.

The benefit cost analysis as shown in **Table 4** reveals a decrease in the total energy cost in using the modified cassava attrition peeling machine as compared to the existing version and manual peeling process. In addition to its increased throughput capacity, the modified cassava attrition peeling machine performed optimally well with 12% and 69% energy cost savings recorded for the existing and manual peeling process, respectively.

Conclusions and Recommendations

The substitution of rounded cylindrical balls with egg shaped balls, together with the introduction of breaker baffles and peeling drum inner surface perforation (embossment) in mechanized cassava attrition peeling improved cassava peeling by eliminating drudgery of pre-operational treatment and excessive loss of tuber flesh even at minimal specific energy consumption. The machine recorded an efficiency of 75.4%, throughput of 119 kg/h, flesh loss of 5.88% and specific energy consumption of 57.1 kJ/kg. Processing time of 17.5 min/batch and cost of N6.25/kg resulted in 42.3% and 25% improvement, respectively. It is therefore recommended, that since peeling constitutes the major bottle neck in cassava processing, attrition peeling mechanism should be maintained in the design of any cassava peeling systems to eliminate drudgery of pre-peeling operations. Government and other agencies should grant loan to farmer to immediately adopt this important innovation for the mass production of cassava products to meet with the growing demand of the Nigerian industries for export.

Ackowledgements

Projects Development Institute (PRODA), Enugu and staff are highly acknowledged for their material and technical supports in the course of this study.

REFERENCES

Adetan, D. A., L. O. Adekoya and O. L. Aluko. 2006. Theory of a mechanical method of peeling cassava tubers with knives. International Agrophysics, 20: 269-276.

Ajibola, O. O. 2000. Adding Value to the Farmer's Harvest. Obafemi Awolowo University Inaugural Lecture Series No.145, Obafemi Awolowo University Press Ltd., Ile-Ife, Nigeria.

Akintunde, B. O., F. A. Oyawale and T. Y. Tunde-Akintunde. 2005. Design and fabrication of a cassava peeling machine. Nigerian Food Journal. Vol. 23, pp 1-8.

Echebiri, R. N. and M. E. I. Edaba 2008. Production and utilization of cassava in Nigeria; prospects for food security and infant nutrition. Production Agriculture Technology, 4(1): 38-52.

Egbeocha, C. C., S. N. Asoegwu and N. A. A. Okereke. 2016. A Review on Performance of Cassava Peeling Machines in Nigeria. Futo Journal Series (FUTOJNLS) Volume-2, Issue-1, pp. 140-168.

Ejovo, O. N, S. Oboli and A. C. C. Mgbeke. 1988. Studies and preliminary design for a cassava tuber peeling machine. Transactions of the American Society of Agric. Engineers, 31(2): 380-385.

Ezekwe, G. O. 1979. Mechanising Cassava Peeling: The PRODA Cassava Nibbling Machine, PRODA Technical Reports No. 1, pp. 1-20.

http:// www.had2know.com. Accessed June, 2016.

Igbeka, J. C., M. Jory and D. Griffon. 1992. Selective mechanization for cassava processing. Journal of Agricultural Mechanization in Asia, Africa and Latin America

Table 3 Processing time and throughput capacities of peeling technologies

Exp. Runs	Mass of cassava (kg)	MANUAL		EXISTING MACHINE (PRODA)		MODIFIED MACHINE	
		Peeling time (mins)	Throughput (kg/h)	Peeling time (mins)	Throughput (kg/h)	Peeling time (mins)	Throughput (kg/h)
1	25	85	17.65	25	60	15	100
2	30	130	13.84	28	64.29	15	120
3	35	148	14.18	30	70	18	116.67
4	40	150	16.00	35	68.57	20	120
5	45	180	16.66	35	85.71	21	150
Mean		138.6	15.67	30.6	69.71	17.5	119

(AMA), Tokyo, 23(1): 45-50.
IITA (International Institute of Tropical Agriculture) 2006. IITA Annual report, 8.
Jimoh M. O. and O. J. Olukunle. 2012. An automated cassava peeling system for the enhancement of food security in Nigeria, Nigerian Food Journal, 30(2): 73-79.
Khurmi, R. S. and J. K. Gupta. 2005. A Textbook of Machine Design (S.I. Units) Eurasis Publishing House (PVT) Limited, New Delhi-110055.
Kolawole, O. P., L. A. S. Agbetoye and A. S. Ogunlowo. 2010. Sustaining world food security with improved cassava processing technologies: The Nigerian Experience on Sustainability, 2: 3681-3694.
Koocheki, A., S. M. A Razavi, E. Milani, T. M. Moghadam, M. Abedini, S. Alamatiyan and S. Izadikhah. 2007. Physical Properties of Water Melon Seed as a Function of Moisture Content and Variety. International Agro Physics, 21: 349-359.
Nwokedi, P. M. 1984. Performance evaluation of cassava peeling machine. In: Tropical root crops: Production and uses in Africa, E.R Terry, E.U. Doku, O.B Arene and N.M Mahungu (eds) Int. Development Research Centre, pp. 108-110.
Odigboh, E. U. 1983a. Cassava production, processing and utilization, In: Chan Jnr, H. T. (ed.), Handbook of Tropical Foods, New York: Mercel Decker Pub. Inc., 145-200.
Odigboh, E. U. 1983b. Model III batch process cassava peeling machine presented at International Conference of Agricultural Engineering Paper No 88.406.
Ohwovoriole, E. N., S. Oboli and A. C. Mgbeke. 1988. Studies and preliminary design for a cassava tuber peeling machine. Transactions of the American Society of Agricultural Engineers (ASAE), 31(2) 380-385.
Olukunle O. J., O. C. Ademosun, A. S. Ogunlowo, A. S. Agbetoye and A. Adesina. 2006. Development of a double action cassava peeling machine. International Conference on prosperity and poverty in globalised world: challenges for agricultural research (www.two-pentag.com)
Olukunle, O. J. and M. O. Jimoh. 2012. Comparative analysis and performance evaluation of three cassava peeling machines. International Research Journal of Engineering Science, Technology and Innovation (IRJESTI), 1(4): 94-102.
Oluwole, O. O. and M. A. Adio. 2013. Design and construction of a batch cassava peeling machine. Journal of Mechanical Engineering and Automation, 3(1): 16-21.
Onwualu, A. P., C. O. Akubuo and I. E. Ahaneku. 2006. Fundamentals of Engineering for Agriculture. Immaculate Publications Ltd, Enugu Nigerian.
Sharma, P. C. and D. K. Aggarwal. 2006. Machine Design. S.K. Kataria and Sons, Nai Sarak Dechi. katria books @ yahoo.com. pp. 19-58, 483-839.
Ugwu, K. C. and R. E. Ozioko. 2015. Development and performance test of cassava peeling and mashing machine. International Journal of Scientific and Engineering Research, 6(6): 1572-1579.
Ukenna, R. U. and V. J. Okechukwu. 2014. Development and modification of cassava peeling and washing machine. Agricultural Engineering Department, B. Eng. Thesis. Federal University of Technology, Owerri (FUTO), Nigeria.

■■

Table 4 Cost Benefit Evaluation

S/N	Manual peeling			PRODA			Modified Cassava Attrition Peeling Machine		
	Mass of cassava (kg)	Amount (₦)	Time taken (mins.)	Mass of cassava (kg)	Amount (₦)	Time taken (mins.)	Mass of cassava (kg)	Amount (₦)	Time taken (mins.)
1	100	2,500	300	100	833	45	100	625	25
2	200	5,000	430	200	1,666	65	200	1,250	40
3	300	7,500	560	300	2,500	80	300	1,875	65
4	400	10,000	600	400	3,333	120	400	2,500	90
5	450	11,250	750	450	3,750	150	450	2,812.5	110
6	500	12,500	950	500	4,166	185	500	3,125	130

	Manual peeling	PRODA	Modified Cassava Attrition Peeling Machine
Average price per kg (N/kg)	100	625	25
Average time taken per kg (min/kg)	200	1,250	40
Throughput capacities (kg/h)	300	1,875	65
Total energy cost (TEC)	400	2,500	90
Energy cost savings per kg of modified machine (ECS)	500	3,125	130

Development a Table Top Centrifugal Dehuller for Small Millets

by

N. A. Nanje Gowda
Research Associate
All India Co-ordinated Research Project on Post-Harvest Engineering & Technology,
University of Agricultural Sciences,
Gandhi Krishi Vignana Kendra, Bengaluru 560065
Karnataka, INDIA
*Corresponding author: nanjegowdana@gmail.com

Satishkumar
Senior Research Fellow
Centre of Excellence for Small Millets,
University of Agricultural Sciences,
Gandhi Krishi Vignana Kendra, Bengaluru 560065
Karnataka, India

Farheen Taj
Senior Research Fellow
Centre of Excellence for Small Millets,
University of Agricultural Sciences,
Gandhi Krishi Vignana Kendra, Bengaluru 560065
Karnataka, INDIA

S. Subramanya
Professor
All India Co-ordinated Research Project on Post-Harvest Engineering & Technology,
University of Agricultural Sciences,
Gandhi Krishi Vignana Kendra, Bengaluru 560065
Karnataka, INDIA

B. Ranganna
Emeritus Scientist
All India Co-ordinated Research Project on Post-Harvest Engineering & Technology,
University of Agricultural Sciences,
Gandhi Krishi Vignana Kendra, Bengaluru 560065
Karnataka, INDIA

Abstract

Millets, nutritious small cereal grains with enormous health benefits, are grown across the world for food and fodder. Due to the typical structure, hardness and small size of grains, dehusking of millets has remained as a constraint. The present investigation deals with the performance evaluation of a low cost table top centrifugal dehuller that was developed. Dehulling experiments were conducted for five millets viz. foxtail, little, proso, kodo, and barnyard millets at three moisture contents (11.1, 13.6 & 16.2% db), and three dehulling speeds (5,000, 5,500 & 6,000 rpm). The moisture content of grains had a significant effect on dehulling performance compared to dehulling speed which had less or negligible effect at times. The highest average dehulling efficiency obtained for foxtail, little and proso millets was 92.7, 91 and 93.5%, respectively, with 13.6% (db) grain moisture content and a dehulling speed of 5,500 rpm. For kodo and barnyard millets, the highest average dehulling efficiency was 80.9% and 74.4%, respectively at 11.1% (db) moisture content and a dehulling speed of 6,000 rpm. For the same experimental combination, the percentage of broken was less than 5% for foxtail, little and proso millets, while for kodo and barnyard millets, it was 5.7 and 9.2%, respectively. The average undehulled grain percentage for foxtail, little, proso, kodo and barnyard was 2.4, 5.7, 2.3, 14.2 and 18.1%, respectively. The approximate cost for converting one kg of millet in to rice is about INR 0.97 ($0.01).

Keywords: millets, dehulling, dehusking, foxtail, proso, centrifugal dehuller

Introduction

Millets are known for their nutritional and health benefits from time immemorial, hence they are also called as nutri-cereals. Millets are found to be the best alternative to the most commonly used cereals, due to their special biochemical composition superior to rice and wheat in certain constituents. Therefore, millets have proved to have potential health benefits such as preventing cancer, cardiovascular diseases, reducing tumour incidence, lowering blood pressure, cholesterol, fat absorption and reducing gastro-intestinal problems, etc. (Salehet al., 2013). The demand for millets by urban population is increasing significantly in the recent years, since these grains , owing to their low glycemic index, release glucose slowly in the blood and reduce the glucose absorption which prevents and maintains diabetes mellitus (ADA, 2005; Shobanaet al., 2009; Kim et al., 2011). Though millet possess several health benefits, few plausible reasons like lack of technical know-how about processing methods, lack of awareness about nutritive value, reluctance among people to buy and consume, and lack of appropriate processing machinery, have made them less popular and has contributed to their poor availability. Owing to the absence of appropriate primary processing technology particularly for dehulling, the production and processing of small millets has remained a constraint. For the past few decades, continuous efforts have been made to develop efficient dehulling machineries. The production and consumption of millets has declined because dehulling is a difficult task, due to their small grain size, and the husk sticking tightly to the grain within. Traditionally at household level, dehulling was performed using a stone grinder, pounding with a wooden staff, while at large scale, stone mills and carborundum rollers were used. Later, improved machineries such as beating cylinders, hammer mills, abrasive stone hullers, and rubber roll hullers were developed. At present, centrifugal dehuller is the most efficient small millet dehuller of the 21st Century.

Fig. 1 Table top centrifugal dehuller for small millets dehulling

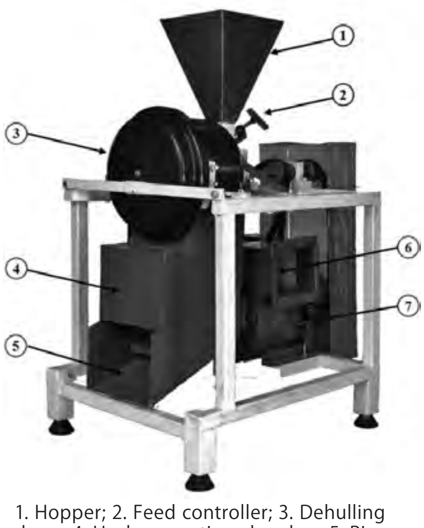

1. Hopper; 2. Feed controller; 3. Dehulling drum; 4. Husk separation chamber; 5. Rice outlet; 6. Husk outlet; 7. Belt & Pulley drive connected to motor

Millets being a staple food and consumed at household levels, processing must be considered both at traditional and industrial levels, involving small, medium and large-scale entrepreneurs. A small to medium size entrepreneur or a family has to dehull small quantities of millets to meet domestic needs by processing about 5-10 kg of millets per batch. Thus, the existing large scale centrifugal dehullers are of unmatched capacity, and cost more than INR 100,000 ($1,470) which makes them unaffordable for a family or small scale processors. Under these conditions, a small capacity (5-10 kg/h), low-priced table-top apparatus would be more ideal need of the hour which would enhance the millets consumption tremendously. Considering these aspects, a study was undertaken to develop a low cost and small capacity table-top centrifugal dehuller to dehull the most commonly grown millets in India. The details of the dehuller are being published elsewhere.

Materials and Methods

Sample Preparation

Five commonly grown millet varieties in India viz. foxtail (*Setaria italica*), little (*Panicum sumatrense*), proso (*Panicum miliaceum*), kodo (*Paspalum scrobiculatum L.*), and barnyard (*Paspalum scrobiculatum*) were procured from All India Coordinated Research Project on Small Millets Centre, University of Agricultural Sciences, Bengaluru. The most commonly grown millets variety of foxtail (var. HMT 100-1), little (var. OLM-36), proso (var. GPU-21), kodo (var. JK-13), and barnyard (var. RAU-11) in south India were selected for this investigation. The millet grains were hand-cleaned and conditioned to three different moisture levels on dry basis, the moisture content values proposed for the study were 11.1%, 13.6%, and 16.2% (d.b). To obtain predetermined moisture levels, a pre-calculated amount of distilled water was added to the grains, followed by sealing the grains in polythene bags and stored at 7°C for about 72 h (NanjeGowdaet al., 2015).

Developed Table-top Centrifugal Dehulling Machine

The table top centrifugal dehuller (**Fig. 1**, developed at All India Coordinated Research Project on Post-Harvest Engineering & Technology, University of Agricultural Sciences, Bengaluru, India) has a dehulling capacity of 6-8 kg/h (depending upon grains), total weight 32.2 kg (without motor), and one labour, was used for dehulling studies. The developed dehuller mainly consists of a hopper with feed controller, dehulling drum, centrifugal impellor, husk separating chamber, centrifugal blower (8.5 m^3/min) with airflow rate control value, one single phase 1HP motor of 2,880 rpm, and pulley & v-belt driving mechanism. The dehulling took place due to simultaneous action of impact and centrifugal forces. Three types of impellor vane designs each with 3-vanes fixed at three different angles were evaluated in preliminary studies. Based upon preliminary study results, the optimised impellor setting was fixed for conducting the present study. In addition, the feed rate of millet grains was adjusted between 6.0-6.5 kg per hour for dehulling studies of all five millet grains.

Dehulling Procedure

In each experiment, about 200g of millets conditioned to three different moisture contents were dehulled in triplicates. The dehulled samples were segregated into: whole kernels (M_w), broken grains (M_b), and undehulled grains (M_u). The term "broken" in the Eq. 2 refers to milled rice fraction retained over 0.85 mm sieve. The dehulling efficiency (DE, %) and percent of broken (B, %) were calculated using Eq.1 and Eq.2 (Singh et al., 2009) as:

$$DE\ (\%) = [1 - (M_u/M)] \times [1 - (M_b/M_t)] \times 100 \quad (1)$$

$$B\ (\%) = (M_b/M_t) \times 100 \quad (2)$$

where, M_t = Total mass of grains taken for de-hulling, g.

Design of Experiments

RSM was employed to study the effect of each experimental variable (initial moisture content and impellor speed) on dehulling parameters using Design Expert 7.0.0 software. Three level factorial designs were used to test significant difference between the samples. For each experimental variable, the centre and range values were based on the results of preliminary trials.

Results and Discussion

Dehulling of Foxtail Millet at Different Initial Moisture Contents and Impellor Speeds

It was evident that the effect of initial moisture content was significant ($p < 0.001$) on dehulling efficiency of foxtail millet, compared to the effect of impellor speed which had leasteffect. However, the interaction of these factors was also non-significant (**Table 1**). The average dehulling efficiency was found to increase from 87% to 92.6% with decreased moisture content from 16.2 to 13.6% (d.b.). With further decrease in moisture content up to 11.1% (d.b.) the dehulling efficiency decreased to 89.9% at various impellor speeds (**Fig. 2a**). The moisture content of grains had significant ($p < 0.001$) effect on broken fraction compared to impellor speed which had little effect, as shown in Figure 2b. The average highest dehulling efficiency (92.8%) of foxtail millet was obtained when 13.6% (d.b.) moisture content grains were dehulled at 5,500 rpm, with less than 5% brokens (**Fig. 2a**). The centrifugal dehuller developed by Ganesan and Varadharaju, (2013) offered a dehulling efficiency of 87.5% with less than 5% broken for foxtail millet having 12% (d.b.) moisture content and dehulled at peripheral speed of 47.29 ms^{-1} and required the grains

Fig. 2a & **2b** Response surface contours for dehulling efficiency (a) and broken percentage (b) of foxtail millet as a function of moisture content and impellor speed. For each contour plots, the third variable is fixed at '0' level

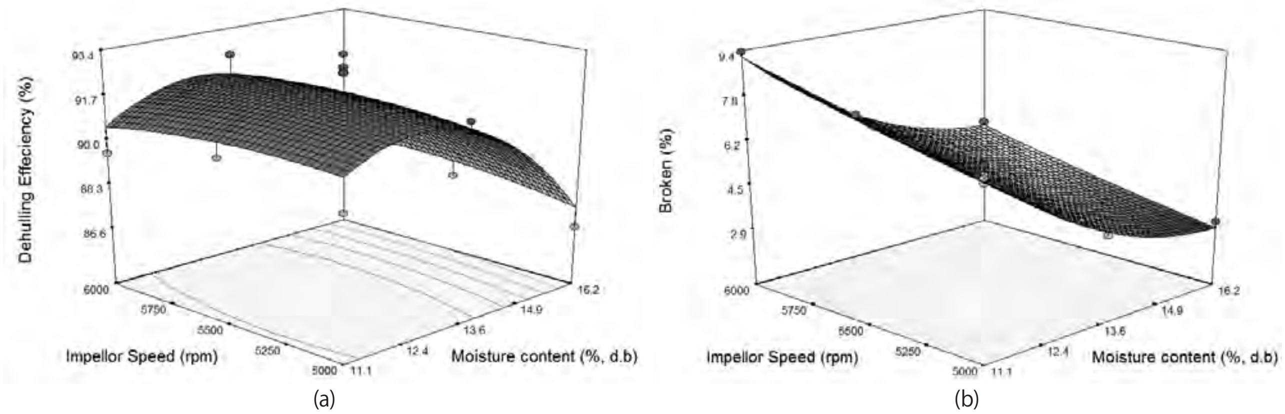

Fig. 3a & **3b** Response surface contours for dehulling efficiency (a) and broken percentage (b) of little millet as a function of moisture content and impellor speed. For each contour plots, the third variable is fixed at '0' level

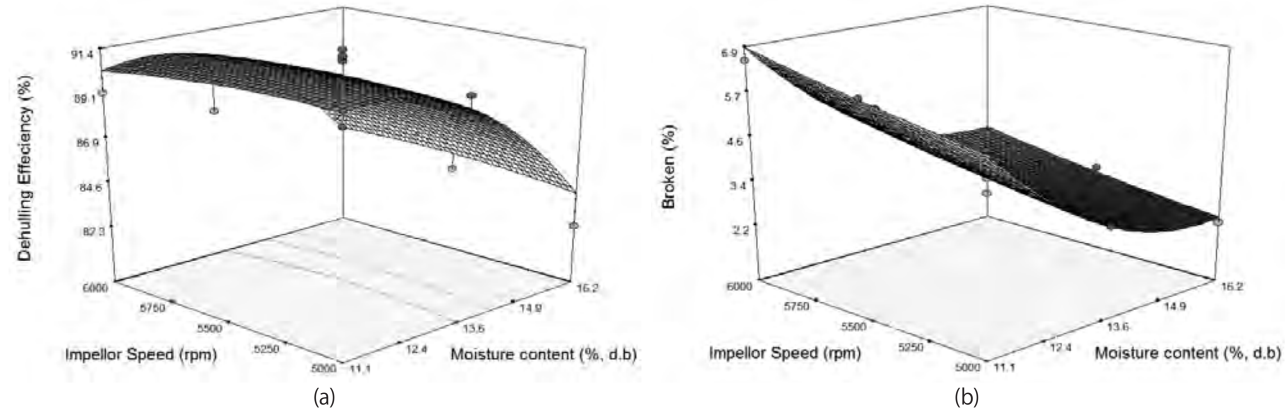

Table 1 Processing time and throughput capacities of peeling technologies

Source	Sum of squares	df	Mean Square	F Value	p-value
Model	6,892.85	17	405.46	122.82	0.0001****
A-Moisture content	316.17	1	316.17	95.77	0.0001****
B-Impellor speed	0.81	1	0.81	0.25	0.6222
C-Millets	6,359.49	4	1,589.87	481.58	0.0001****
AB	1.83	1	1.83	0.56	0.4597
AC	117.80	4	29.45	8.92	0.0001****
BC	4.10	4	1.02	0.31	0.8698
A2	71.03	1	71.03	21.52	0.0001****
B2	1.18	1	1.18	0.36	0.5523
Residual	155.16	47	3.30		
Lack of Fit	153.94	27	5.70	Std. Dev	1.82
Pure Error	1.22	20	0.061	Mean	82.72
Correlation Total	7048.01	64		C.V (%)	2.20

*$p \leq 0.05$, significant; **$p \leq 0.01$, significant; ***$p \leq 0.001$, significant; ****$p \leq 0.0001$, significant

to undergo two passes for dehulling. Nevertheless, the table-top centrifugal dehuller reported in the present study found to offernearly 5% higher dehulling efficiency under single pass for foxtail millet. This might be due to the vane design and vane angle used in the impellor offered an effective dehulling of millets.

Dehulling of Little Millet at Different Initial Moisture Contents and Impellor Speeds

Fig. 3a & **3b** shows the effect of initial moisture content and impellor speed on dehulling efficiency and percentage broken for little millet, respectively. The effect of moisture content was found to be significant ($p < 0.001$), compared to the impellor speed on dehulling efficiency and broken percentage for little millet (**Table 1**). The increase in moisture content from 11.1 to 13.6% (d.b.) showed an increase in dehulling efficiency of little millet from 89.6% to 91% and then gradually deceased to 83.8% at a fixed impellor speed of 5,500 rpm (**Fig. 3a**). The polynomial behaviour of dehulling efficiency with decreased moisture content beyond 13.6% (d.b.) and with increased impellor speed beyond 5,500 rpm was because of formation of more broken at lower moisture level and at higher impellor speed. Similarly, an increase in moisture content from 11.1% to 16.2% (d.b.) decreased the formation of broken from 6% to 3%, respectively (**Fig. 3b**). Therefore, when foxtail millet with 13.6% (d.b.) moisture content was dehulled at 5,500 rpm, it resulted in a highest dehulling efficiency of 91% with minimum broken of 3.5%. Increase in broken percentage with increased impellor speed and decreased moisture content is expected since at low moisture, grains tends to be more hard and are subject to high impact force under higher dehulling speed. The highest dehulling efficiency (91.3%) of little millet reported in the present study was 4.6% higher than the dehulling efficiency obtained with the dehuller developed by Ganesan and Varadharaju, (2013). It is reported that about 86.75% dehulling efficiency with less than 5% broken were obtained when little mille twith 12% (d.b.) moisture content was dehulled at a peripheral speed of 47.29 ms^{-1}, with two passes.

Dehulling of Proso Millet at Different Initial Moisture Contents and Impellor Speeds

Similar to the dehulling of foxtail and little millet, dehulling efficiency and broken percentage of proso millet was significantly ($p < 0.001$) effected by moisture content of grains, followed by impellor speed (**Table 1**). During dehulling of proso millet, the average dehulling efficiency was found to increase from 87.8% to 93.5% with decreased moisture content from 16.2 to 13.6% (d.b.). A further decrease in moisture content to 11.1% (d.b.) the dehulling effi-

Fig. 4a & **4b** Response surface contours for dehulling efficiency (a) and broken percentage (b) of proso millet as a function of moisture content and impellor speed. For each contour plots, the third variable is fixed at '0' level

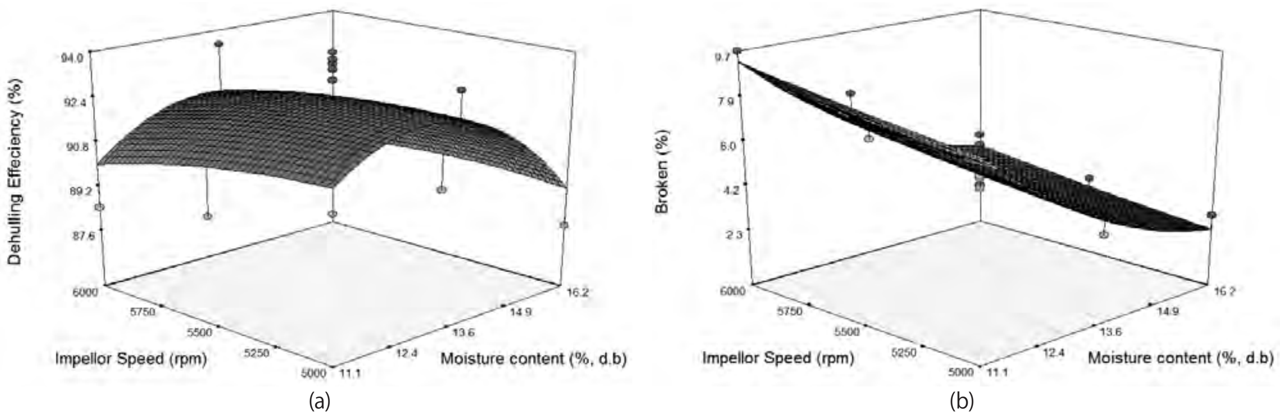

ciency was found to decrease drastically to 89.5% as shown in **Fig. 4a**. The average broken percentage of proso millet was found to increase drastically from 3.4% to 9.0% with increased impellor speed (5,000 to 6,000 rpm) and decreased moisture content (16.2% to 11.1% d.b.), as shown is **Fig. 4b**. The best combination of variables that resulted highest dehulling efficiency (93.5%) for proso millet was when grains with 13.6% (d.b.) moisture content dehulled at impellor speed of 5,500 rpm. Under the same experimental condition, the broken percentage (4.3%) recorded was under acceptable range.

Dehulling of Kodo Millet at Different Initial Moisture Contents and Impellor Speeds

Unlike in dehulling of foxtail, little and proso millets, the average dehulling efficiency of kodo millet at different speeds was found to increase linearly from 71.1 to 80.2% with decrease in moisture content from 16.2-11.1% (d.b.) as shown in

Fig. 5a, **5b** & **5c** Response surface contours for dehulling efficiency (5a), un-dehulled percentage (5b) and broken percentage (5c) of kodo millet as a function of moisture content and impellor speed. For each contour plots, the third variable is fixed at '0' level

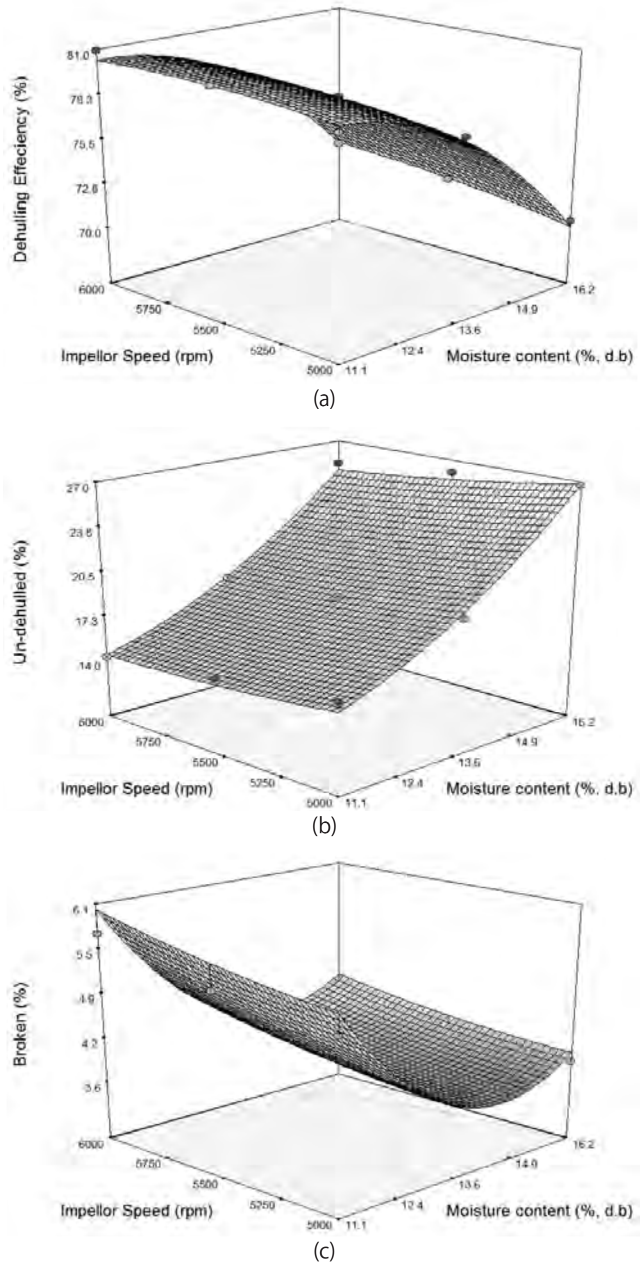

Fig. 6a, **6b** & **6c** Response surface contours for dehulling efficiency (6a), un-dehulled percentage (6b) and broken percentage (6c) of barnyard millet as a function of moisture content and impellor speed. For each contour plots, the third variable is fixed at '0' level

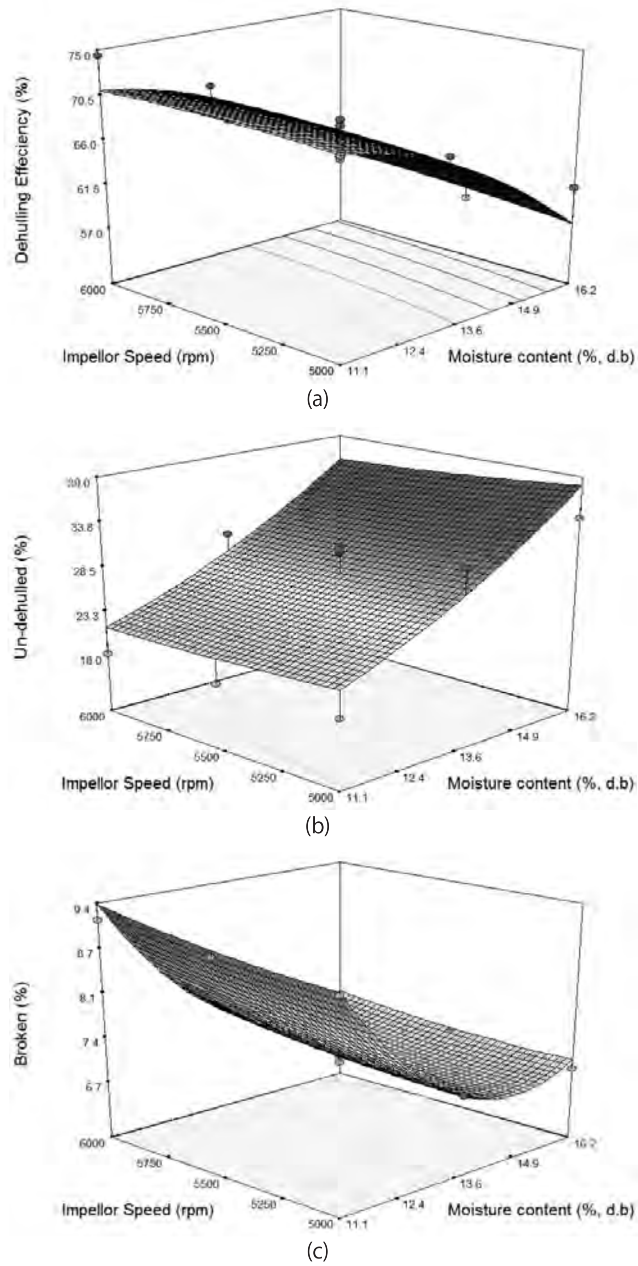

Fig. 5a. Though the moisture content had a significant ($p < 0.001$) effect on dehulling of kodo millet, the overall dehulling efficiency obtained was not on par with other grains. As the average dehulling efficiency of kodo millets obtained at a moisture content of 11.1% (d.b.) was about 80.5%, and was slightly less than the acceptable range (**Fig. 5a**). The impellor speed did not show any significant effect on dehulling efficiency, this was due to the fact that kodo millet is known to be enclosed by multiple layers of husk andis very hard to break, which may require appropriate pre-treatments for effective dehulling. Nearly about 26%, 18.6% and 15.2% of kodo grains were un-dehulled at 16.2%, 13.6% and 11.1% (d.b.) moisture content, respectively (**Fig. 5b**). Consequently, the average broken percentage of 3.9, 4.2 and 5.4 % were observed at 16.2%, 13.6% and 11.1% (d.b.) moisture contents (**Fig. 5c**). In the present study, both the broken and un-dehulled fractions together had an adverse effect on decreasing the dehulling efficiency of kodo millet. Therefore, hydrothermal treatments like parboiling or steaming may play a vital role in dehulling of kodo millet for complete removal of husk and reducing the broken and un-dehulled fractions. Shrestha, (1972) and Chandi and Annor, (2016) have reported that parboiling helps in easy dehusking of kodo millet. Varadharaju and Ganesan, (2013) have also reported an increase in dehulling efficiency of 21.8-27.5% forkodo millet subjected to hydrothermal treatment at different levels of soaking temperature, soaking time and steaming periods.

Dehulling of Barnyard Millet at Different Initial Moisture Contents and Impellor Speeds

In comparison with dehulling of foxtail, little, proso, and kodo millets, the dehulling efficiency of barnyard millet was found to be the lowest among other grains. The dehulling efficiency as affected by moisture content and impellor speed is shown in **Fig. 6a**. Both the moisture content and impellor speed had an insignificant effect on dehulling of barnyard millet. The average highest dehulling efficiency varied between 73.6 to 74.4% for barnyard millets at 11.1% (d.b.) moisture content and dehulled at different speeds. However, on the other had the dehulling of grains with 11.1% (d.b.) moisture content resulted in about 9-10% broken and about 18-19.2% of un-dehulled grains (**Fig. 6b** & **6c**). The poor dehulling efficiency of barnyard millet was because of the tight bond between outer husk and the kernel (rice). It was found that, unlike kodo millet the barnyard millet may also require some pre-treatment like hydrothermal treatment in order to loosen the outer husk and enhance the kernel separation. In addition, the study suggests that, centrifugal or impact dehulling principle may not be an appropriate mechanism for dehulling of barnyard millet. This is because, the husk of barnyard millet is not as thick and hard as other millets, and thus any application of higher impact force would cause damage to the kernel and would in turn results in higher broken and powder fractions. Therefore, dehulling of barnyard millet using abrasive or frictional type hullers might be an appropriate method, which was not tested in present study. Nevertheless, an appropriate pre-treatment before dehusking of barnyard millet in a centrifugal dehuller may also improve the dehulling performance, which was not tested. Varadharaju and Ganesan, (2013) have also reported that barnyard millet subjected to hydrothermal treatment at different temperature, soaking time, and steaming period increased the dehulling efficiency by about 20.8-26.2% compared to untreated grains.

Cost Economics

The capacity of the table-top centrifugal dehuller was found to vary between 6-8 kg/h depending upon the type of millet dehusked. The total cost of developed dehuller is less than 25,000 rupees (370$) per unit. The cost involved in processing one kg of millet grains into rice was approximately rupees 0.97 (0.01$) and the operating cost of machine was around 5.81 rupees (0.09$) per hour.

Conclusions

The developed small scale dulling unit hasa capacity of about 6-8 kg/h can be effectively used by small scale entrepreneurs, SHGs of women, and at households. The availability of appropriate low-cost dehulling machinery may enhance the business opportunities of upcoming entrepreneurs and increase the millet consumption. The tested dehuller can be used for efficient dehulling of foxtail, little, proso millets (single pass), kodo and barnyard millets (multi pass), provided that the grains have a moisture content of less than 13.6% (d.b.) during dehulling. The dehuller performs simultaneous operations of dehusking and husk separation by single pass for foxtail, little and proso millets, while kodo and banyard millets require multi pass for efficient dehulling operations. The machine is best suitable for efficient dehulling of foxtail, little and proso millets without any need of pre-treatments like soaking, parboiling, and streaming. The maximum dehulling efficiency of about 92.7%, 91%, and 93.5% for foxtail, little and proso millets, respectively was obtained for the combination of 13.6% (d.b.) moisture content and 5,500 rpm impellor speed. The operational cost of machine was around 0.09$ per hour and the cost for processing millets into rice was found to be less than 0.97 rupees (0.01$) per kilo gram of small millet grains.

Acknowledgement

Authors gratefully acknowledge the Directorate of Research, UAS, GKVK, Bengaluru for the financial support and the Centre of Excellence on Small Millets, UAS, GKVK. The AICRP on PHET, UAS, GKVK, Bengaluru facilitated the fabrication of the unit.

Nomenclature

ANOVA: analysis of variance
M_w: mass of whole kernel,g
M_b: mass of broken, g
M_u: mass of un-dehulled, g
M_t: total mass of grains, g
DE: dehulling efficiency, %
B: broken, %
m^3/min: cubic metre per minute
ms^{-1}: metre per second
rpm: revolution per minute
d.b.: dry basis
kg: kilogram
H: hour
cm: centimetre
HP: horse power
%: percent

REFERENCES

American Diabetes Association. 2005. Diagnosis and classification of diabetesmellitus. Diabet Care, 28:37?42.

Chandi, G. K. and G. A. Annor. 2016. The Cereal Grains- Minor Millets.Reference Module in Food Sciences.Elsevier Ltd. *http://dx.doi.org/10.1016/B978-0-08-100596-5.00012-3*.

Ganesan, S.and N. Varadharaju. 2013. Optimization of machine parameters of centrifugaldehuller for dehulling of foxtail and little millet. National Seminar on Recent Advancesin Processing, Utilization and Nutritional Impact of Small Millets. Madurai Symposium, Thamukkam Grounds, Madurai, 13 September 2013.

NanjeGowda, N. A., K. Alagusundaram and C. V. Kavitha Abirami. 2015. Modelling of Thin-Layer Drying of Black Gram.Journal of Agricultural Engineering, 52 (4): 17-27.

Kim, J. S., T. K. Hyun and M. J. Kim. 2011. The inhibitory effects of ethanol extractsfrom sorghum, foxtail millet and proso millet on α-glucosidaseanda-amylase activities. Food Chem., 124: 1647-51.

Saleh, A. S., Q. Zhang, J. Chen and Q. Shen. 2013. Millet grains: nutritional quality, processing, and potential health benefits. Comprehensive reviews in food science and food safety, 12(3): 281-295.

Shobana, S., Y. N. Sreerama and N. G. Malleshi. 2009. Composition and enzymeinhibitory properties of finger millet (*Eleusinecoracana L*.) seed coatphenolics: mode of inhibition of a-glucosidase and pancreatic amylase. FoodChem., 115(4): 1268-73.

Shrestha, K. B. 1972. Dehusking of varagu and its ulilization for edible purposes.Thèsedemaîtrise. University of Mysore, Karnataka, Inde.

Varadharaju, N and S. Ganesan. 2013. Effect of parboiling on de-hulling and cooking qualitiesofkodo and barnyard millet. National Seminar on Recent Advancesin Processing, Utilization and Nutritional Impact of Small Millets.MaduraiSymposium, Thamukkam Grounds, Madurai, 13 September 2013.

■■

Design, Development and Evaluation of Manually-Operated Check Row Planter for Dry Sowing of Rice

by
Ajay Kumar Verma
Professor & Principal Scientist
Dept. of Farm Machinery and Power Engineering,
Faculty of Agril. Engineering,
IGKV, Raipur, Chhattisgarh, INDIA
ajayaverma@rediffmail.com

Abstract

A manually operated check row planter for dry seeding of rice, capable of planting two rows of rice at a spacing of 25 cm × 25 cm was designed, fabricated and tested. The effective field capacity of the planter was found 0.023 ha/h with field efficiency 47.38% and seed rate was 10.1 kg/ha. The miss index, multiple index and seed damage was found to be 6.6%, 13.3% and 2.1% respectively. Comparative studies were conducted to evaluate the performance of the check row planter, transplanting and dibbling in System of Rice Intensification (SRI). For sowing one hectare of land the planter required Rs. 853/ha (One US \$ ≈ 72 Rs.) which was less as compared to manually transplanting in SRI and dibbling. The developed machine saves 66.7% and 72.4% of money over manual transplanting and dibbling methods.

Introduction

Worldwide, rice is grown on 161 million hectares, with an annual production of about 678.7 million tons (FAO, 2009). More than 90 % of rice is consumed in Asia, where it is a staple for a majority of the population (Mohanty, 2013). Rice provides 30-75% of the total calories to more than 3 billion Asians (Khus, 2004; Von Braun and Bos, 2004). Traditionally, nursery seedlings are raised and transplanted in standing water manually. This transplanting system not only helps in controlling the weeds but also ensures premium quality rice. SRI method of rice cultivation is getting popular in states of India like Andhra Pradesh, Tripura, Karnataka, Kerala and Chhattisgarh etc. Transplanting 12-14 day's old seedlings in 25 cm × 25 cm rows is required in SRI system. In SRI system field is puddled with suitable puddling device, transplanted manually and weeding is done by using suitable weeder. Subbaiah et al., 2006 collected data for two seasons of rice crop and found SRI to be more promising in terms of grain yield. Considering the benefits of planting in 25 cm × 25 cm row maintaining plant distance, has been discussed in many platforms to find out suitable means to use similar type of spacing in dry condition with suitable planter. Direct seeding of rice refers to the process of establishing the crop from seeds sown in the field, rather than by transplanting seedling from nursery (Farooq et al., 2011). To minimize the time consumption and labour

Fig. 1 Development and Fabrication of planter

(a) Seed box (b) Compaction wheel (c) Seed dropping cell

(d) Seed rate controller unit (e) Cut off wheel requirement during sowing operation and to increase the efficiency, appropriate technology was required to be introduced for sowing the rice crops suitable for farmers. It was anticipated that the farmers desire a low cost and low powered device for sowing crops like rice, with higher rate of work. Therefore, manually operated efficient planter was needed to utilize the potential of the available man power. Considering the above factors, manually operated check row planter for dry seeding of rice was design and developed. The check row planter was powered by one man and can sow rice at higher rate of work than traditional transplantation. The planter will sow the rice seeds at 25 cm × 25 cm row to row and plant to plant distance.

Materials and Method

Brief Description of Machine

Check row planter enabled operator to perform hill planting at definite spacing (in checks or squares). Separate seed hopper was provided in planter for each row. Seed hopper bottoms for row crops have rotating agitator feeding mechanism that was rotated in small circular pipes. It has small opening for passing the seeds. A small cell was attached below each hopper where seeds were dropped at desired intervals. Two or three seeds were received in cell at a time. After receiving the seeds, the cell opened and closed using a cut-off mechanism. Seeds then dropped in a valve and remained there until the valve is tripped like a trap door to drop the seeds into the furrow or hill. The planter can be set to plant 2 to 3 seeds per hill. A wide range of spacing could be obtained by using metering roller and star wheel which was fixed on side of the hopper and rotate with the help of metering shaft. This star wheel performed the cut-off of seed by adjusting the number of blade on star wheel to maintain the cut off operation by which plant to plant distance was maintained.

Development of Check Row Planter

The handle of the implement was designed on the basis of the standing posture of the operator. Length of the handle of the implement and angle of operation were independent. The length and height of handle were kept as 1,030 mm and 850 mm, keeping in view the lower angle between point of pulling and vertical plane, in order to reduce strain on hands of operator. The length of crossbar was kept as 400 to 500 mm on the basis of anthropometry data of elbow-elbow breadth. The optimum grip diameter recommended is 25-37.5 mm, the length of grip depends on hand width and its value was taken as 130 mm (Gite et al., 2009).

The trapezoidal shaped seed box was developed. The inclination of front and rear walls was kept 400. Seeds fall freely from the agitator type feeding mechanism through the small opening (adjustable) of circular body fixed in the bottom of seed hopper. Seed then passed to the seed dropping unit cutoff action took place and seed dropped from the bottom of the furrow openers. Pegged type ground wheel (diameter 400 mm) was made by 32 × 5 mm MS Flat. Soil compaction wheel was attached behind both the seed box for covering the seeds into soil. Both the compaction wheel were made by a pair of two wheels and in this pair both the wheel tapered from outside to center for better compaction therefore diameter of wheel at outer side was 15 cm and 14 cm at center. Cut-off wheel was the part of cut-off mechanism which was fixed on metering shaft and rotates with the shaft. Cut-off wheels blades play the main role to maintain distance between seed to seed in planter.

Evaluation Procedure

Check row planter was calibrated in laboratory and field tests were done at Faculty of Agricultural Engineering, Raipur for 3 plots selected, of size 20 × 10 m^2. The methods of rice planting (25 cm × 25 cm), by check row planter, transplanting manually in SRI and dibbling of rice seeds manually were evaluated. All the plots were prepared with two passes of cultivator, one pass of rotavator and one pass of planker. Spring dynamometer was used to measure the required pull force to operate the check row planter (**Fig. 2**).

Fig. 2 Measurement of pulling force by spring type dynamometersr

Fig. 3 Testing of check row planter

Result and Discussion

Physical Properties of Seeds

Popular rice variety MTU 1010 of Chhattisgarh was selected for the study. **Table 1** shows the physical properties of rice seeds used in the laboratory and field tests of the planter. The bulk density of seeds was in range of 644.5-658.0 kg/m^3 with moisture content ranging from 6.5-7.0%.

Uniformity of Placement of Seeds

Accuracy and precision of seed placement affects plant population which in turn controls crop growth and yield. The placements of rice seeds were at uniform depth under a range of 2 cm to 3.2 cm and an average of 3 cm with a minimum SD of 0.67 cm (**Table 2**). The CV was found to be 36.5% and 30.8% which indicates that rice seeds were placed very close to the target depth of 2.5 cm with an acceptable limit and uniformity (**Fig. 3**).

The number of missing hills during operation in field reflects the functionality and effectiveness of the seeder mechanism. Plant spacing variability (PSV) can be described by the standard deviation (SD) of consecutive plant-to-plant spacing within the row (**Table 3**). **Table 3** Distance between seeds and missing hill

The PSV calculated by field test of check row planter was found to be 5.65 cm with missing index of 6.67 % and multiple index 13.33% (**Table 4**). The missing hills and multiple hills perhaps was due to the jerk or vibration which produced opening of seed dropping unit during operation. It may also be due to the clogging/segregation motion of rice seeds in agitator mechanics (**Fig. 3**).

It was observed that the machine was operated at average speed of 0.97 km/h and no skidding was observed during the experiment (**Table 5**). The theoretical field capacity was 0.048 ha/h whereas, the effective field capacity was found to be 0.023 ha/h due to turning of machines and other extraneous unavoidable circumstances. Performance and economic analysis (**Tables 6** & **7**) revealed that the time required for sowing operation was minimum for check row planter and highest in dibbling in dry seeds. The cost of operation was also minimum for check row planter (Rs 653/ha) and maximum for dibbling in dry seeds (Rs. 2,777/ha). In all types of methods check row planting was more profitable as compared to transplanting and dibbling of dry seeds.

The energy consumed during sowing operation of rice under different method of sowing is depicted in **Table 7**. The dibbling of seeds consumed 3.71 times more energy and transplanting consumed 3.08 times more energy as compared to the check row planter.

Force Limit for Operation of Check Row Planter

The maximum pushing/pulling power of the hand during standing work has been studied by many researchers (Gite, 1985).The manually operated planter transmits the power from ground wheel to metering shaft. Since the machine was to be operated by a man the power required to operate the machine was considered as 0.1 hp. In this machine the power given to the ground wheel is transmitted to the metering shaft and cut off mechanism. The rpm of the ground wheel and metering shaft will be the same because

Table 1 Bio physical characteristics of rice seeds

S. No.	Length of seed, mm	Width of seed mm	Thickness of seed, mm	Unit mass of seed, g	Geometric mean diameter, mm	Sphericity
Mean	9.47	2.43	2.14	0.0276	3.61	0.37
SD	8.70-10	2.2-2.60	2-2.8	0.023-0.032	3.47-3.84	0.36-0.40
Range	0.496	0.129	0.074	0.0032	0.0117	0.0139
CV%	5.32	5.30	3.45	11.59	3.24	3.75

Table 2 Distance between seeds and missing hill

Particulars	Depth of sowing, cm		Average
	Row 1	Row 2	
Mean	2.42	2.4	2.41
SD	0.867	0.869	0.868
Range	2.3-3.2	2.2-3.3	2.25-3.25
CV%	35.82	36.20	36.00

Table 3 Distance between seeds and missing hill

Particulars	Seed distance, cm			Average
	Field 1	Field 2	Field 3	
Mean	26.3	27.78	26.31	26.79
SD	4.90	6.32	5.75	5.65
CV%	18.63	27.75	21.85	22.74
Missing hill	1	2	1	1.33
Missing index %	5	10	5	6.66

Table 4 Multiple Index

Particulars	Seed drop/hill			Average
	R1	R2	R3	
Total hill drop	20	20	20	20
No. of Multiple hill	3	2	3	2.66
Multiple index %	15	10	15	13.33

ground wheel rotates on metering shaft. The pulling force varied from 13 to 17.5 kg at 32.850 angle of inclination. The draft accordingly computed varied from 10.97 kgf (107.6 N) to 14.77 kgf (144.8 N). The average draft recorded was 13.02 kgf (127.7 N), which was considered to be very well within pulling capacity of man.

Cost of Operation

The cost of operation of the machine per hour as well as per ha is represented in Table 8. For sowing one ha of land the planter required Rs. 1,503/ha which was much less compared to transplanting in SRI and dibbling of dry seeds which required 19.23 and 23.14 man days/ha respectively and required additional of Rs. 4,807 and Rs. 5,765/ha. Thus, the newly developed machine saves 68.7% and 73.9% of money over transplanting manually and dibbling of seeds.

Conclusion

1. The check row planter can perform planting at a designed spacing between seeds (26.7 cm) and rows (25 cm) at an acceptable seed rate (10.1 kg/ha).
2. The placement of seeds was at uniform depth under a range 2.4 cm to 3.25 cm. The missing index was found 6.6%, whereas the multiple index was observed 13.3%. The seed damage was observed only 2.1%, which was within acceptable limit.
3. The theoretical field capacity was 0.048 ha/h, at a speed of 1.05 km/h whereas, the actual field capacity was found 0.023 ha/h and field efficiency 47%.
4. The check row planter being light, simple in design and easy to operate can also be fabricated from locally available materials.
5. The machinery cost per hour was calculated as Rs. 34.54/h. For sowing one ha of land the planter required 5.44 man days which was much less as compared to manually transplanting in SRI and dibbling dry seeds. The planter saves 68.7% and 73.9 % of money over transplanting and dibbling of rice seed manually.

Acknowledgement

The authors are grateful to ICAR New Delhi, Niche Area of Excellence Programme- Farm Mechanization in Rainfed Agriculture, for granting financial assistance during the course of investigation.

REFERENCES

Food and Agriculture Organisation, 2009. FAO STAT Database, FAO, Rome, Italy, www.faostat.fao.org (accessed June 2010).

Gite, L. P. 1985. Ergonomic con-

Table 5 Test result of check row rice planter

Field No.	Speed, km/h	TFC, ha/h	AFC ha/h	η_e, %	Time req., h/ha	Seed rate, kg/ha
A.	1.04	0.050	0.024	47.66	41.66	9.40
B.	0.98	0.048	0.023	47.40	43.47	10.12
C.	0.94	0.046	0.022	47.10	45.45	10.75
Avg.	0.97	0.048	0.023	47.38	43.52	10.09

Table 6 Comparison of different method of planting of rice

Method of planting Manual (25 × 25 cm) for SRI	EFC, ha/h	Time req., h/ha	Man-days, required /ha	Cost/ha, Rs.
Check row rice planter	0.023	43.52	5.45	1,360
Transplanting y	0.0065	153.84	19.23	4,807
Dibbling	0.0054	185.18	23.14	5,765

Table 7 Energy consumption for different method of rice sowing

S.No.	Method of rice sowing	Energy consumption MJ/ha
1	Dry seeding by Check row planter	2,370.00
2	Transplanting of nursery in SRI	5.00
3	Dry seeding rice seeds by manually	240.00

Table 8 Calculation of cost work with check row rice planter

S.No.	Particulars	Amount
1	Cost of machine, Rs.	2,370.00
2	Life of the machine (y)	5.00
3	Annual use (h)	240.00
5	Depreciation, Rs.	213.3
6	Interest, Rs.	182.49
Sum of (5 & 6)	Fixed cost (Rs/Year) annul use is 240 h	396.19
A	Fixed cost (Rs./h)	2.30
B	Operational	
1.	Wage of 1 operator (Rs. 250/day*), Rs./h	31.25
C	Variable cost	
1.	Repair and maintenance, Rs/h	0.987
Total of (A + B + C)	Cost of operation with check row planter, (Rs./h)	34.537
a.	Cost of operation, Rs. /ha	1,503
b.	Saving over manually transplanting, Rs./ha	3,305
c.	Saving over manual transplanting percentage	68.75
d.	Saving over dry seeding manually, Rs./ha	4,262
e.	Saving over dry seeding manually, percentage	73.91

* 1 day i.e. 8 hour of work

sideration in design of mechanical weeders. proceeding design course on agricultural machinery, CIAE, Bhopal.1-8.
Gite, L. P., J. Majumdar, C. R. Mehta and A. Khatadkar. 2009. Anthoropometric and Strength Data of Indian Agricultural Workers for Farm Equipment Design. Central Institute of Agricultural Engineering, Bhopal, India.
Khus, G. S. 2004. Harnessing science and technology for sustainable rice-based cropping systems. Proc. FAO Rice Conference 'Rice is Life". Int. Rice Comm. News, 53: 17-23.
Mohanty, S. 2013. Trends in Global Rice Consumption.Rice Today. 12(1): 44-45.
Subbiah, S. V., M. Kumar and J. S. Bentur. 2006. DRR's experience of SRI method of rice cultivation in India. Paper for international dialogue on rice and water: exploring option for food security and sustainable environments, IRRI, Los Banos, March 7-8.
Von Brun, J. and M. S. Bos. 2004. The challenging economics and politics of rice: Implecation for food security, Globalization and Environment Sustainability. IRRI and Japan Int. Res. Centre for Agril, Sciences, 7-20.

■■

ABSTRACTS

The ABSTRACTS pages is to introduce the abstracts of the article which cannot be published in whole contents owing to the limited publication space and so many contributions to AMA. The readers who wish to know the contents of the article more in detail are kindly requested to contact the authors.

1751

Development and Performance Evaluation of Inclined Plate Planter for Rice Cultivation Under Rainfed Condition:

Ajay Kumar Verma, Manisha Sahu

Yield potential of rice crop largely depends on the crop establishment technique to ensure optimal population. More than 21 percent of total cost of production is accounted for transplanting operation alone. Therefore, adoption of alternative rice culture, which requires less input and possible increase in yield, is highly desirable under rainfed condition. Therefore, the inclined plate seed metering mechanism for direct seeding of rice seeds to maintain plant to plant distance at reduced seed rate was developed. The part modelling was done to optimized inclined plate (inclination angle of inclined plate 450 with horizontal, rotor speed 0.17 m/s, area of single cell 28 mm^2 and forward speed 5 km/h). The prototype of machine was developed and field tested in 20 ha area in research farm and about 100 ha in farmer's field. Its field capacity was 0.77 ha/h with field efficiency 83%. The seed rate required for sowing of rice seeds was 20 kg/ha (20 × 10 cm spacing at 2 seeds per cell), which was low in comparison to seed rate of fluted roller metering seed drill as 82 kg/ha. The average plant population was found 105 plants/ m^2 with inclined plate planter. Study revealed that sowing by inclined plate planter with inverted T type furrow opener was more advantageous in view of crop management under rainfed rice cultivation.

■■

Development of Semi Mechanised Tools for Cutting and Splitting of Jack Fruit for Bulb Separation

by

C. Nickhil
RM.Tech. Scholar.
Dept. of Agril. Engg.
University of Agricultural Sciences,
Gandhi Krishi Vignan Kendra, Bangalore 560065
Karnataka, INDIA

N. A. Nanje Gowda
Research Associate
All India Co-ordinated Research Project on Post-Harvest Engineering & Technology,
University of Agricultural Sciences,
Gandhi Krishi Vignana Kendra, Bengaluru 560065
Karnataka, INDIA
*Corresponding author: nanjegowdana@gmail.com

B. Ranganna
Contractual Scientist.
All India Co-ordinated Research Project on Post-Harvest Engineering & Technology,
University of Agricultural Sciences,
Gandhi Krishi Vignan Kendra, Bengaluru 560065
Karnataka, INDIA

S. Subramanya
Professor
All India Co-ordinated Research Project on Post-Harvest Engineering & Technology,
University of Agricultural Sciences,
Gandhi Krishi Vignana Kendra, Bengaluru 560065
Karnataka, INDIA

Abstract

Jackfruit is the favourite fruit for many, owing to its sweetness; yet it is one of the important underutilized fruit. Although extensive work on value addition of jackfruit has been done; the mechanical processing of jackfruit to separate the bulbs has remained a major concern. Therefore, a semi mechanised machine was developed for jackfruit core removing and fruit splitting to facilitate easy bulb extraction. Trials were conducted to process the three different size fruits based on their length viz. small (15-30 cm), medium (30-45 cm) and large (45 cm & above) at different cutting speeds of 600, 700, 800 rpm. When the developed machine operated at a cutting speed of 800 rpm offered a core removing efficiency of 96%, 89.5% and 71.3% and bulb damage percentage of 12.2%, 8.6% and 4.1% for small, medium and large size fruits, respectively. The total time required to cut and separate the bulbs using developed machine was 7.10, 10.0 and 12.4 min which was lesser than the manual processing by an expert requiring 13.25, 18.07 and 27.20 min for small, medium and large fruits, respectively. The throughput capacity of machine for small, medium and large size fruits were 66 kg/h, 114 kg/h and 144 kg/h, respectively. The total cost of developed tool was about 20,000 rupees ($295) and the total operating cost was about 52 rupee ($0.77) per hour. The developed machine can be operated by a common person with least drudgery and would be ideal for small to large scale processors and entrepreneurs.

Keywords: jackfruit, jack, mechanical tool, core cutting.

Introduction

Jackfruit (*Artocarpus heterophyllus Lam*) is one of the most consumed and underutilized fruit in several parts of the world. India is the second biggest producer of the fruit and is considered as the motherland of jackfruit. The total production of jackfruit during 2014-15 was estimated to be around 2.08 million tonnes, but only 7 percent of fruits produced are processed in India, which is very low when compared to Thailand (30%), Brazil (70%), Philippines (78%) and Malaysia (80%) (Anon (2002), Munishamanna et al. (2012), NHB (2016)). Jackfruit is rich in several nutrients such as vitamin B and C, potassium, calcium, phosphorus, iron, proteins, fats, β Carotene, and high level of carbohydrates that yields up to 98 kcal of energy per 100 g fruit (Kumar et al. (1988), Devi et al. (2014)). Apart from its use as a table purpose, jackfruit has also played a significant role in the Indian agriculture from the time immemorial and is a popular fruit for preparation of several home dishes, sweets, bakery products and other beverages. Although the fruit is one of the most liked and nutritious, utilization of this fruit is very limited because of its unique biological and physical characteristics which make the fruit difficult to process and extract the bulbs.

Review of Literature

A vast amount of work has been done on value addition of jackfruit to develop ready to eat products. While the work on the development of a mechanical tools or machine for processing of ripe jackfruit is found to be very limited from the literature review. However attempts have been made to develop hand operated jack fruit slicing blade to cut the whole fruit vertically or horizontally into 3 to 4 pieces. The usage of knife coated with edible vegetable oil to prevent latex sticking to knife surface while cutting ripened jackfruit was reported by APAARI (2012) and Munishamanna et al. (2012). Devi et al. (2014) have demonstrated a hand operated ripened jack fruit slicer to cut the whole jack fruit into two pieces. The mechanism is similar to hand operated shear cutter, where the cutting blade will slice through the jackfruit when the handle bar is pulled from the top towards cutting platform. Anon (2015) has developed a semi mechanised jack fruit peeling tool to remove the peel from whole tender jackfruit. The unit consists of tubular knife, toothed cutting edge and elongated guide. The toothed cutting edge was designed in such a way that could cut through a body of jackfruit and fixed elongated guide telescopically positioned within the tubular knife to direct the toothed cutting edge towards the jackfruit. The mechanism for moving the tubular knife towards the cutting pad and through the body of a jackfruit includes leveraged means designed to reduce the force required to peel the jackfruit through tubular knife, which peels off the skin of jackfruit. Vasudev Murthy (2016) has developed a tender jackfruit peeling machine which resembles a simple lathe machine used in automobile industries. The machine can be used to peel tender jackfruit alone which commonly used as vegetable and cannot be used to process ripened jackfruit. The tender jackfruit peeling machines are also developed and sold by various industries across the globe such as Luohe Hiyoung Machinery Manufacturing Co., Ltd. China, Tianjin Joy Machinery and Equipment Co., Ltd. China and Viet Loyal Import Export Co., Ltd. Veitnam. Dhanusha et al. (2017) have developed a peeling machine for large sized cylindrical vegetables which was found to be useful in peeling of tender jackfruit and cannot be used to cut ripe jackfruits. A survey was also conducted in Karnataka state prior to this study which showed the absence of appropriate mechanised tools or machinery for ripe jackfruit processing. This study also revealed the use traditional tools such as kitchen knife (62.8%), sickle (23.1%), axe (9.5%), steel blade and others (4.2%) across parts of Karnataka state.

Despite several attempts have made to develop mechanical tools for jackfruit processing, these methods are found to be cumbersome and generally cut the fruits either into two halves or into several slices resulting nearly 20-25% damage to fruit bulbs or pulp. As a result of this, these techniques or tools neither got popularized nor adapted by growers and processors. Therefore, lack of appropriate tools for jackfruit processing have led knife or sickle smeared with edible vegetable oil as the only option for cutting jackfruits. However, these crude methods are very difficult to follow by a common man since it is very risky to handle sharp cutting tool and found to be drudgery. These traditional jackfruit processing techniques is possible to follow by an expert alone who is involved in this activity for particular time period. From the literature review, it is observed that attempts made over past few years in development of appropriate tool for jack fruit processing was unsuccessful. Due to the lack of appropriate tool for jack fruit cutting and extracting bulbs with minimum damage with maximum convenience has remained a major concern for the growers, processors as well as consumers. In order to address these issues, this study aimed to develop mechanical tools for jackfruit cutting, splitting and facilitate easy and efficient bulbs separation.

Materials and Methods

Sample Preparation

The most cultivated local variety was selected and procured directly from the growers near Doddaballapur taluk of Bangalore. The fruits were graded into three categories viz. small, medium and large based on the average length of fruits. In this study, the fruits length of 15-30 cm was assumed as small size, 30-45 cm as medium size and 45 cm and above as large size. Since the jackfruits bulbs are mainly attached with inner core of the fruits, the complete cutting and removing of inner core is essential for easy bulb separation. Therefore, to understand the correlation between inner core size variations with respect to outer fruit dimensions, about ten fruits of each size were manually cut and inner core sizes were measured manually.

Development of Semi Mechanised Tools Jack Fruit Rind Cutting and Fruit Splitting

The jack fruit core cutting and rind cutting are subsequent operations; two separate mechanised tools for core cutting and fruit splitting were fabricated at workshop of All India Co-ordinated Research Project on Post-Harvest Engineering & Technology, University of Agricultural Sciences, Gandhi Krishi Vignan Kendra, Bengaluru.

Development of Jack Fruit Core cutting unit

Fig. 1 shows the schematic design of core cutting unit, which consists of a rotating hollow spindle (SS 304 grade), stationary nylon rod to push the core out of spindle, 0.5 HP 3-phase motor (1,400 rpm), adjustable fruit holding jaws, a plat form to hold the fruit vertically, a bevel gear assembly coupled with chain-sprocket mechanism that will transfer the rotating motion of handle to move the coring assembly in vertical axis and a main supporting frame. The bottom end of spindle was fixed with saw toothed cutter with similar diameter that of the spindle. The inner diameter of spindle is 50 mm which was fixed based on average core size measured and averaged during the preliminary studies. The core removing spindle was fixed inside hollow bearings along the length of spindle to enable free frictionless rotating motion. The top end of spindle pipe was fixed with a pulley which was driven by motor through a v-belt. This core cutting tool was used to remove the central core of jackfruit from stalk side of fruit at the bottom end.

Development of Pedal Operated Jack Fruit Splitting Unit

The schematic design of pedal operated fruit splitting unit is shown in **Fig. 2** and it mainly consists of a plat form to hold the fruit horizontally, a fruit splitting tines (SS 304 grade), and a spring loaded horn shaped sliding mechanism to pull the tines by holding the fruit rind on to the frame. The one end of sliding mechanism is connected to splitting tines while the other end is connected to a pedal through wire cable.

Performance Evaluation of Developed Jack Fruit Cutting and Splitting Tools

The developed semi mechanised jackfruit core removing and fruit splitting units are shown in **Fig. 3** and **Fig. 4** respectively. The developed tools were evaluated for core removing efficiency (%), bulb/pulp damage (%), throughput (kg/h), and total time for cutting and bulb separation (min). After every individual operation, the mechanical (machine) damage to fruit bulbs was evaluated by visual inspection and the percentage of bulb damage was calculated. The core removing efficiency (%), bulb damage (%), and throughput (kg/h) were calculated using Eq. 1, Eq. 2 and Eq. 3, respectively.

Core removal effeciency (%) = (Weight of core removed (kg)) / (Total weight of core (kg)) (1)

Bulb damage (%) = (Weight of damaged bulbs (kg)) / (Total weight of bulbs separated (kg)) (2)

Throughput (kg/h) = (Weight of fruit Processed (kg)) / (Processing time (h)) (3)

Comparative Performance Evaluation of Developed Jack Fruit Cutting and Splitting Tools vs. Manual Cutting and Separation of Jack Fruit Bulbs

Fig. 1 Schematic design of jack fruit cutting tool

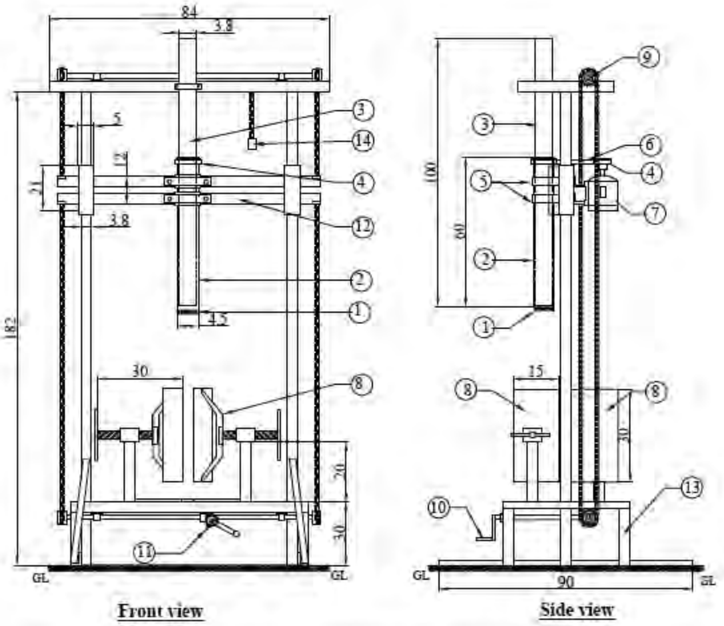

Part number	Description	Part number	Description
1	Saw tooth cutter	8	Fruit holding jaws
2	Spindle	9	Chain & Sprocket
3	Nylon rod	10	Handle
4	Pulley	11	Bevel gear
5	Bearings	12	Coring assembly
6	V-belt	13	Frame
7	Electric motor	14	Latch

Fig. 2 Schematic design of jack fruit splitting tool

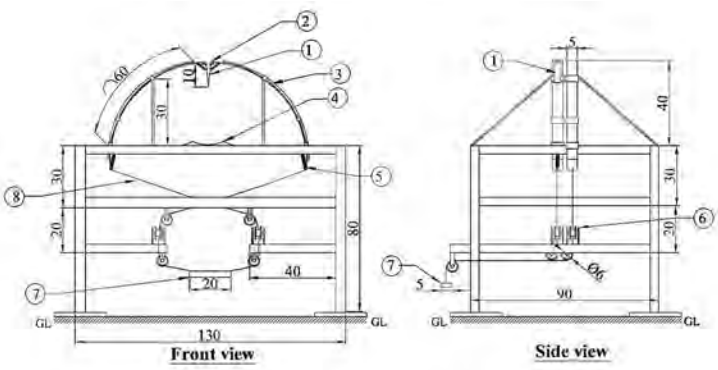

Part number	Description	Part number	Description
1	Splitting tyne	5	Tension spring
2	Sliding bars	6	Pulleys
3	Sliding guide	7	Foot pedal
4	Fruit resting platform	8	Metal wire

To evaluate the performance of developed machine in comparison with manual cutting and separation of bulbs, trails were conducted to cut different size fruits using developed machine and also manually by an expert. After each core cutting operation by machine, the left-over portion of core was removed and weighed manually to calculate the core removing efficiency. The collected bulbs were hand sorted into damaged and undamaged to calculate percentage of bulb damage. Similarly, manual cutting and separation of bulbs from the fruit was also carried out employing a skilled labour and the results were compared with to assess the overall performance, economics, drudgery and easiness of operation by developed machine.

Experimental Design

Response surface methodology was employed to study the effect of each variable on responses using Design Expert 7.0.0 software. A one factor design with linear model was used to test significant difference between the samples by considering the fruit size as categoric factor. For each experimental variable, the centre values and the ranges were fixed based on preliminary studies. The cost economics of the developed semi mechanised machine was also worked out by considering the fixed and variable costs.

Fig. 3 Developed semi mechanised jackfruit core cutting unit

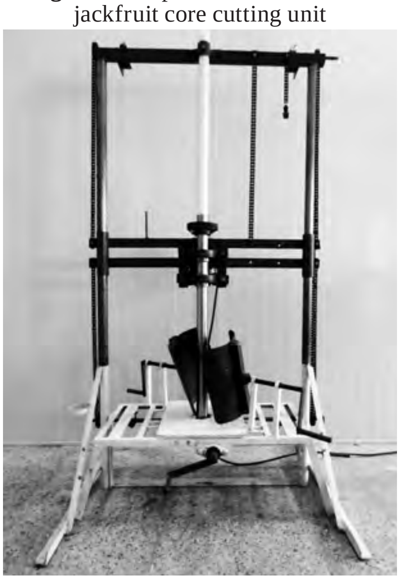

Fig. 4 Developed semi mechanised jackfruit splitting unit

Results and Discussion

Operation of Developed Semi Mechanised Jack Fruit Coring and Splitting Machine

The different sequential operations performed using developed semi mechanised jackfruit core cutting unit (**Fig. 3**) and fruit splitting unit (**Fig. 4**) are shown in **Fig. 5**. The jack fruit has a fibrous central core and a thick outer rind; one has to cut and remove this core before splitting the fruit for bulbs extraction. Before start of fruit cutting operation using developed gadget; the cutting spindle was smeared with vegetable oil to avoid the latex sticking problem. The fruit is then loaded onto platform such that stack side is in straight line to spindle and fruit is held rigidly by adjusting the fruit holding jaws. The coring unit is switched on by operating the handle, the rotating spindle assembly is moved down until the spindle come through the bottom of fruit. Subsequently, the coring assembly in moved up, and the nylon rod pushes the core out of spindle allowing the spindle ready to cut the next fruit. The coring unit is switched off and the coring assembly is locked at the top by a latch. Now the fruit is unloaded and the rind was manually cut to required depth using knife and loaded onto splitting unit. The fruit is held in horizontal posi-

Fig. 5 Different operations performed while processing of jackfruit using developed tools

Oil dipping for spindle

Jackfruit loaded & locked between holding jaws

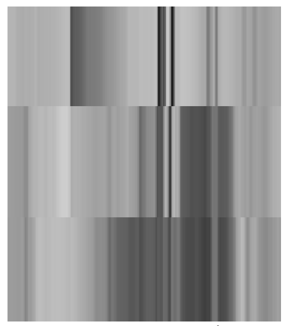

Fruit core coming out during coring operation

Jackfruit core removed by spindle

Jackfruit core removed by spindle

Jackfruit ready to harvest bulbs after splitting tion and the splitting tines are inserted between rind and pedal is pressed to split and expose the fruit inside out for easy separation of bulbs. The complete removal of core breaks the bond between bulbs and fruit, thus facilities easy plucking of bulbs.

Core Removing Efficiency (%)

The effect of fruit size and spindle speed on coring removing efficiency is shown in **Fig. 6**. The fruit size had a significant ($p < 0.0001$) effect on coring removing efficiency, compared to cutting speed which had negligible effect (**Table 1**). The average coring removing efficiency deceased from 96% for small fruits to nearly 72% for large fruits under various spindle speeds of 600-800 rpm. The highest coring removing efficiency recorded was 96% for small size fruits at a cutting speed of 600 rpm. However, an increase or decrease in spindle speed had no effect on coring removing efficiency. The linear decrease in core removing efficiency with increase in fruit size was due to the incomplete removal of core from medium and large size fruits by the spindle with inadequate diameter. This was due to fact that the inner core size varies significantly with respect to fruit size and does not remain constant throughout the length of the fruit, which requires different spindle sizes for cutting small, medium and large fruits.

Table 1 ANOVA for core cutting efficiency

Source	Sum of squares	df	Mean Square	F Value	p-value
Model	1,490.50	3	496.83	1,546.23	0.0001****
A-Speed	0.16	1	0.16	0.50	0.4907
B-Size	1,490.34	2	745.16	2,319.09	0.0001****
Residual	3.53	11	0.32		
Lack of Fit	3.53	5	0.70	Std. Dev	0.56
Pure Error	0	6	0	Mean	85.72
Cor. Total	1,494.03	14		C.V (%)	0.66

*$p \leq 0.05$, significant; **$p \leq 0.01$, significant; ***$p \leq 0.001$, significant; ****$p \leq 0.0001$, significant

Table 2 ANOVA for percentage of bulb damage

Source	Sum of squares	df	Mean Square	F Value	p-value
Model	166.39	6	27.73	3,422.95	0.0001****
A-Speed	0.00	1	0.00	0.07	0.8040
B-Size	165.46	2	82.73	10,211.25	0.0001****
AB	0.32	2	0.16	19.56	0.0008***
A^2	0.62	1	0.62	76.05	0.0001****
Residual	0.06	8	0.01		
Lack of Fit	0.06	2	0.03	Std. Dev	0.09
Pure Error	0.00	6	0.00	Mean	8.24
Cor Total	166.45	14		C.V (%)	1.09

*$p \leq 0.05$, significant; **$p \leq 0.01$, significant; ***$p \leq 0.001$, significant; ****$p \leq 0.0001$, significant

Percentage of Bulb Damage

The percentage of bulb damage during core cutting at different spindle speeds is shown in **Fig. 7**. The highest bulb damage percentage ranged between 11.4-12.2% for small fruits, which was found to decrease to 3.5-4.1% for large fruits. The percentage of bulb damage significantly ($p < 0.001$) varied with respect to fruit size, this was due to variation of core size among different sized fruits (**Table 2**). The percentage of bulb damage increased linearly with decrease in fruit size from large to small fruits at various spindle speeds between 600-800 rpm. The small size fruits found to have smaller core size; thus the selected spindle diameter was larger than the core diameter of small fruits which led to excess cutting of core along some portion of fruit bulbs resulting in higher damage percentage. On other hand, the spindle speed had no effect on bulb damage and it was found to remain constant for all three fruit sizes. The percentage of pulp damage in developed semi mechanised tool is nearly 20-25% lesser than the method reported by Devi et al. (2014). This is because the spindle of developed method cut and removes the centre core without disturbing or damaging the fruit pulp. Whereas

Fig. 6 Effect of spindle speed and fruit size on core removing efficiency

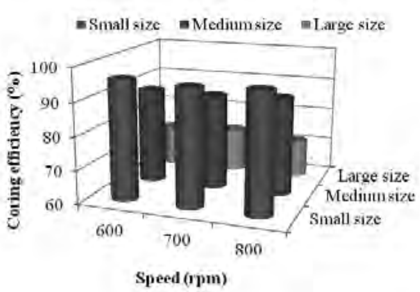

Fig. 7 Effect of cutting speed and fruit size on bulb damage

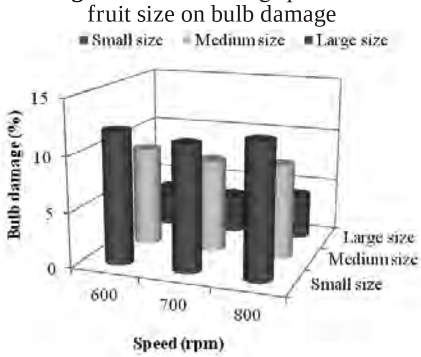

Fig. 8 Effect of fruit size and cutting speed on throughput

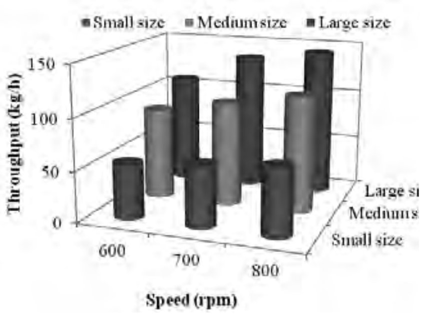

Table 3 ANOVA for through put capacity

Source	Sum of squares	df	Mean Square	F Value	p-value
Model	13,726.8	5	2,745.36	381.3	0.0001****
A-Speed	1728	1.00	1728	240.00	0.0001****
B-Size	11,710.8	2.00	5,855.4	813.25	0.0001****
AB	288	2.00	144	20.00	0.0005***
Residual	64.8	9.00	7.2		
Lack of Fit	64.8	3.00	21.6	Std. Dev	2.68
Pure Error	0	6.00	0	Mean	96.60
Cor. Total	13,791.6	14.00	13,791.6	C.V (%)	2.78

*$p \leq 0.05$, significant; **$p \leq 0.01$, significant; ***$p \leq 0.001$, significant; ****$p \leq 0.0001$, significant

Table 4 ANOVA for total time for jackfruit processing

Source	Sum of squares	df	Mean Square	F Value	p-value
Model	74.13	5	14.83	1,627.19	0.0001****
A-Speed	2.08	1	2.08	228.66	0.0001****
B-Size	71.96	2	35.98	3,948.88	0.0001****
AB	0.09	2	0.04	4.76	0.0390*
Residual	0.08	9	0.01		
Lack of Fit	0.08	3	0.03	Std. Dev	0.10
Pure Error	0.00	6	0.00	Mean	9.83
Cor. Total	74.21	14		C.V (%)	0.97

*$p \leq 0.05$, significant; **$p \leq 0.01$, significant; ***$p \leq 0.001$, significant; ****$p \leq 0.0001$, significant

the conventional jackfruit slicing methods will cut the fruit vertically into 2-3 pieces by simultaneously damaging the bulbs throughout the cut region which accounts a high per cent of bulb damage up to 25%.

Throughput Capacity (kg/h)

The throughput capacity of the machine was found to be higher for large fruits and lower for small size fruits. It was observed that, both the cutting speed and the fruit size together had a significant ($p < 0.001$) effect on the capacity of the machine (**Table 3**). However, the throughput capacity was largely dependent on fruit size than the spindle speed as shown in **Fig. 8**. This was because of the mass of fruits processed per unit time was found to be higher in large fruits compared to small and medium size fruits. In addition, the higher spindle speeds assisted in quick core cutting in short period of time irrespective of fruit size. Therefore, the large size fruits processed at higher spindle speed of 800 rpm offered the highest throughput capacity. The highest throughput capacity observed was 66 kg/h (small fruits), 114 kg/h (medium fruits) and 114 kg/h (large fruits) at a cutting speed of 800 rpm. Though the throughput capacity was found to be higher for large fruits, the coring efficiency for large size fruits was very low due to the incomplete removal of inner core which is very important for easy bulb separation. Therefore, it was noticed that the spindle size fixed was found to be best for cutting core in small and medium fruits and was not adequate for large fruits.

Total Time for Jack Fruit Processing

The total processing time is the time taken for mechanical core cutting, rind cutting, fruit splitting and manual separation of bulbs from the fruit. The average total time taken for processing the jack fruit was significantly ($p < 0.001$) affected by both fruit size and spindle speed (**Table 4**). The average time taken for processing different size jack fruit by developed machine is shown in **Fig. 9**. The time required for cutting and splitting operations increased with increase in fruit size, whereas the total time decreased slightly when cutting speed is increased from 600 to 800 rpm. The average total time taken for cutting and splitting of small, medium and large fruit were 07.10 min, 10.00 min and 12.40 min, respectively. The total time taken was mainly dependent on fruit size, the incomplete cutting of core by the spindle in large fruits requires an extra time for removing the left-over core portion. Subsequently, the leftover portion of core in large fruits made the splitting operation more difficult, thus requiring an extra force and time for splitting and harvesting of bulbs from these fruits. The complete cutting of core by spindle in small and medium fruits assisted in quick fruit splitting and easy bulb separation.

Fig. 9 Effect of fruit size and cutting speed on total processing time

Fig. 10 Total time taken for cutting jackfruit by mechanical and manual methods

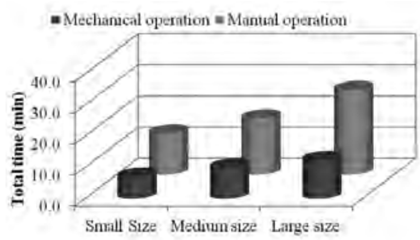

Comparative Study of Developed Mechanical mMethod with Traditional (Manual) Method of Processing

The comparison between the average time taken for core cutting, fruit splitting and bulb separation by developed mechanical method and conventional manual method is shown **Fig. 10**. The lowest processing time of 7:10 min, 10:00 min and 12:40 min for small, medium and large size fruit, respectively was observed in developed mechanical method. The mechanical cutting assists uniform core cutting from top to bottom of fruit in quick time, thus the manual bulb separation become too easy after complete removal of core irrespective of fruit size. On other hand, in manual processing the operator requires more time for complete cutting and removing of core. For an instance, the manual operation required additional time of 6:20 min, 8:10 min and 14:08 min for processing small, medium and large fruits, respectively. This extra time was the time incurred in core cutting and fruit splitting.

In addition, the mechanical method showed the highest percentage of bulb damage of about 12% which was due to variation of core size throughout the fruit length, while in manual processing damage percentage was less than 5%. Though the manual operation offers least bulb damage percentage, it was found that the manual processing is a time consuming operation and involves risk for operator to handle sharp tools and drudgery.

Cost Economics

The total cost of the developed semi mechanised machine for jackfruit processing was about 20,000 rupees ($295) only. The total operational cost of the machine was about 52 rupee ($0.77) per hour having a throughout capacity of up to 22 fruits per hour. The cost benefit ratio of the developed jack fruit processing tool was nearly 1:3.

Conclusions

The developed mechanised gadgets eliminates some of the problems faced in manual processing such as longer time for processing, risk of handling sharp tools, latex sticking to the hands and reduces the drudgery. The method also assists in quick cutting and splitting of fruits for easy bulb separation by a common person without need of an expert. For developed machine, the highest core removing efficiency varied between 71.3-96.0% with 3.5-12.0% bulb damage. The semi mechanised tool is best suitable for cutting, splitting of fruit for easy bulb separation from small and medium fruits. However, with slight modification in core cutting spindles by having three spindles with different diameter based on size of fruit to be processed will make these tools more efficient and effective. The semi mechanized tools will benefit a large number of jackfruit growers across the globe. Making available an appropriate fruit cutting and bulb separation tool will enhance the proper utilization and also enhances higher returns to growers and traders. This will go a long way in the proper utilization the under-utilized jackfruit, besides causing enforcing reduction in post-harvest losses.

Acknowledgement

Authors gratefully acknowledge the Directorate of Research, UAS, GKVK, Bengaluru for the financial support and AICRP on PHET, UAS, GKVK, Bengaluru for facilitated the fabrication of the unit.

Nomenclature

ANOVA: analysis of variance
M_w: mass of whole kernel,g
M_b: mass of broken, g
M_u: mass of un-dehulled, g
M_t: total mass of grains, g
DE: dehulling efficiency, %
B: broken, %
cfm: cubic feet per minute
ms^{-1}: metre per second
rpm: revolution per minute
w.b.: wet basis
kg: kilogram
h: hour
cm: centimetre
HP: horse power
%: percent

REFERENCES

Anon. 2015. Jackfruit peeling machine, Fruit Peeler Master. Available: *https.//www.youtube.com watch?v=MijbvKZTmwc* [30.01.2015].

APAARI. 2012. Jackfruit Improvement in the Asia-Pacific Region- A Status Report. Asia-Pacific Association of Agricultural Research Institutions, Bangkok, Thailand. 182 p.

Devi, S. P., S. Talaulikar, M. J. Gupta, M. Thangam and N. P. Singh. 2014. A Guide on Jack Fruit - Cultivation and Value Addition. Technical Bulletin No. 41, ICAR (RC), Goa.

Dhanusha, K. V. 2017. M.Tech. Theses. Development of a peeling machine for large sized cylindrical vegetables. Orissa University of Agriculture and Technology. India.

ICUC. 2002. Status report published by International Centre for Underutilized Crops (ICUC), Underutilized Tropical Fruits in Asia Net Work (UTFANET) News Letter, March 2002.

Kumar, S., A. B. Singh, A. B. Abidi, R. G. Upadhyaya and A. Singh. 1988. Proximate composition of jackfruit seeds. Journal of Food Science and Technology, 25: 308-309.

Munishamanna, K. B., B. Ranganna, K. B. Suresha, K. Srinivasappa and V. Palanimuthu. 2012. Jackfruit cultivation and value addition. Technical Bulletin, AICRP on post-harvest technology, UAS, GKVK, Bangalore.

NHB. 2016. National Horticulture Board. Available at: *http://apeda.in/agriexchange/India%20Production/India_Productions.aspx?cat=fruit&hscode=1047*.

Vasudev, Murthy. 2016. Tender Jackfruit is a Healthy Veggie: Univ. Bangalore Mirror Bureau. *http://www.thehindu.com/news/cities/bangalore/now-get-to-the-jackfruit-without-getting-your-hands-sticky/article8256249.ece*. Accessed date: 23/11/2017. ■■

Co-operating Editors


B Kayombo


M F Fonteh


S A Ndindeng


S E Abdallah


A A K El Behery


Ahmad Addo


R J Bani


I K Djokoto


A N GITAU


D K Some


K Houmy


O A Oyelade


Umar B Bindir


J C Igbeka


E U-Odigboh


K C Oni


U L Opara


N G Kuyembeh


A H Abdoun


A B Saeed


A I Khatibu


S Tembo


H A Cetrangolo


I de A Nääs


A E Ghaly


E J Hetz


M A L Roudergue


R Aguirre


O Ulloa-Torres


Y M Mesa


P P Rondon


S G C Magaña


H Ortiz-Laurel


A I Luna Maldonado


G C Bora


M R Goyal


A K Mahapatra


S M Farouk


Daulat Hussain


M A Mazed


R Ali


Chetem Wangchen


M A Basunia


Minzan Li


Xiwen Luo


S M Ilyas


Surya Nath


Indra Mani


C R Mehta


A M Michael

malopez@udec.cl

Roberto Aguirre
Assoc. Prof., National Univ. of Colombia, A.A. 237, Palmira, COLOMBIA. TEL+57-572-271-7000, ra@palmira.unal.edu.co

Omar Ulloa-Torres
Prof., Escuela de Agricultura de la Region, Tropical Humeda(EARTH), Apdo. 4442- 1000, San Jose, COSTA RICA. TEL+506-255-2000, o-ulloa@ns.earth.ac.cr

Yanoy Morejón Mesa
Agril. Engineer Univ. Agraria de La Habana, Facultad de Ciencias Técnicas Autopista Nacional y Carretera de Tapaste Apartado, 18-19 San José de las Lajas, Mayabeque, CP 32700 CUBA. ymm@unah.edu.cu

Pedro Paneque Rondon
Assoc. Prof., Universidad Agraria de La Habana, Facultad de Ciencias Técnicas, Autopista Nacional y Carretera de Tapaste, Apartado 18-19, San José de las Lajas, Mayabeque, CP 32700 CUBA. paneque@unah.edu.cu

S. G. Campos Magaña
PhD. and Prof., Paseo de los Claveles #398, Colonia Parques de la Cañada. CP 25080, Saltillo, Coahuila, MEXICO. camposg_1999@yahoo.com

Hipolito Ortiz-Laurel
Head of Agric. Eng. and Mechanization Dept./ Postgraduate College, Iturbide 73, Salinas de Hgo, S.L.P., C.P. 78600, MEXICO. TEL+52-496-30448

Alejandro Isabel Luna Maldonado
Prof. and Head of the Dept. of Agricultural and Food Engineering, Autonomous University of Nuevo Leon, Nuevo León, MEXICO. alejandro.lunaml@uanl.edu.mx; alejlun@yahoo.com

Ganesh C. Bora
Associate Prof., Dept. of Agricultural and Biological Engineering, Mississippi State Univ., 130 Creelman St., Room 242, P.O. Box 9632, MS 39762, U.S.A. gcbora@abe.msstate.edu

Megh R. Goyal
Senior Acquisitions Editor, Agric. & Biomedical Eng. and Retired Professor in Agric. & Biomedical Eng. Univ. of Puerto Rico, Mayaguez P.O. BOX 86, Rincon, PR-00677, U.S.A. goyalmegh@gmail.com

Ajit K. Mahapatra
Agric. & Biosystems Eng. Dept., South Dakota State Univ., P.O. Box 2120 Brookings, SD 57007-1496, U.S.A. TEL+1-605-688-5291, mahapata@sdstate.edu

-ASIA and OCEANIA-

Shah M. Farouk
Prof. (Retd.), Farm Power & Machinery Dept., Bangladesh Agril. Univ., Mymensingh 2202, BANGLADESH. TEL+880-1711-801923, smf1941@yahoo.com

Daulat Hussain
Dean, Faculty of Agric. Eng. and Technology, Bangladesh Agril. Univ., Mymensingh-2202, BANGLADESH. TEL+880-91-52245

Mohammed A. Mazed
Member-Director, Bangladesh Agri. Res. Council, Farmgate, Dhaka, BANGLADESH. mamazed@barcbgd.org

Rostom Ali
Prof., Dept. of Farm Power and Machinery, Bangladesh Agricultural University, Mymensingh-2202, BANGLADESH. rostomfpm@bau.edu.bd

Chetem Wangchen
Programme Director Agril. Machinery Centre Ministry of Agric. Royal Government of Bhutan, Bondey Paro Bhutan 1228, BHUTAN. krtamc@druknet.bt

Mohammad Ali Basunia
Associate Prof., Mechanical Engineering Programme, Institute Teknologi Brunei (ITB), Jalan Tungku Link, Gadong BE 1410, BRUNEI DARUSSALAM. ali.basunia@itb.edu.bn

Minzan Li
Prof. of College of Information and Electrical Engineering, China Agricultural University, P.O. Box 125, China Agricultural University (East Campus), Qinghua Donglu 17, Haidian District, Beijing, 100083, CHINA. limz@cau.edu.cn

Xiwen Luo
Prof. of South China Agricultural University; Academician of Chinese Academy of Engineering, Wushan, Guangzhou, 510642, CHINA. xwluo@scau.edu.cn

S. M. Ilyas
Prof. Green View Apartment, Flat-699; Pocket-2; Sector-19; Dwarka, NEW DELHI-110 075, INDIA. Tel+91-95608 48971, smilyas15@gmail.com

Surya Nath
Flat #1143, G Block, Galaxy North Avenue, GC-3, Gaur City, Greater Noida. UP. 201009, INDIA. TEL +234-042-771676, surya.nath@rku.ac.in

Indra Mani
Prof., Head of Division of Agril. Eng. IARI, New Delhi-110012, INDIA. maniindra99@gmail.com

C. R. Mehta
Project Coordinator, AICRP on Farm Implements and Machinery, ICAR - Central Institute of Agricultural Engineering, Nabi-bagh, Berasia Road, Bhopal - 462 038, INDIA. crmehta65@yahoo.co.in

A. M. Michael
1/64, Vattekunnam, Methanam Road, Edappally North P.O., Cochin, 682024, Kerala State, INDIA. kmichael65@eth.net

B. S. Pathak
Adjunct Prof., Indian Agril. Research Institute, KC5, Kavi Nagar, Ghaziabad- 201002, INDIA. bspathakprof@gmail.com

Vilas M. Salokhe
Prof., Flat B-1, Royal Gateway Apartment Near Yallama Temple, Main Road Kasaba Bawada Kolhapur - 416006, INDIA. vsalokhe@yahoo.com

Gajendra Singh
Adjunct Professor, Indian Agricultural Research Institute (IARI), 86-C, Millennium Apartments, Sector-61, NOIDA, U. P. 201301, INDIA. TEL+91-99-71087591, prof.gsingh@gmail.com

Sitaram Dagdupant Kulkarni
Dr., Flat No. 105, Guruprasad Apptts., Plot No. 85 & 86, Survey No. 78, Left Bhusari Colony, Kothrud, Pune - 411038, INDIA. sdkulkarnispu@gmail.com

S. R. Verma
Ex-Dean & Prof. of Agr. Eng., H. No. 14, Good Friends Colony, Barewal Road, Ludhiana 141012. Punjab, INDIA. TEL+91-161-2551096, srverma10@yahoo.com

Peeyush Soni
Associate Prof., Dept. of Agricultural and Food Engineering, Indian Institute of Technology Kharagpur, Kharagpur, West Bengal -721302, INDIA. TEL+91-3222-283100, soni@iitkgp.ac.in


B S Pathak


V M Salokhe


G Singh


S D Kulkarni


S R Verma


P Soni


Kamaruddin Abdullah


M Behroozi-Lar


Saeid Minaei


A Mahdavian


A M Abdul-Munaim


H Hasegawa


B A Snobar


J H Chung


In-Bok Lee


M Z Bardaie


Enkhbayar Gonchigdorj


M P Pariyar


H P W Jayasuriya


Alamgir A Khan


A Q A Mughal


M S Mirjat


N A Abu-Khalaf


R M Lantin


R P Venturina


S A Al-Suhaibani


A M S Al-Amri


S G Illangantileke


Suming Chen


S Krishnasreni

Kamaruddin Abdullah
The Graduate School/Renewable Energy, Darma Persada University, Jl. Radin Inten II, Pondok Kelapa, East Jakarta, 13450, INDONESIA. TEL+64-21-8649051, kabdullah0997@yahoo.com

Mansoor Behroozi-Lar
Prof., Emeritus Tehran Uni. Agr. Eng., Ph. D., Jalal All Ahmad Nasim St. Nasim Danesh Complex Block #35, second floor Tehran, IRAN. Behroozil@Yahoo.com

Saeid Minaei
Assoc. Prof., Dept. of Agr. Machinery Eng., Tarbiat Modarres Univ., P.O.Box 14115-336, Tehran, IRAN. TEL+9821-44180537, minaee@modares.ac.ir

Alireza Mahdavian
Assistance Prof., Department of Biosystems Engineering, Tarbiat Modares Univ., P.o.Box 14115-336, Tehran -14977-13111, IRAN. TEL +98-912-3346506, al.mahdavian@gmail.com; a.mahdavian@modares.ac.ir

Ali Mazin Abdul-Munaim
Assistant Prof., Dept. of Agril. Machines and Equipments, College of Agric., Univ. of Baghdad, IRAQ. TEL+964-778-4561, old2a3y@yahoo.com

Hideo Hasegawa
Assoc. Prof., Institute of Science and Technology, Niigata University, 8050 Ikarashi 2-no-cho, Nishi-ku, Niigata 950-2181 JAPAN. +81-25-262-6690, hsgw@agr.niigata-u.ac.jp

Bassam A. Snobar
Prof., Univ. of Jordan, Faculty of Agriculture, Amman 11492, JORDAN. snobar@ju.edu.jo

Jong Hoon Chung
Prof., Dept. of Biosystems & Biomaterials Science and Eng., College of Agril. and Life Sciences, Seoul National Univ., Bldg 200 Rm 2216 1 Gwanangno, Gwanak-Gu, Seoul, 151-742, KOREA. TEL+82-2-880-4601, jchung@snu.ac.kr

In-Bok Lee
Prof., Laboratory of Aero-Environmental & Energy Engineering (A3EL), Dept. of Rural Systems Eng., College of Agril. & Life Sciences, Seoul National Univ., San 56-1, Shillim-dong, Gwanak-gu, Seoul-city, KOREA. TEL+82-2-880-4586, iblee@snu.ac.kr

Muhamad Zohadie Bardaie
Prof., Dept. of Agril. and Biosystems Eng., Univ. Putra Malaysia, 43400 upm, Serdang, Selangor, MALAYSIA. TEL+60-3-8946-6410

Enkhbayar Gonchigdorj
Director, School of Eng. & Technology, Mongolian University of Life Sciences, Ulaanbaatar, Zaisan, 17024, MONGOLIA. TEL+60-976-11-341554 enkhbayar@muls.edu.mn

Madan P. Pariyar
Consultant, Rural Development through Selfhelp Promotion Lamjung Project, German Technical Cooperation. P.O. Box 1457, Kathmandu, NEPAL.

Hemanatha P. W. Jayasuriya
College of Agril. and Marine Sciences, P.O. Box 34, PC 123Al-khod, Muscat Sultanate, OMAN. TEL+968-2414-1223, hemjay@squ.edu.om

Alamgir A. Khan
Research Engineer, Agricultural Mechanization Research Institute, Multan, PAKISTAN. alamgirakhtar@hotmail.com

A. Q. A. Mughal
Research Professor, Greenwich Univ., DK-10, Street 38t, Darakshan, DHA Phase-6, Karachi-75500, PAKISTAN. dr.aqmughal@greenwich.edu.pk

Muhammad Saffar Mirjat
Dean, Faculty of Agril. Eng., Sindh Agriculture Univ. Tandojam, PAKISTAN. TEL+92-221653160, drmirjat@hotmail.com

Nawaf A. Abu-Khalaf
Assistant Prof., Palestine Technical Univ. -Kadoorie (PTUK), P.O.Box 405, Hebron, West Bank, PALESTINE. TEL+972-2-2227-846/7, nawafu@hotmail.com

Reynaldo M. Lantin
Retired Professor, College of Engineering and Agro-Industrial Technology, University of the Philippines Los Banos, College, Laguna 4031, PHILIPPINES. TEL+63-49-536-2792, reylantin@gmail.com

Ricardo P. Venturina
PHILIPPINES.

Saleh Abdulrahman Al-suhaibani
Prof., Agril. Eng. Dept.,College of Agric., King Saud Univ., P.O. Box 2460 Riyadh 11451, SAUDI ARABIA. salsuhaibani@gmail.com

Ali Mufarreh Saleh Al-Amri
Prof., Dept. of Agril. Systems Eng., College of Agril. Sciences & Food, King Faisal Univ., P.O.Box 55035, Al-Ahsa, 31982 SAUDI ARABIA. aamri@kfu.edu.sa

Sarath G. Illangantileke
Prof., Sarath Ilangantileke, Consultant in Agric Engineering, Mechanization and Education, 4/567 Victoria Range Bungalows, Kengalla, SRI LANKA. sageilan@gmail.com

Suming Chen
Prof., Dept. of Bio-Industrial Mechatronics Eng., National Taiwan Univ., 1, Section 4, Roosevelt Road, Taipei, TAIWAN. TEL+886-2-33665350, schen@ntu.edu.tw

Suraweth Krishnasreni
Emeritus Prof. 24/77 Baan Kasemsan 1, Soi Kasemsan 1 Rama 1 Rd., Wangmai, Pathumwan, Bangkok 10330, THAILAND, surawethk@gmail.com

Surin Phongsupasamit
President, Institute for Promotion of Teaching Science and Technology, 924 Sukumit Rd. Klong Toey Bangkok, THAILAND, surin1950@hotmail.com

Akkapol Senanarong
Agricultural Engineering Research Institue Department of Agriculture, 50 Phaholyothin Rd., Jatuchak Bangkok 10900, THAILAND, akkapol@ksc.th.com

Can Ertekin
Prof., Dpt. of Farm Machinery and Technologies Eng., Faculty of Agril., Akdeniz University, 07070, Antalya, TURKEY. ertekin@akdeniz.edu.tr

Imad Haffar
Managing Director, Palm Water Jumeirah Village (Slte Office Gate #10) Al Khail Road, P.O. Box 215122, Dubai, U.A.E. Tel+971-4-375-1196, imad.haffar@palmwater.ae

Nguyen Hay
Prof., President of Nong Lam Univ., Linh Trung Ward, Thu Duc District, Ho Chi Minh City, VIET NAM. nguyenhay@gmail.com

Pham Van Lang
VIET NAM. langvcd@yahoo.com

-EUROPE-

Tihomir Hristov Katardjiev
General Manager at Yogurtson Trade Ltd., Omachi 216-74, Ichikawa-shi, Chiba-ken 272-0801, Japan


S Phong-supasamit


A Senanarong


C Ertekin

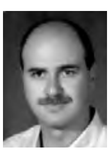
I Haffar


N Hay


P V Lang


T H Katardjiev


P Kic


J Müller


K P Ferentinos


Nick Sigrimis


E Gasparetto


W B Hoogmoed


Y Lobachevsky


M Martinov


J Ortiz-Cañavate


Brian G Sims

Retirement Co-editors' Name List

Co-editor's name	Nationality	Inaugural year	Retired year	Co-editor's name	Nationality	Inaugural year	Retired year
Adrian Moens	Netherlands	1972	1989	Suppiah Kathirkamathamby	Sri Lanka	1981	1991
Bala Krishna Shrestha	Nepal	1972	1991	Armed Hossain Mirdha	Mexico	1982	1991
Chul Choo Lee	Korea	1972	2014	A. A. Valenzuela	Chile	1982	2013
Chau Van Khe	Vietnam	1972	1980	David Boakye Ampratwum	Ghana	1982	2011
Manbahadur Gurung	Bhutan	1972	2006	Kshirode Chandra Roy	Bangladesh	1982	1985
Merle L. Esmay	U. S. A.	1972	1990	M. H. Abdel Aziz	Saudi Arabia	1982	1991
Giuseppe Pellizzi	Italy	1973	2012	Krishna Prakash Srivastava	Ethiopia	1983	1989
Mohamed A. Bedri	Sudan	1973	1987	Muhammad Siddique Chaudhry	U. S. A.	1983	1991
Shahansha-Uddin Choudhury	Bangladesh	1973	1991	Wimala Tissa Weerakoon	Zambia	1983	1985
T. B. Muckle	U. K.	1973	1978	Harry D. Henderson	Lebanon	1984	1985
Chang Joo Chung	Korea	1975	2014	Mohammad Afzal	Pakistan	1984	1994
T. Touggaard Pedersen	Denmark	1975	1990	A. P. Kaloyanov	Bulgaria	1985	2013
Bilash Kanti Bala	Bangladesh	1976	1982	Soedjatmiko	Indonesia	1986	2014
George B. Hanna	Egypt	1976	1988	Aalbert Anne Wanders	Netherlands	1988	2007
Jun Sakai	Japan	1976	2015	Ali Mahmoud El Hossary	Egypt	1988	2010
Siswadhi Soepardjo	Indonesia	1976	1985	Chanchai Rojanasaroj	Thailand	1988	2011
Tieng-Song Peng Taiwan	Taiwan	1976	2015	Edward A. Baryeh	Zimbabwe	1988	2014
Mohammad Ilyas	Pakistan	1977	1981	T. P. Ojha	India	1988	2015
Amala Prasad Sharma	Fiji	1978	1981	Eltag S. Eldin Mahmoud	Sudan	1990	2011
Arumugam Kandiah	Ethiopia	1978	1989	Henrik Have	Denmark	1990	2009
Bherulal T. Devrajani	Pakistan	1978	2004	Graeme Ross Quick	Australia	1995	2015
John Kilgour	U.K.	1978	2014	Rafiq ur Rehman	Pakistan	1995	2015
Satish Chandra	Fiji	1979	1990	Abdulsamad Abdulmalik Hazza'a	Yemen	1999	2014
Jitendra P. Mittal	Nigeria	1980	1993	Yunus Pinar	Turkey	1983	2016
Naresh Chandra Saxena	India	1980	1988	William J. Chancellor	U.S.A	1972	2017
Paris Andereou	Lebanon	1980	1984	Kunihiro Tokida	Japan	2016	2017
Wang Wanjun	China	1981	2012	Shujun Li	China	2012	2018
Allah Ditta Chaudhry	Pakistan	1981	2015	S. F. (Sen-Fuh) Chang	Taiwan	1987	2018
Allan L. Phillips	U. S. A.	1981	2004	Jan Pawlak	Poland	2002	2019
Julien G. Van Lancker	Brundi	1981	1989	Oleg S. Marchenko	Russia	2003	2019

Back Issues

AGRICULTURAL MECHANIZATION IN ASIA, AFRICA AND LATIN AMERICA

(Vol.49, No.1, Winter, 2018-)

◇ ◇ ◇

Vol.49, No.1, Winter 2018

◇ ◇ ◇

Vol.49, No.2, Spring 2018

◇ ◇ ◇

Vol.49, No.3, Summer 2018

◇ ◇ ◇

Vol.49, No.4, Autumn 2018

■■

INSTRUCTIONS TO AMA CONTRIBUTORS

The Editorial Staff of the AMA requests of articles for publication to observe the following editorial policy and guidelines in order to improve communication and to facilitate the editorial process:

Criteria for Article Selection

Priority in the selection of article for publication is given to those that –

a. are written in the English language;
b. are relevant: to the promotion of agricultural mechanization, particularly for the developing countries;
c. have not been previously published elsewhere, or, if previously published are supported by a copyright permission;
d. deal with practical and adoptable innovations by, small farmers with a minimum of complicated formulas, theories and schematic diagrams;
e. have a 50 to 100-word abstract, preferably preceding the main body of the article;
f. are printed, double-spaced, under 3,000 words (approximately equivalent to 6 pages of AMA-size paper) ; and those that
g. art: supported by authentic sources, reference or bibliography.
h. written in MS DOS format.

Rejected/Accepted Articles

a. As a rule, articles that are not chosen for AMA publication are not returned. At the earliest time possible, the writer(s) is advised whether the article is rejected or accepted.
b. When an article is accepted but requires revision/modification, the details will be indicated in the return reply from the AMA Chief Editor in which case such revision/modification must be completed and returned to AMA within three months from the date of receipt from the Editorial Staff.
c. The AMA does not pay for articles published.
d. Complimentary copies: Following the publishing, three successive issue are sent to the author(s).

Procedure

a. Articles for publication (original and one-copy) must be sent to AMA through the Co-operating Editor in the country where the article originates. (Please refer to the names and addresses of Co-operating Editors in any issue of the AMA). However, in the absence of any Co-operating Editor, the article needs to be sent to Co-operating Editor in the writer's neighboring country. Please note that it is AMA Chief Editor that decide whether publish each submitted paper on AMA or not. Even if Co-operating Editor found your manuscript suitable for publication on AMA, it can not the case with AMA Chief Editor.
b. Contributors of articles for the AMA for the first time are required to attach a passport size ID photograph (black and white print preferred) to the article. The same applies to those who have contributed articles three years earlier. In either case, ID photographs taken within the last 6 months are preferred.
c. The article must bear the writer(s) name, title/designation, office/organization, nationality and complete mailing address.

Format/Style Guidance

a. Article must be sent by E-mail with Word File and PDF File attached.
b. The data for graphs and photographs must be saved into piecemeal data and enclosed (attached) with the article.
c. Whether the article is a technical or popular contribution, lecture, research result, thesis or special report, the format must contain the following features:
(i) brief and appropriate title;
(ii) the writer(s) name, designation/title, office/organization; and mailing address;
(iii) an abstract following ii) above;
(iv) body proper (text/discussion);
(v) conclusion/recommendation; and a
(vi) bibliography
d. Tables, graphs and diagrams must be numbered. Table numbers must precede table titles, e.g., "Table 1 Rate of Seeding per Hectare". Such table number and title must be typed at the top center of the table. On the other hand, graphs, diagrams, maps and photographs are considered figures in which case the captions must be indicated below the figure and preceded by number, e.g., "Fig. 1 View of the Farm Buildings".
e. Papers are printed in black and white. Tables and figures must be made so as to be clearly understood in black and white.
f. **The data for the graph must also be included. (e.g. EXCEL for Windows)**
g. Tables and figures must be preceded by texts or discussions. Inclusion of such tables and figures not otherwise referred to in the text/discussion must be avoided.
h. Tables must be typed clearly without vertical lines or partitions. Horizontal lines must be drawn only to contain the sub-title heads of columns and at the bottom of the table.
i. Express measurements in the metric system and crop yields in metric tons per hectare (t/ha) and smaller units in kilogram or gram (kg/plot or g/row).
j. Indicate by footnotes or legends any abbreviations or symbols used in tables or figures.
k. Convert national currencies **in US dollars** and use the later consistently.
l. Round off numbers, if possible, to one or two decimal units, e.g., 45.5 kg/ha instead of 45.4762 kg/ha.
m. When numbers must start a sentence, such numbers must be written in words, e.g., Forty-five workers..., or Five tractors..."instead of 45 workers..., or, 5 tractors.

SUBSCRIPTION/ORDER FORM

AGRICULTURAL MECHANIZATION IN ASIA, AFRICA AND LATIN AMERICA (AMA)

Issued Quarterly

AMA has Achieved an IMPACT FACTOR!!

AMA has been read by those involved in agricultural machinery and industry all over the world since the first publishment in 1971. Thanks to many contributions from both the readers and writers, in 2012, we have achieved an Impact Factor, established by Thomson Reuters in U.S.A. AMA is the only Japanese agricultural machinery and industry related magazine which achieved an Impact Factor.

Subscription Rate (includes surface mail postage)

Annual (4 issues).......................... ¥8,000
Single copy....................................... ¥2,500

(Check one)
☐ Please send me/us an invoice
☐ I/We enclose remittance for ¥ __________
☐ Please charge my/our credit card
☐ VISA
☐ MASTER Card. No. ______________________

Exp. date ______________________

Signature ______________________

We deeply appreciate your payment by credit card (NO EXTRA CHARGE NEEDED).
We charge you extra 4,000 JPY when paid by check or wire transfer.

****

Name: ____

Firm: ____

Position: ____

Address: ____

(block letters)

FARM MACHINERY INDUSTRIAL RESEARCH CORP.
1-12-3 Kanda-Nishikicho, Chiyoda-ku, Tokyo 101-0054, Japan
Tel. +81-3-3291-3674, Fax. +81-3-3291-5717
URL: http://www.shin-norin.co.jp
E-Mail: ama@shin-norin.co.jp


MOROOKA TECHNOLOGY to WORLDWIDE JOBSITE
HST SYSTEM AND RUBBER CRAWLER
MOROOKA developed Rubber Crawler about 40 years ago with joint development with Bridgestone. Rubber Crawler provides high performance even on irregular ground, stable moving on the sloping ground or snowy land.
Team MOROOKA Helps You ! Here's Experts in Each Field !!
Best Buddy in Muddy Fields
Tough and stable Rubber Crawler Forklift
Powerful and Invinsible Hero
Carrier Dump for a large amount
For fertilizer transportation
For sugar cane plant transportation
For potato transportation
Specialties of MOROOKA Products
Pioneer of the rubber crawler
● Seamless and durable rubber crawler assures high performance movement with low ground pressure.
● Simple and compact design allows easy operation for everybody.
● Ship structure underbody and rotary bogie system absorb the impact and allow the stable movement.
● Rubber crawler is used as base body of wide range of industrial machines.
● Rubber crawler and HST (hydrostatic transmission) system enables easy control for smooth & stable movement and huge driving power.
For forestry
For agriculture and multipurpose
ROTARY SCREEN
FORWARDER
MOBILE WOOD CRUSHER
FORKLIFT
SHOVEL LOADER
CARRIER
MOROOKA
MOROOKA Co., Ltd.
358, Shoubeeshindenmachi, Ryugasaki city, Ibaraki Prefecture, 301-0031, Japan
TEL : +81-297-66-2111 FAX : +81-297-66-3110 E-mail : info@morooka.co.jp
URL : www.morooka.co.jp (Japanese) www.morooka.com (English)